Snapshots of protein dynamics and posttranslational modifications in one experiment – β-catenin and its functions

Multiplexe Analyse des dynamischen β-Catenin/Wnt Signalweges

Dissertation

der Mathematisch-Naturwissenschaftlichen Fakultät
der Eberhard Karls Universität Tübingen
zur Erlangung des Grades eines
Doktors der Naturwissenschaften
(Dr. rer. nat.)

vorgelegt von
Katrin Luckert
aus Waiblingen

Tübingen
2010

Tag der mündlichen Qualifikation:	23.11.2010
Dekan:	Prof. Dr. Wolfgang Rosenstiel
1. Berichterstatter:	Prof. Dr. Stefan Stevanović
2. Berichterstatter:	Prof. Dr. Thilo Stehle

Acknowledgement

This thesis was performed at the Natural and Medical Sciences Institute at the University of Tuebingen in the department of biochemistry. In the context of the liver systems biology project *Hepatosys*, an experimental part of this thesis was performed at the Harvard Medical School, Boston, MA, USA in the department of Prof. Dr. Peter Sorger.

First of all, I would like to thank my advisor Prof. Dr. Stefan Stevanović for excellent supervision of this thesis. I would like to acknowledge Prof. Dr. Thilo Stehle for the agreement to supervision of my thesis as the 2nd examiner.

I am especially indebted to Dr. Thomas Joos and Dr Oliver Pötz for all kind of support during this thesis, for untiring effort, commitment and encouragement. Many thanks to Thomas for inspiring me for a research stay abroad and mostly for initiating and supporting this. I would especially like to thank Olli for a plenty of enlightening and helpful discussions, good ideas and encouraging words.

Furthermore, I am grateful for an excellent collaboration with Prof. Dr. Andreas Hecht who gave scientific support, provoked interesting thoughts and provided valuable sample material.

It is a pleasure to thank Prof. Dr. Peter Sorger for giving me the opportunity to join his lab in summer 2008 and 2009 and to spend a very impressive time abroad with a variety of unforgettable personal experiences.

Furthermore, I would like to acknowledge Boehringer Ingelheim Fonds for the financial support of both research stays in Boston.

I would like to thank all of my colleagues at the NMI for all kind of assistance, inspiring discussions, but also for the friendly atmosphere. Especially I would like to thank Conny Kazmaier for assistance and good conversations in the lab and beyond. Many thanks go to the graduate students David, Nadja, Michael, Steffi, Yvonne and Sonja for a lot of fun during the last 3 years.

It is a pleasure to thank my parents who made my university education possible and who supported me in all respects. My very special thanks go to my brothers Hansjörg and

Thomas - Saturday afternoon soccer sessions have always been fun - and my all friends for a great time beyond work.

Finally, and most importantly, I would like to thank my beloved husband Philipp. Philipp - thanks you for your understanding and patience during busy weeks, but also for a great time and wonderful moments together.

Table of contents

1	**Introduction**	**1**
1.1	Systems biology	1
1.2	The Wnt pathways	2
1.3	β-catenin and its roles in the canonical Wnt pathway	3
1.4	The role of Wnt/β-catenin signaling in normal and transformed hepatocytes	6
1.5	Non-canonical Wnt5a signaling	6
1.6	Protein microarrays	8
1.6.1	Platforms and applications	8
1.6.2	Analytical tools for cell signaling studies	11
1.7	Goal of doctoral thesis	11
2	**Materials and methods**	**13**
2.1	Reagents and chemicals	13
2.2	Buffers	15
2.3	Antibodies	17
2.4	Consumables	18
2.5	Devices and programs	19
2.6	Bacteria strains, plasmids and recombinant proteins	20
2.7	Suspension bead array	21
2.7.1	Covalent immobilization of proteins to beads	21
2.7.2	Non-covalent immobilization of proteins to beads	21
2.7.3	β-catenin bead array	22
2.7.4	β-catenin sandwich immunoassay	22
2.8	Molecular biological methods	23
2.8.1	Expression and purification of GST-ECT and GST-TCF4	23
2.8.2	Expression and purification of GST-β-catenin	23
2.9	Cell culture methods	24
2.9.1	Cell lines	24
2.9.2	Primary mouse hepatocytes	25
2.9.3	TCF reporter assay	25
2.10	Biochemical methods	26
2.10.1	Sample preparation for the β-catenin bead array panel	26
2.10.2	Protein quantification	26
2.10.3	β-catenin fishing (GST-pulldown)	26
2.10.4	LDS-Polyacrylamide gel electrophoresis	27
2.10.5	Coomassie staining	27
2.10.6	Western blot	27
3	**Results**	**29**
3.1	β-catenin bead array panel	29

3.1.1 Assay development - β-catenin bead array panel 29
3.1.2 Technical reproducibility of the β-catenin bead array panel 33
3.1.3 Cross-validation of the µ-fishing assay 34
3.1.4 Linearity of µ-fishing assay for active β-catenin 38
3.1.5 Specificity and linearity of phospho-specific β-catenin sandwich immunoassays 39
3.2 β-catenin/Wnt signaling in HEK293 40
3.2.1 Time-dependent Wnt signaling in HEK293 40
3.2.2 Origin and characteristics of active β-catenin signaling in HEK293 43
3.3 β-catenin/Wnt signaling in primary mouse hepatocytes 45
3.3.1 Time-dependent Wnt signaling in primary mouse hepatocytes 45
3.3.2 Origin and characteristics of active β-catenin signaling in primary mouse hepatocytes 48
3.4 β-catenin/Wnt signaling in human HCC derived cell lines HepG2 and FOCUS 50
3.4.1 HepG2 – model system for hepatocytes harboring an activating β-catenin mutation 50
3.4.2 FOCUS - model system for hepatocytes undergoing EMT 53
3.5 Non-canonical and canonical Wnt signaling in HCC cell lines 55
3.5.1 Time-dependent β-catenin signaling in response to Wnt5a 55
3.5.2 Does non-canonical Wnt5a impair Wnt3a-mediated activation of canonical β-catenin/Wnt signaling? 56

4 Discussion 60

4.1 Development and validation of the β-catenin bead array panel 60
4.2 β-catenin/Wnt signaling in HEK293 62
4.2.1 Time-dependent β-catenin/Wnt signaling in HEK293 62
4.2.2 Origin and characteristics of active β-catenin signaling in HEK293 66
4.3 β-catenin/Wnt signaling in primary mouse hepatocytes 68
4.3.1 Time-dependent β-catenin/Wnt signaling in primary mouse hepatocytes 68
4.3.2 Origin and characteristics of active β-catenin signaling in primary mouse hepatocytes 71
4.4 β-catenin/Wnt signaling in human HCC cell lines 72
4.4.1 HepG2 – model system for hepatocytes harboring an activating β-catenin mutation 72
4.4.2 FOCUS - model system for hepatocytes undergoing EMT 73
4.5 Non-canonical canonical Wnt signaling in HCC cell lines 75
4.5.1 Time-dependent β-catenin signaling in response to Wnt5a 76
4.5.2 Does non-canonical Wnt5a impair the Wnt3a-mediated activation of canonical β-catenin/Wnt signaling? 77
4.6 The β-catenin bead array panel – a tool for a systems biology approach? 79

5 Summary 81

6 Zusammenfassung 82

7 References 83

8 Supplementary material 95

8.1 Supplementary material 1: Relative expression levels of β-catenin in HEK293, FOCUS, HepG2 and primary mouse hepatocytes 95

8.2 Supplementary material 2: Relative levels of the E-cadherin/β-catenin and the N-cadherin/β-catenin complex in HEK293, FOCUS, HepG2 and primary mouse hepatocytes 96

8.3 Supplementary material 3: Demasking experiment 97

8.4 Supplementary material 4: Expression of Wnt signaling genes in FOCUS and HepG2 99

9 List of publications 101

10 Akademische Lehrer 102

11 Lebenslauf 103

List of Tables

Table 1 Reagents and chemicals 13
Table 2 Buffers 15
Table 3 List of antibodies 17
Table 4 List of consumables 18
Table 5 List of devices and programs 19
Table 6 Bacteria strains, plasmids and recombinant proteins 20
Table 7 List of cell lines 24
Table 8 Inter- and intra-assay variances of the β-catenin bead array panel 34
Table 9 Comparison of recorded changes in active β-catenin signaling in HEK293. 36

List of Figures

Figure 1 Important interaction partners of β-catenin and its structure. 3
Figure 2 Canonical Wnt signaling. 5
Figure 3 Phosphorylation sites of β-catenin. 6
Figure 4 Overview of Wnt5a signaling pathways. 8
Figure 5 Overview planar and bead-based microarrays. 10
Figure 6 Sandwich immunoassay. 11
Figure 7 Overview β-catenin bead array panel. 29
Figure 8 Workflow of the analysis of β-catenin using the β-catenin bead array panel. 31
Figure 9 Validation of the β-catenin bead array panel. 32
Figure 10 Cross-validation of the µ-fishing assay with HEK293 lysates. 35
Figure 11 Cross-validation of the µ-fishing assay with lysates of primary mouse hepatocytes. 37
Figure 12 Linearity of µ-fishing assay for active β-catenin. 38
Figure 13 Validation of sandwich immunoassays specific for phosphorylated β-catenin. 39
Figure 14 Time-dependent Wnt activation in HEK293 with rWnt3a. 41
Figure 15 Time-dependent Wnt activation in HEK293 cells through GSK-3 inhibition. 42
Figure 16 Origin and characteristics of active β-catenin signaling in HEK293 cells. 44
Figure 17 Time-dependent Wnt activation in primary mouse hepatocytes with rWnt3a 46
Figure 18 Time-dependent Wnt activation in primary mouse hepatocytes through GSK-3 inhibition. 47
Figure 19 Origin and characteristics of active β-catenin signaling in primary mouse hepatocytes. 49
Figure 20 Time-dependent Wnt activation in HepG2 using rWnt3a. 52
Figure 21 Time-dependent Wnt signaling in FOCUS using rWnt3a. 54
Figure 22 Impact of Wnt5a on Wnt3a-mediated activation of β-catenin signaling in FOCUS. 58
Figure 23 Impact of Wnt5a on Wnt3a-mediated activation of β-catenin signaling in FOCUS. 59
Figure 24 Workflow - from the cell culture experiment to the analysis of β-catenin. 61
Figure 25 Iinvestigated phospho acceptor sites and the corresponding protein kinase 63
Figure 26 Comparison of rWnt3a-induced β-catenin signaling in different cell types. 69
Figure 27 Wild type and truncated β-catenin in HepG2. 72
Figure 28 Cellular rearrangements during EMT. 74

Abbreviations

Aa	Amino acid
Ab	Antibody
APC	Adenomatosis polyposis coli
AU	Arbitrary units
BSA	Bovine serum albumin
CK	Casein kinase
Co-ip	Co-immunoprecipitation
Dky	Donkey
DMEM	Dulbecco's Modified Eagle's Medium
DMSO	Dimethyl sulfoxide
ECL	Enhanced chemiluminescence
E.coli	Escherichia coli
ECT	E-cadherin cytosolic tail
EDC	1-Ethyl-3-[3-dimethylaminopropyl]carbodiimide hydrochloride
EDTA	Ethylenediaminetetraacetic acid
ELISA	Enzyme-linked immunosorbent assay
FBS	Fetal bovine serum
FPLC	Fast protein liquid chromatography
Fz	Frizzled
GSK	Glycogen synthase kinase
GST	Glutathione S-transferase
Gt	Goat
HCC	Hepatocellular carcinoma
HRP	Horseradish peroxidase
ICAT	Inhibitor of β-catenin and TCF4
IPTG	Isopropyl β-D-1-thiogalactopyranoside
JNK	C-Jun N-terminal kinase

kDa	Kilodalton
LDS	Lithium dodecyl sulfate
LEF	Lymphoid enhancer factor
LRP	Low-density lipoprotein receptor-related protein
MFI	Median fluorescence intensity
MOPS	3-(N-Morpholino)propanesulfonic acid
Ms	Mouse
NLK	Nemo-like kinase
OD	Optical density
Page	Polyacrylamide gel electrophoresis
PBS	Phosphate buffered saline
PCR	Polymerase chain reaction
PE	Phycoerythrin
PKA	Protein kinase A
Rbt	Rabbit
Rpm	Round per minute
RT	Room temperature
s-NHS	N-hydroxysulfosuccinimide
TAK	Transforming growth factor-beta-activated kinase
TBST	Tris buffered saline Tween-20
TCF	T cell factor
Tris	Tris(hydroxymethyl)aminomethane
Triton X-100	4-(1,1,3,3-Tetramethylbutyl)phenyl-polyethylene glycol
Tween 20	Polyethylene glycol sorbitan monolaurate
w/v	Weight per volume
w/w	Weight per weight

Abstract

β-catenin plays multiple roles in the canonical Wnt signaling pathway and in cell-cell adhesion complexes. In addition, β-catenin is a proto-oncogene and activating β-catenin mutations play a significant role in the genesis of colorectal, hepatocellular and other common cancers. Different functions of β-catenin as transcriptional co-activator or cell adhesion molecule are orchestrated by changes in concentration and phosphorylation as well as its ability to complex with proteins such as cadherins or transcription factors.

In the context of this thesis a novel suspension bead array assay panel for the analysis of the different forms of β-catenin was developed. This assay only requires sample material in the lower µg range and is able to relatively quantify total β-catenin concentration, the extent of β-catenin phosphorylation at multiple sites and the ratio of complexed and free cytoplasmic β-catenin. The assay combines for the first time three biochemical methods – sandwich immunoassay, co-immunoprecipitation and protein-protein interaction assay – in one suspension bead array panel.

The assay panel was used to study dynamic changes in the concentration of eight different β-catenin forms in primary mouse hepatocytes as well as in HEK293, FOCUS and HepG2 cells. Taking advantage of the novel assay, new insights into the dynamics of Wnt/β-catenin signaling were gained which can be used for computational modeling of the Wnt/β-catenin signaling in the context of the Hepatosys project.

This study could define a signaling-active pool of distinct forms of β-catenin (free β-catenin and pS45, pS552 and pS675 β-catenin) which mediates the canonical Wnt signaling on protein level in β-catenin wild type cells. Furthermore, it was demonstrated that this signaling active pool originates from de-novo protein biosynthesis only, but not from membrane release.

1 Introduction

1.1 Systems biology

"The computer simulation of life." *Kitano, Nature 2003*

Several decades of science have regularly delivered new insights into the complex biology of different organisms coinciding with the development of innovative techniques and more and more comprehensive approaches. The “omics” disciplines delivered gene expression patterns (genomics) [1, 2], maps of transcriptional regulation networks (transcriptomics) [3, 4], broad metabolism studies (metabolomics) [5] as well as large-scale protein expression data sets (proteomics) [6]. While “omics” and systems biology both focus on the resolution of biological processes, they totally differ in the concept of data generation and analysis. From the perspective of a systems biologist, cellular communication system and interaction is too complex to be narrowed down to a single molecule, to a cellular event or to a simple reaction. Thus, for the understanding of biological processes systems biology claims to monitor dynamic time-resolved cellular processes and to analyze interactions at the molecular level as well as physiological functions of the whole organism including its regulatory structure [7, 8]. For this purpose experiments are systematically designed and contain multiple perturbations in several concentrations which are applied over a broad time frame. Up to now, the generation of huge data sets is still limited by suitable existent experimental and analytical methods. Multiple time points and perturbations demand for a miniaturized cell culture format, for instance, to enhance the sample throughput and to reduce material cost. To further analyze the coincidentally enhanced number of samples, analytical systems are necessarily needed which enable a fast and preferentially multi parametric analysis.

The description of cell signalling processes basically relies on the construction of a network of involved components. Systematic screens of mRNA expression, protein interactions and protein abundance and modifications [9, 10] using high-throughput methods deliver huge data sets on network level. These approaches are complemented by literature research [11, 12]. In contrast to gene expression analysis, protein data sets describing the characteristics of proteins such as its interaction, modification, abundance or localization, are more complex since multiple parameters need to be measured to add as much information as possible for each component of the network. These data sets are heterogeneous since they are

unavoidably generated using different assay systems or technical platforms, respectively [7, 13, 14]. Gaudet et al. [14] proved the usage of heterogeneously collected protein data for computational modeling of cell signaling networks. Heterogeneity of collected data coincides with the challenge of data management, combination and storage. For instance, a software tool named *DataRail* was built to combine and simplify data gaining and model construction [15].

Currently, two complementary approaches exist in systems biology. As described above, one strategy aims to collect as many information as possible to obtain a “molecular snapshot” of the cellular network. In contrast to these data-driven approaches, *in silico* experiments define smaller networks and simulate the temporary and spatial changes of the network components. These computational models are necessarily needed to overcome remaining experimental limitations and to understand the interconnection of different components of the system. Furthermore, the *in silico* description of cellular processes allows testing whether the consisting model reflects the data or allows generating a new hypothesis. For instance, Schilling et al. [16] currently studied in a combined theoretical and experimental approach hardly detectable ERK signaling details in correlation with cell fate decisions.

The Hepatosys project was initiated in 2001 in order to establish a systems biology network in Germany aiming to design a model for a fairly complex cell type – the hepatocyte. In the context of that systems biology approach, regeneration and differentiation of hepatocytes as well as critical hepatocyte processes as endocytosis, detoxification and iron metabolism were investigated (www.hepatosys.de). The analysis of cell signaling using both experimental and computational methods was embedded in different subprojects. One of these subprojects focused on the description of the Wnt signaling pathway in primary mouse hepatocytes.

1.2 The Wnt pathways

The Wnt signaling pathway is involved in the regulation of embryonic development, cell differentiation, cell polarity [17-19] and in mature organism, adult tissue maintenance by regulation of stem cell pluripotency [20]. Dysregulation of the Wnt pathway is associated with various types of cancer, including colorectal and hepatocellular carcinoma [21-23].

Up to now 19 mammalian Wnt genes (http://www.stanford.edu/~rnusse/wntwindow.html) have been discovered which all encode for secreted hydrophobic and dynamically modified glycoproteins [24]. These proteins function as extracellular Wnt ligands which induce diverse signaling cascades. They were first categorized into canonical and non-canonical Wnt ligands according to their transforming ability as for instance the induction of embryonic axis duplication in Xenopus embryos [25] and the accumulation of cytoplasmic β-catenin [26]. Based on this classification of Wnt ligands, the associated downstream pathways are known

as canonical and non-canonical Wnt pathways. From the classical perspective of Wnt signaling, distinct ligands trigger the defined intracellular responses depending on the nature of the ligand itself (reviewed in [27]).

However, several current studies showed that distinct Wnt pathway activity is not induced by a distinct Wnt ligand, but by the sum of signals triggered by different Wnt receptors [27]. The receptor complexes are composed of a Frizzled (Fz) receptor [28] and the LDL receptor-related protein 5/6 (LRP-5/6) co-receptor or alternatively a receptor belonging to the receptor tyrosine kinases (RTKs) of the Ryk [29] and Ror subfamilies [30, 31]. From this perspective, cell type- or context-specific expression of the receptor types and their assembly define which pathways are activated downstream the receptor complex.

In summary, two complementary Wnt signaling concepts for a cellular decision which distinct branch of the Wnt pathway is activated were proposed. Basing on the criteria, the two concepts are further termed as either ligand-based or receptor-based view.

1.3 β-catenin and its roles in the canonical Wnt pathway

β-catenin is a key molecule in the Wnt pathway and its different cellular functions are orchestrated by changes in its concentration, phosphorylation state, and the extent of binding to proteins such as cadherins and transcription factors. It belongs to the armadillo protein superfamily [32] which is characterized by a positively charged superhelix as a signature motif – the Armadillo repeats [33]. This structural element allows the interaction with various factors like cadherins or TCF [34-38]. However, although N- and C-terminus are lacking such structural elements, they modulate interactions regulating its transcriptional activity [39, 40] or, as suggested by Gottardi et al. [41], a switch between two isoforms either active in signaling or cell-adhesion. Figure 1 summarizes the most important interactions of β-catenin and displays schematically the full-length structure of β-catenin.

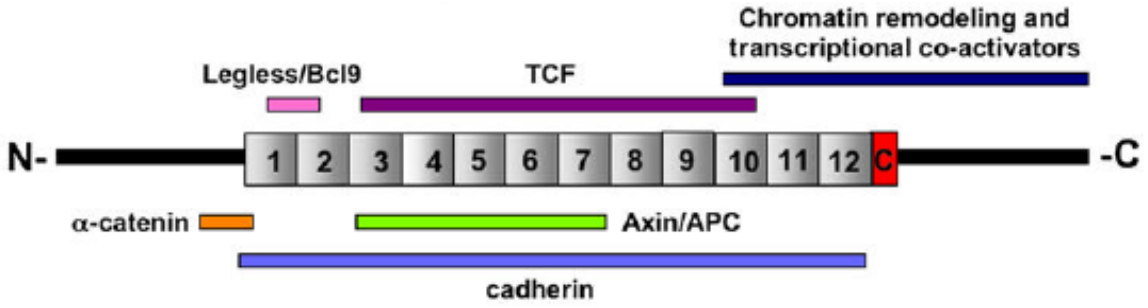

Figure 1 Important interaction partners of β-catenin and its structure.

β-catenin and its main interaction partners are displayed. The structure of full-length β-catenin is composed of flexible regions at the N- and C-terminus and the central 12 armadillo repeats including Helix C. Source [42].

In the absence of Wnt growth factors, β-catenin is mainly found at the membrane functioning as a cell-adhesion molecule [43]: here β-catenin interacts with the cytoplasmatic tail of E-cadherin [44, 45] and α-catenin which is linked to the actin cytoskeleton [46, 47]. Complex formation with both partners can be influenced by growth factors which mediate tyrosine phosphorylation of Y654 β-catenin [48, 49] or Y142 β-catenin [50]. Both modifications lead to a reduced binding of β-catenin to E-cadherin or α-catenin, respectively. However, the linkage between β-catenin involved in either cell-adhesion or Wnt signaling is not yet fully understood (reviewed in [51]).

Figure 2 shows canonical Wnt signaling in the absence and presence of a Wnt ligand. Newly synthesized β-catenin, which is not sequestered in cell-adhesion complexes, is fed into a phosphorylation-dependent degradation process. In the destruction complex composed of GSK-3β, CK1α, Axin and APC, β-catenin is sequentially targeted for degradation by CK1α-mediated phosphorylation at S45 [52] and GSK-3β-mediated phosphorylation at S33, S37, and T41 [53] followed by β-TrCP-mediated ubiquitination [54] and proteasomal degradation [55-57]. In the nucleus, co-repressors such as Groucho bind TCF and prevent TCF/β-catenin-mediated transcription of Wnt target genes [58, 59].

In the presence of a Wnt ligand, 2 types of membrane receptors are required to transfer the extracellular signal into the cell: following the current opinion the LDL receptor-related protein 6 (LRP-6) co-receptor assembles with the Frizzled (Fz) receptor [28], then its intracellular domain gets phosphorylated in a dual-kinase mechanism by GSK-3β and CKI [60-62] and recruits Axin to the membrane via the phosphorylation sites [63]. In parallel, Dishevelled (Dsh) binds the receptor complex and is phosphorylated (not shown in Figure 2) [64]. Both mechanisms were described to contribute to the stabilization of β-catenin. The destruction complex dissociates by an unknown process, β-catenin starts to accumulate and then translocates into the nucleus. β-catenin forms a complex with either of the TCF/LEF family of transcription factors (T-cell-specific transcription factor/lymphoid enhancer-binding factor 1) [65-67] and therewith it promotes expression of Wnt-response genes including c-*myc*, *cyclin D1*, c-*jun*, *Tcf-1*, *Lef-1*, *Conductin/Axin2*, and the *metalloproteinase matrilysin* (*MMP7*) (http://www.stanford.edu/~rnusse/wntwindow.html). Within the nucleus, co-activators such as TBP (TATA-binding protein [68]) or p300/CBP [69, 70] enhance the transcriptional activity of β-catenin, whereas Chibby [71] or ICAT [70, 72] impair the transcriptional activity as a competitor for C-terminal activation sites of β-catenin. Axin 2 induction represents a negative feedback loop for the Wnt pathway [73-75].

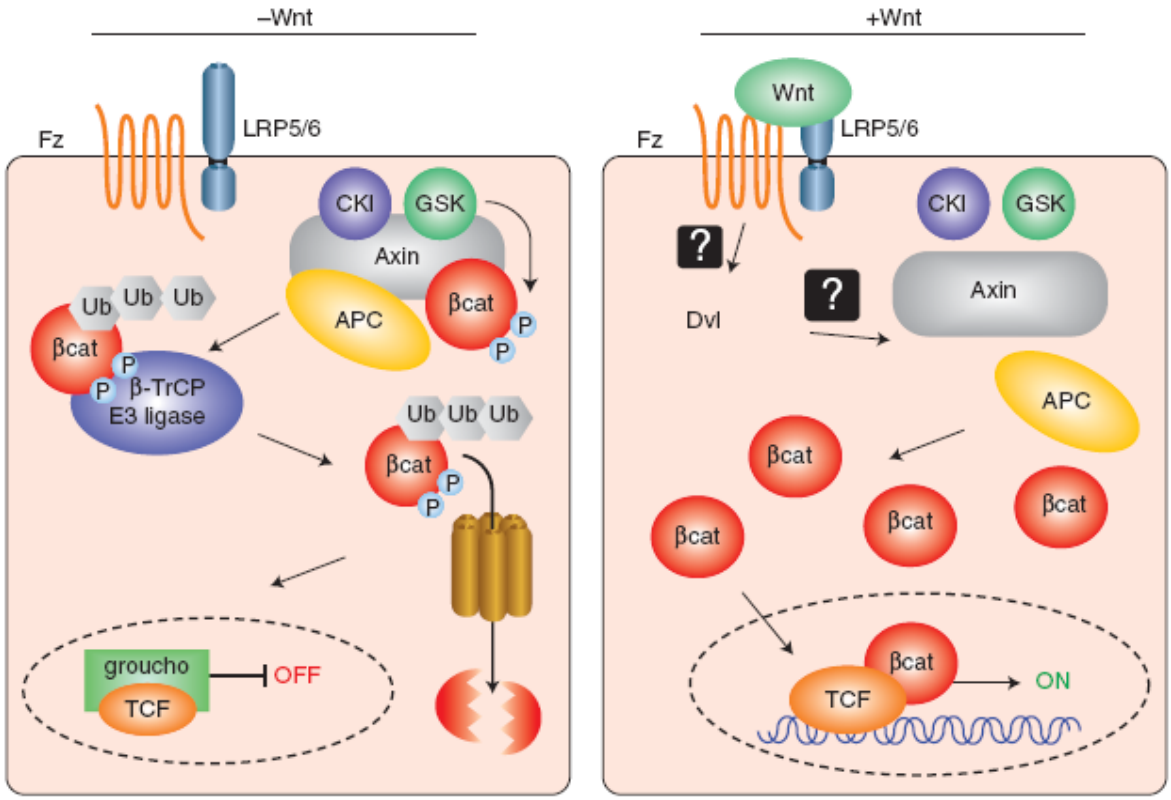

Figure 2 Canonical Wnt signaling.

The cartoon displays a summary of canonical Wnt signaling in the absence (left) and presence (right) of a Wnt ligand. In the absence of a Wnt ligand, the cytosolic pool of β-catenin is kept low by the so-called destruction complex composed of CK1, GSK-3, Axin and APC. The lack of intracellular mediator and the presence of transcriptional repressors down regulate Wnt signaling. When a canonical Wnt ligand binds to the Fz/LRP membrane complex, the destruction of β-catenin is stopped. β-catenin translocates into the nucleus and activates TCF/β-catenin –mediated transcription of Wnt target genes. Source [76].

β-catenin function can also be regulated through posttranslational modifications that are not Wnt receptor triggered: for example, the phosphorylation of β-catenin at S675 through protein kinase A (PKA) stabilizes the protein and influences positively the transcriptional activity of β-catenin [77]. Wnt-dependent and Wnt-independent modifications are likely to compete or cooperate in the regulation of β-catenin function depending on cell state (reviewed in [78]). Figure 3 shows a selection of phosphorylation sites of β-catenin.

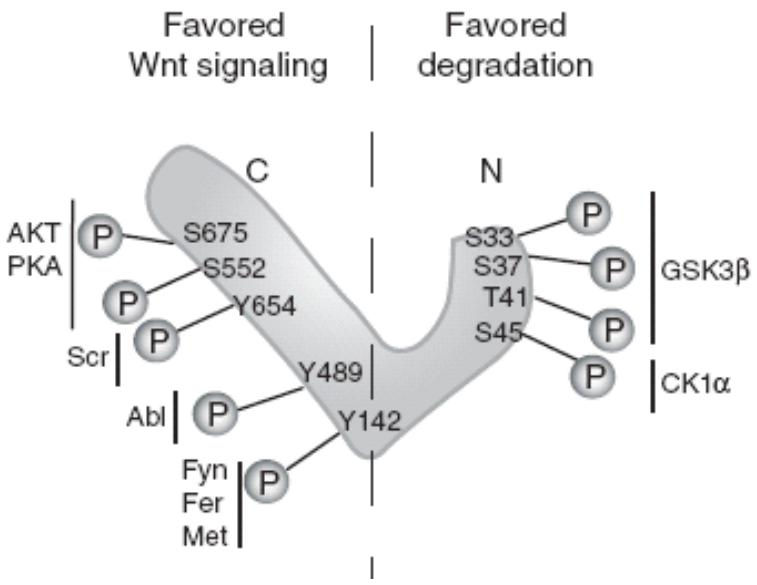

Figure 3 Phosphorylation sites of β-catenin.

Multiple cellular signals impinge on β-catenin by posttranslational modifications. Speaking generally, these modifications can be divided into their role in the regulation of Wnt signaling. Here, modifications which favor Wnt signaling or degradation, respectively, are displayed. Source [51].

1.4 The role of Wnt/β-catenin signaling in normal and transformed hepatocytes

The Wnt pathway is given a crucial role in the liver due to its versatile functions within this complex organ. During liver development, the temporal regulation of β-catenin/Wnt signaling is an important modulator of differentiation and growth processes as well as hepatic maturation [79, 80]. In the adult liver, Wnt signaling regulates regeneration, zonation, liver metabolism and oxidative stress (reviewed in [81, 82]).

In many cancers including hepatic tumors a hyper-activated β-catenin/Wnt pathway was found. Mutations in *APC* [83], *CTNNB1* [84], *AXIN1* and *AXIN2* [85] were monitored to occur in hepatoblastoma, whereas mutations in *CTNNB1* [86], *AXIN1* and *2* [85], as well as up regulation of *FZD7 [87]* and inactivation of GSK-3β [88] were detected in hepatocellular carcinoma (HCC), both resulting in hyper-activated β-catenin signaling.

1.5 Non-canonical Wnt5a signaling

As described in 1.2, Wnt signaling was historically divided into β-catenin-dependent (canonical) or β-catenin-independent (non-canonical) intracellular signaling which comprises pathways such as the planar cell polarity (PCP) pathway discovered in Drosophila [89] or the

Wnt/JNK pathway [90] as well as the Wnt/Ca^{2+} pathways [91]. However, this classification might be modified since context-specific responses as species-, tissue- or stage-specificity for instance have been shown to play a role with respect to the cellular outcome (reviewed in [27, 92]). A striking example is Wnt5a which has been described as the most prominent and well-investigated non-canonical Wnt ligand. But Mikels and Nusse [30] published a first surprising result by demonstrating that Wnt5a is able to activate or inhibit β-catenin/TCF signaling through distinct receptor/co-receptor expression in human 293 embryonic kidney (HEK293) cells (Figure 4E). This result underlines that the experimental outcome can vary due to subtle differences in the expression of individual Wnt ligands, receptors and repressors as well as their interplay for transduction of a Wnt signal.

Basically, Wnt5a was shown to mediate a broad spectrum of cellular processes (Figure 4, reviewed in [93]). Wnt5a-mediated PCP pathway regulates important cellular movements of organization, orientation and morphogenic processes throughout normal development. Furthermore, Wnt5a triggers various Ca^{2+} signaling and JNK-dependent signaling pathways. Modulation of β-catenin levels and β-catenin-dependent signaling by Wnt5a is still controversially discussed: Ishitani et al. [94] reported about the TAK-NLK pathway which interferes with β-catenin/TCF-mediated transcription, while Topol et al. [95] proposed a Wnt5a inducible mechanism of GSK-3-independent degradation of β-catenin. Additionally, Torii et al. [96] described an activation of TCF/β-catenin signaling on protein and transcriptional level involving PKA activation and GSK-3β inhibition (Figure 4F).

In summary, it still remains unclear how Wnt5a determines the specific activation of a distinct pathway.

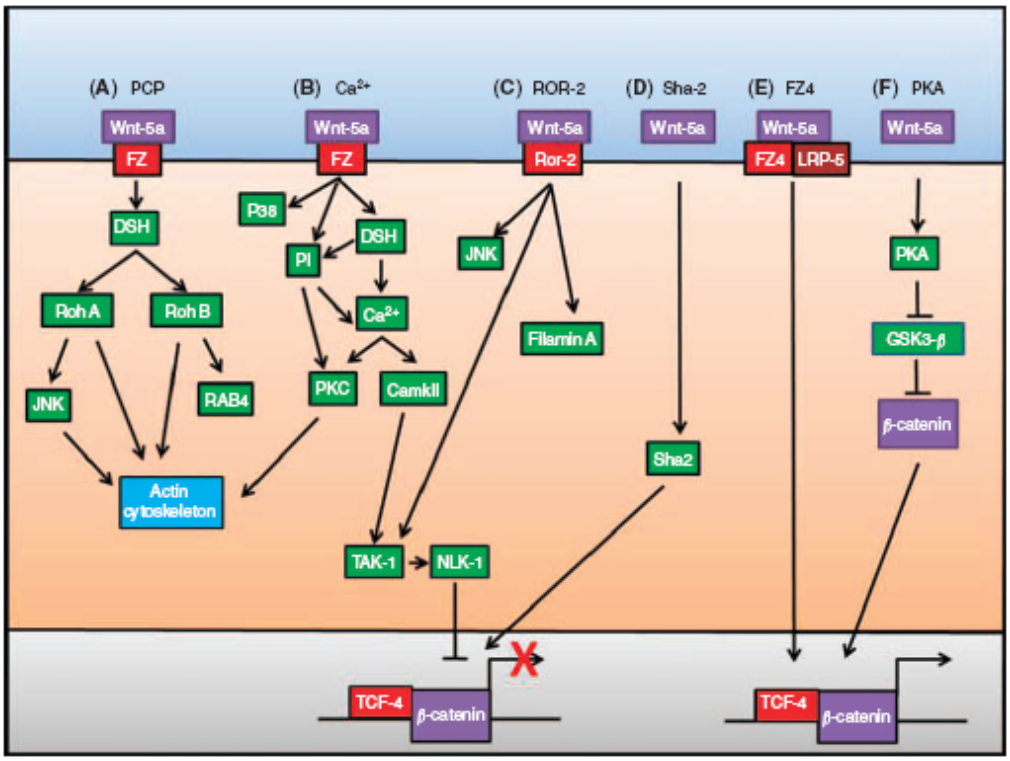

Figure 4 Overview of the Wnt5a signaling pathways.

The non-canonical Wnt pathways comprise various pathways that do not promote β-catenin activation. Wnt5a activates the planar cell polarity pathway (A) and Ca^{2+} signaling (B) both leading to cell movement. Wnt5a-mediated signaling was found to modulate the transcriptional activity of TCF4/β-catenin negatively (C and D) as well as positively (E and F). Source [93].

1.6 Protein microarrays

1.6.1 Platforms and applications

In the past, microarrays have been successfully established and applied for DNA-based research up to genome-wide approaches [97, 98]. Lots of efforts were required before consisting technologies and knowledge could be used to develop similar array-based tools for proteomic analysis. Nowadays protein microarrays comprise alternative tools for various purposes such as the detection of biomarkers [99], quantification of proteins in clinical samples [100] or the measurement of functionality and activity [101].

But, the design and generation of highly-specific protein profiling arrays depend on the availability of specific capture molecules [102, 103]. This is not a problem for microarrays involving nucleic acid molecules. Based on the primary sequence of the target DNA, specific DNA capture sequences can be determined according to the well-defined principle of complementary base pairing. In contrast, it is impossible to predict high-affinity capture

molecules for proteins from their primary amino acid sequence. This is due to the diverse tertiary structures of proteins and the manifold possibilities of interacting with each other. Protein interaction depends on a variety of molecular forces such as strong electrostatic forces, hydrogen bonds, hydrophobic or weak Van der Waals interactions but most often, all of the above in combination. Moreover, post-translational modifications such as glycosylation or phosphorylation impact on protein interactions and activity. Additionally, proteins often appear in complexes and simultaneously interact with different binding partners. All these factors combined necessitate that protein capture molecules must be generated individually and screened, not only for affinity, but also for specificity and cross-reactivity.

The basic principle of microarrays was published by Roger Ekins [104]. According to his ambient analyte theory, tiny amounts of capture molecule used in microarrays do not capture significant amounts of analyte in a sample, but bind the analyte in a ratio directly reflecting the concentration in the sample. This fact enables on the one hand quantification in a miniaturized format and on the other hand the multiplexed detection of several analytes in one sample.

According to their solid support, protein microarrays can be divided into planar and bead-based arrays (Figure 5) [106].

In the case of planar arrays (Figure 5, left), microspots of either capture molecules (forward phase array) or cell lysates (reversed phase array) are immobilized on slides as a surface to analyze many parameters in one sample (forward phase array) or to investigate one analyte in many spotted samples (reversed phase array). Bound analytes are visualized using target specific labeled detection antibodies. Printed in replicates, protein arrays enable the analysis of hundreds of parameters from tiny amounts of sample material in parallel.

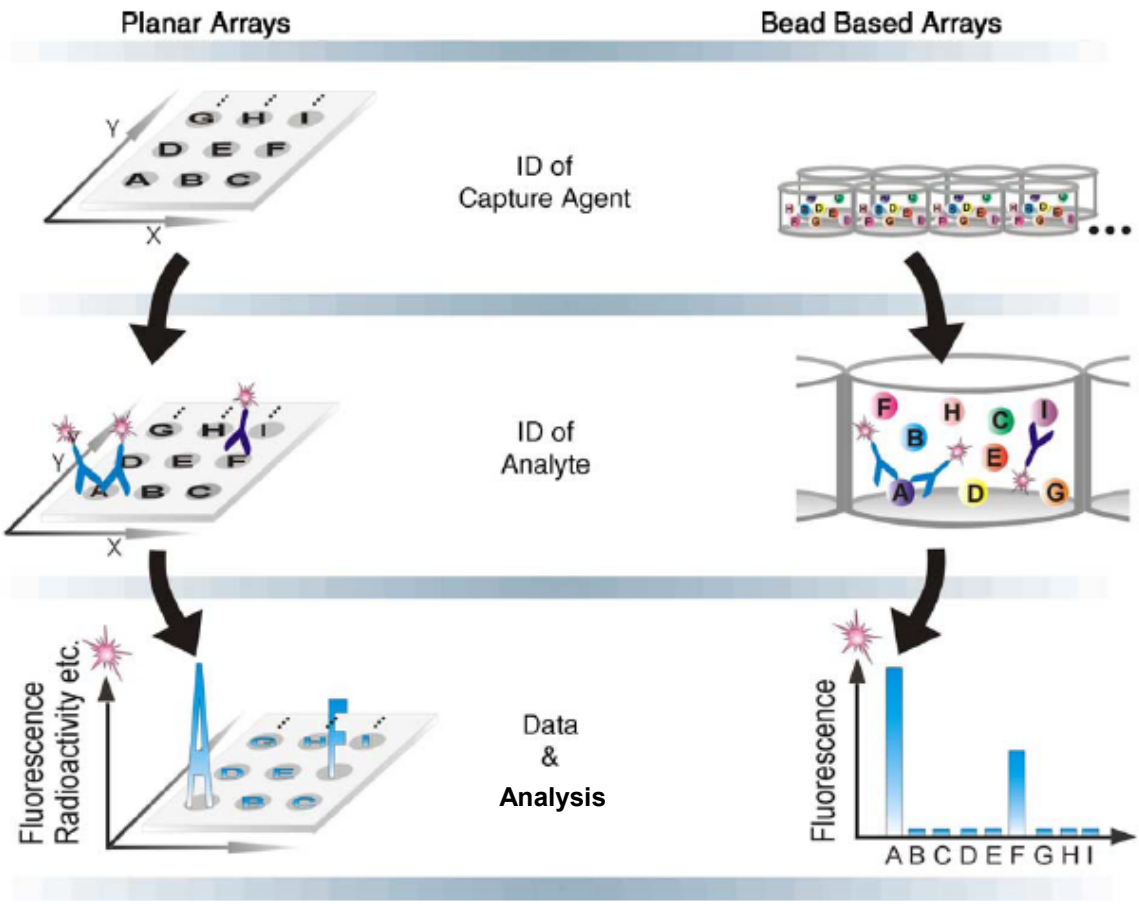

Figure 5 Overview planar and bead-based microarrays. Source: [106].

Bead-based microarrays - also called suspension bead arrays - rely on the usage of different, distinguishable populations of beads as a solid support for the capture molecules (Figure 5). Suspension bead arrays constitute a highly flexible platform for the measurement of up to 500 analytes in a multiplex manner. In principle, beads as the solid phase are distinguished by size or color using analyzers resembling flow cytometers (Luminex, Austin, TX, USA). Individual bead types are coated with specific capture molecules and are probed with sample material. Bound analytes are monitored using an analyte-specific fluorescently-labeled reporter detection system and are subsequently quantified on each individual bead (Figure 6). The most prominent bead-based assay format is the multiplexed sandwich immunoassay. In comparison to classical microtiter plate based ELISAs, sensitivity, accuracy and reliability of miniaturized and parallelized immunoassays are in a comparable range [107, 108].

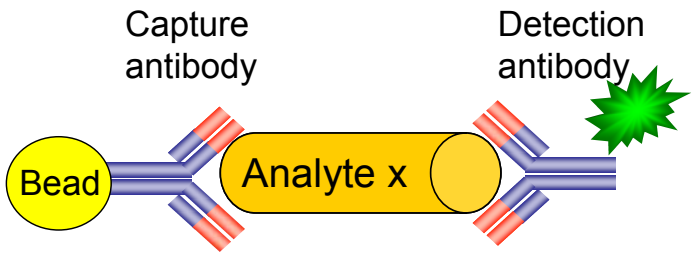

Figure 6 Sandwich immunoassay.

Bead-based sandwich immunoassays consist of a capture antibody immobilized on a bead as well as a detection antibody which is labeled with a reporter molecule.

1.6.2 Analytical tools for cell signaling studies

A basic prerequisite for the analysis of cell signaling on a network level is detailed knowledge of the principle components. Which molecules are involved? How are they activated? What is the method of choice to detect the transition between the active and inactive state? For the investigation of such fundamental biological questions, established biochemical methods such as Western blots for instance are routinely applied. But with increasing detailed knowledge about the analytes of interest, high throughput techniques are required to measure protein abundance, modification and complexation of the analytes of interest. Time-dependent studies in combination with different cellular states to be tested boost the number of data points dramatically thereby stressing the demand for techniques which allow high throughput experiments. Thus, protein microarrays are perfectly suited for the analysis of cell signaling. For instance, complex kinase signaling was recently addressed with several complementary approaches all using microarray technology: Nielsen et al. [109] studied dynamic receptor tyrosine kinase signaling using a planar antibody array, while Ciaccio et al. [110] described a microwestern array for a systems-level analysis of dynamic EGF receptor (EGFR) signaling and Du et al. [111] profiled 62 receptor tyrosine kinases with a bead-based approach.

1.7 Goal of doctoral thesis

The dynamic description of complex cellular communication processes requires accurate quantitative data sets comprising protein abundance, modification and activity as fundamental parameters for a mathematical modeling. It revealed time- and material-consuming for systematic analysis of pathway activity in different conditions and cell types when accomplishing such approaches with traditional methods such as quantitative Western blots, co-immunoprecipitation and reporter assays. As complementary methods, miniaturized

and parallelized ligand binding assays can be applied for the analysis of complex cell signaling processes.

In the liver, β-catenin Wnt signaling regulates regeneration, zonation, liver metabolism as well as oxidative stress and consists a crucial factor during development. On the molecular level, β-catenin plays multiple roles in the canonical Wnt signaling pathway and in cell-cell adhesion complexes. In addition, it is a proto-oncogene which plays - when mutated - a significant role in the genesis of colorectal, hepatocellular and other common cancers. Different functions of β-catenin as transcriptional co-activator or cell adhesion molecule are orchestrated by changes in concentration and phosphorylation as well as its ability to complex with proteins such as cadherins or transcription factors.

Detailed quantitative and time-resolved analysis of various forms of β-catenin is required to understand the dynamics of β-catenin-mediated signaling itself and moreover to decipher diverse signals impinging on β-catenin. Focusing on β-catenin-mediated signaling in primary mouse hepatocytes, data sets describing fundamental β-catenin signaling dynamics should be generated as a part of this thesis. The impact of growth factors beside canonical Wnt3a as well as small molecules perturbing the Wnt pathway should reveal potential crosstalk between β-catenin mediated signaling and surrounding cell signaling cascades.

For that purpose, the goal of this thesis was the development of a bead-based array using antibodies and bait proteins to study the phosphorylation status and function of β-catenin. This bead array panel should enable the investigation of dynamic effects of growth factors and chemical inhibitors on β-catenin´s abundance, function and posttranslational modification in cell cultures and primary mouse hepatocytes. Data from those experiments should support mathematical models to complement the current view of the Wnt pathway.

2 Materials and methods

2.1 Reagents and chemicals

Table 1 Reagents and chemicals

Name	**Distributor**
Acetic Acid	Fluka (Sigma-Aldrich), St. Louis, MO, USA
Ampicillin	Carl Roth, Karlsruhe, Germany
Bacto™ Tryptone	BD Biosciences, Franklin Lakes, NJ, USA
Bacto™ Yeast extract	BD Biosciences, Franklin Lakes, NJ, USA
Benzonase® Nuclease	Merck KGaA, Darmstadt, Germany
Blocking reagent for ELISA	Roche Diagnostics, Mannheim, Germany
BSA	Carl Roth, Karlsruhe, Germany
Complete Protease Inhibitor	Roche Diagnostics, Mannheim, Germany
Coomassie® Brilliant Blue R250	Serva, Heidelberg, Germany
DMEM	PAA Laboratories GmbH, Pasching, Austria
DC Protein Assay	BioRad, Hercules, CA, USA
DMSO	Sigma-Aldrich, St. Louis, MO, USA
Donkey serum	Sigma-Aldrich, St. Louis, MO, USA
ECL plus WB Detection System	Thermo Fisher Scientific, Waltham, MA, USA
EDC	Thermo Fisher Scientific, Waltham, MA, USA
Ethanol	Carl Roth, Karlsruhe, Germany
Foetal bovine serum	PAA Laboratories GmbH, Pasching, Austria
L-Glutamine	PAA Laboratories GmbH, Pasching, Austria
Glutathion	Sigma-Aldrich, St. Louis, MO, USA
Glycerol	Fluka (Sigma-Aldrich), St. Louis, MO, USA
Goat serum	Sigma-Aldrich, St. Louis, MO, USA

HCl	Carl Roth, Karlsruhe, Germany
IPTG	Carl Roth, Karlsruhe, Germany
Lysozyme	Biomol, Hamburg, Germany
Methanol	Merck KGaA, Darmstadt, Germany
NuPAGE® Antioxidant	Invitrogen, Carlsbad, CA, USA
NuPAGE® MOPS	Invitrogen, Carlsbad, CA, USA
NuPAGE® Transfer Buffer	Invitrogen, Carlsbad, CA, USA
Na_2HPO_4	Fluka (Sigma-Aldrich), St. Louis, MO, USA
NaCl	Carl Roth, Karlsruhe, Germany
NaN_3	Merck KGaA, Darmstadt, Germany
NaOH	Fluka (Sigma-Aldrich), St. Louis, MO, USA
PBS	PAA Laboratories GmbH, Pasching, Austria
Penicillin/Streptomycin	PAA Laboratories GmbH, Pasching, Austria
Phosphatase Inhibitor Cocktail	Sigma-Aldrich, St. Louis, MO, USA
Recombinant human Wnt3a	R&D Systems, Minneapolis, MN, USA
Recombinant mouse Wnt5a	R&D Systems, Minneapolis, MN, USA
SB216763	Sigma-Aldrich, St. Louis, MO, USA
SeeBlue® Plus2 Pre-Stained Standard	Invitrogen, Carlsbad, CA, USA
Sulfo-NHS	Thermo Fisher Scientific, Waltham, MA, USA
Tris	Sigma-Aldrich, St. Louis, MO, USA
Triton X-100	Sigma-Aldrich, St. Louis, MO, USA
Trypsin	PAA Laboratories GmbH, Pasching, Austria
Tween 20	Merck KGaA, Darmstadt, Germany

2.2 Buffers

Table 2 Buffers

Buffer	Component	Concentration
Activation buffer	Na_2HPO_4 pH 6.2	100 mM
Coupling buffer	MES pH 5.0	50 mM
Washing buffer	PBS pH 7.4	1x
	Tween 20	0.05%
Assay buffer	Blocking reagent for ELISA	1x
	Tris pH 7.4	50 mM
	NaCl	150 mM
	Gelatine	1%
Sample dilution buffer	NaCl	150 mM
	Tris pH 7.4	50 mM
	Triton X-100	1%
Washing buffer	PBS	1x
	Tween 20	0.1%
Cell culture medium	DMEM	1x
	L-Glutamine	2 mM
	Penicillin/Streptomycin	1%
	Foetal Bovine Serum	10%
Cell lysis buffer	NaCl	150 mM
	Tris pH 7.4	50 mM
	Triton X-100	1%
	Complete protease inhibitor	1x
	Phosphatase Inhibitor Cocktail 1, 2	1x
	Benzonase Nuclease	1x
IPN150 buffer	Tris pH 7.6	50 mM

	$MgCl_2$ NP-40 NaCl Na_3VO_4 NaF PMSF Phosphatase Inhibitor Cocktail 1, 2 Complete protease inhibitor	5 mM 1% 150 mM 0.1 mM 1 mM 1 mM 1x 1x
LDS-Page running buffer	NuPAGE MOPS	1x
Coomassie staining solution	Coomassie Brilliant Blue R250 Methanol Acetic Acid	0.2% 50% 10%
Destaining solution I	Ethanol Acetic Acid	50% 10%
Destaining solution II	Ethanol Acetic Acid	10% 5%
Transfer buffer	NuPAGE Transfer Buffer Antioxidant Methanol	1x 0.1% 10%
Ponceau staining solution	Ponceau-S Acetic Acid	0.1% (w/v) 1%
TBST	NaCl Tris pH 7.4 Tween 20	150 mM 20 mM 0.05%

2.3 Antibodies

Table 3 List of antibodies

Specificity	Distributor	Species	Label	Used as
Total β-catenin	R&D systems	gt		Capture
E-cadherin	R&D systems	gt		Capture
C-terminal β-catenin	BD Biosciences	ms		Detector
GST	GE Healthcare	gt		Capture
Total β-catenin	Invitrogen	rbt		Detector
pS33/pS37/pT41 β-catenin	Cell signaling technology	rbt		Capture
pS45 β-catenin	Cell signaling technology	rbt		Capture
pS552 β-catenin	Cell signaling technology	rbt		Capture
pS675 β-catenin	Cell signaling technology	rbt		Capture
Rabbit IgG (H+L)	Jackson ImmunoResearch Inc.	dky		Capture
Mouse IgG (H+L)	Jackson ImmunoResearch Inc.	gt	R-PE	Reporter
Rabbit IgG (H+L)	Jackson ImmunoResearch Inc	dky	R-PE	Reporter
Rabbit IgG (H+L)	Jackson ImmunoResearch Inc.	gt	HRP	Reporter
Mouse IgG (H+L)	Jackson ImmunoResearch Inc.	gt	HRP	Reporter

2.4 Consumables

Table 4 List of consumables

Consumables	**Company**
1.5 mL reaction tubes	Vetter Laborbedarf, Ammerbuch, Germany
1.5 mL reaction tubes	Starlab, Ahrensburg, Germany
PCR tubes	Biozyme Scientific, Oldendorf, Germany
Pipetting tips	Mettler-Toledo, Gießen, Germany Starlab, Ahrensburg, Germany Biozyme Scientific, Oldendorf, Germany
96-well PCR plate	Brand, Wertheim, Germany
96-well microplate, round bottom	Greiner Bio-One, Frickenhausen, Germany
96-well microplate, half area flat bottom, non-binding surface	Corning, New York, NY, USA
96-well filter plate	Millipore, Billerica, MA, USA
96-well microplate, half area flat bottom	Corning, New York, NY, USA
Microplate Assay Sealing Film	Thermo Fisher Scientific, Waltham, MA, USA
MagPlex™ -C Microspheres	Luminex, Austin, Texas, USA
GST Hitrap FF 1mL	GE Healthcare, Uppsala, Sweden
Reagent reservoir, sterile	Brand, Wertheim, Germany
Cell culture dish 10 cm	Greiner Bio-One, Frickenhausen, Germany
Cell culture flask T75 and T175	Greiner Bio-One, Frickenhausen, Germany
24-well cell culture plate	Corning, New York, NY, USA
96-well cell culture plate	Greiner Bio-One, Frickenhausen, Germany
Needle 18 G x 1½″	Carl Roth, Karlsruhe, Germany
Single-use syringe Omnifix, 10 mL	Braun Melsungen, Melsungen, Germany
Serological pipettes Costar	Corning, New York, NY, USA
Cell strainer	BD Biosciences, Franklin Lakes, NJ, USA

Nitrocellulose transfer membrane	Schleicher & Schuell Bioscience, Dassel, Germany
Whatman gel blotting paper	Schleicher & Schuell Bioscience, Dassel, Germany
4-12% Bis Tris NuPAGE Gel	Invitrogen, Carlsbad, CA, USA

2.5 Devices and programs

Table 5 List of devices and programs

Device and Software	**Company**
Äkta FPLC	GE Healthcare, Uppsala, Sweden
Balance Explorer	Ohaus, Pine Brook, NJ, USA
Biophotometer	Eppendorf, Hamburg, Germany
Cell Counter & Analyzer Casy TT	Innovatis AG, Reutlingen, Germany
Cell culture incubator	Binder, Tuttlingen, Germany
Centrifuge C5415D, 5417R, 5810	Eppendorf, Hamburg, Germany
Centrifuge Universal 25	Hettich, Tuttlingen, Germany
C25 Incubator Shaker	New Brunswick Scientific, Edison, NY, USA
Digital Science Image Station 440F Software Kodak digital science V 3.0	Kodak, Rochester, NY, USA
FLUOstar Optima FLUOstar Optima Software 1.32 R2	BMG Labtechnologies, Offenburg, Germany
GeneAmp PCR System 2400	Applied Biosystems, Foster City, USA
GFL water bath	Gesellschaft für Labortechnik GmbH, Burgwedel, Germany
KingFisher 96	Thermo Fisher Scientific, Waltham, MA, USA
Laminar flow	BDK GmbH, Sonnenbühl-Genkingen, Germany

Luminex 100 Software X-Ponent Software Solutions IS 2.2	Luminex, Austin, TX, USA
Magnetic separator	Invitrogen, Carlsbad, CA, USA
Multichannel pipette	Eppendorf, Hamburg, Germany
Multichannel adapter, Vacuboy	INTEGRA Biosciences, Fernwald, Germany
pH meter 766	Knick, Berlin, Germany
Pipetus®	Hirschmann Laborgeräte, Eberstadt, Germany
Pipettors	Gilson, Middleton, WI, USA
Power Ease 500	Invitrogen, Carlsbad, CA, USA
Rotating mixer RM5	Glaswarenfabrik Karl Hecht, Sondheim, Germany
Sonification bath Sonorex	Bandelin Electronics, Berlin, Germany
Thermo Mixer Comfort	Eppendorf, Hamburg, Germany
Vacuum manifold	Milipore, Billerica, MA, USA
Vortex Genie 2	Scientific Industries, Bohemia, NY, USA
XCell II Blot Module	Invitrogen, Carlsbad, CA, USA
XCell SureLock Mini-Cell	Invitrogen, Carlsbad, CA, USA

2.6 Bacteria strains, plasmids and recombinant proteins

Table 6 Bacteria strains, plasmids and recombinant proteins

***E.coli* strain**	**Plasmid**	**Provided by**	**Protein**	**Protein [kDa]**
BL21 DE3	pGEX-ECT	A. Hecht [55]	GST-ECT	46
TOP10F’	pGEX-TCF4	A. Hecht	GST-TCF 4	34
BL21 DE3	pGEX-β-catenin	R. Kemmler [112]	GST-β-catenin	114

2.7 Suspension bead array

2.7.1 Covalent immobilization of proteins to beads

Capture antibodies for β-catenin (R&D Systems, Minneapolis, MN, USA or BD Biosciences, Franklin Lakes, NJ, USA), E-cadherin (R&D Systems, Minneapolis, MN, USA), GST (GE Healthcare, Uppsala, Sweden) and species-specific anti rabbit antibodies (Jackson ImmunoResearch, West Grove, PE, USA) were covalently immobilized on different carboxylated magnetic beads (Luminex Corp., Austin, TX, USA) according to the manufacturer's protocol.

200 µL of each bead set (2.5 x 10^6 beads) were pelleted using a magnetic separator (Invitrogen, Carlsbad, CA, USA) and the supernatant was removed. The beads were washed twice with Na_2HPO_4 (Merck KGaA, Darmstadt, Germany) solution, 0.1 M, pH 6.2 (activation buffer) and resuspended in 80 µL of activation buffer. Solutions (50 mg/mL) of N-hydroxysulfosuccinimide sodium salt (Sulfo-NHS; Thermo Fisher Scientific, Waltham, MA, USA) and 1-ethyl-3-(3-dimethylaminopropyl) carbodiimide hydrochloride (EDC; Thermo Fisher Scientific, Waltham, MA, USA) were prepared in activation buffer and 10 µL of each solution was added to each tube. Activation was carried out at RT in the dark under rotation. After 20 min the beads were washed with 500 µL of 50 mM MES (Sigma-Aldrich, St. Louis, MO, USA) pH 5.0 (coupling buffer) followed by the addition of 250 µL protein solution (80-100 µg/mL) prepared in coupling buffer. The beads were vortexed and incubated at room temperature in the dark for at least 2 h under rotation. The beads were washed in 0.5 mL 0.1% Tween 20 (Merck KGaA, Darmstadt, Germany) in PBS pH 7.4 and then resuspended in 100 µL blocking reagent for ELISA (Roche Diagnostics, Mannheim, Germany) containing 0.05% NaN_3 (w/v). Coated beads were stored in the dark at 2-8°C.

2.7.2 Non-covalent immobilization of proteins to beads

Each of the phospho-specific β-catenin antibodies (2.3) was incubated separately with a defined number of beads coated with anti-rabbit antibody (2.5 µL antibody for 1x 10^5 beads) and 50 µL PBS for 4 h at room temperature under rotation. Each of the GST-tagged bait proteins (1 µg of each protein for 1x 10^5 beads) was incubated in 50 µL PBS for 6 h at room temperature under rotation with different bead populations coated with anti-GST antibody (2.3). The beads were washed three times with 200 µL PBS using a magnetic separator (Invitrogen, Carlsbad, CA, USA) and resuspended in 100 µL assay buffer (Blocking reagent for ELISA, Roche Diagnostics, Mannheim, Germany).

2.7.3 β-catenin bead array

25 or 50 µg protein extracts were adjusted to a volume of 40 µL using sample dilution buffer, while the beads (directly or indirectly coated with capture proteins) were diluted in assay buffer (Blocking reagent for ELISA, Roche Diagnostics, Mannheim, Germany). Protein extracts were incubated with 20 µL of beads (2,000 per set/well) overnight at 4°C in a 96-well microtiter plate (non-binding surface, Corning, New York, NY, USA). The incubation was performed in a thermo mixer (Eppendorf, Hamburg, Germany) at 750 rpm. The assays were then transferred from the microtiter plate to a pre-incubated PCR plate (Brand, Wertheim, Germany). The following steps were all carried out on a semi-automated platform (KingFisher 96, Thermo Fisher Scientific, Waltham, MA, USA) with magnetic rods that move the sample particles through the various steps. A protocol for magnetic particle-based methods was established using the associated KingFisher software. The required solutions were pipetted onto PCR plates (50-100 µL/well) before the protocol was started. The detection antibody and the secondary antibody were diluted with assay buffer containing 0.1% Tween 20 (Merck KGaA, Darmstadt, Germany) in the concentration as described below.

The beads were transferred from the incubation plate to a wash plate containing 100 µL/well PBS 0.1% Tween 20 (Merck KGaA, Darmstadt, Germany). The beads were washed twice after each of the following steps. 50 µL of β-catenin-specific antibody (1 µg/mL, BD Biosciences, Franklin Lakes, NJ, USA) were incubated with the beads for 1 h at RT before goat anti-mouse phycoerythrin-conjugated antibody (2.5 µg/mL, Jackson ImmunoResearch, West Grove, PE, USA) containing 1% donkey serum (Sigma-Aldrich, St. Louis, MO, USA) and 1% goat serum (Sigma-Aldrich, St. Louis, MO, USA) was added and applied for 45 min at RT. After the final washing step, the beads were transferred into 100 µL assay buffer containing 0.1% Tween 20 and analyzed with a Luminex 100 IS system (Luminex Corp, Austin, TX, USA). Mean fluorescence intensities of at least 100 beads per assay were recorded for each sample. Standard deviation was calculated based on biological triplicates for the time course experiments. For calculation of intra- and inter-assay variation 4 technical replicates performed on the same day or 4 technical replicates performed on 4 different days were used.

2.7.4 β-catenin sandwich immunoassay

Antibodies specific for C-terminal β-catenin (BD Biosciences, Franklin Lakes, NJ, USA) and total β-catenin (Invitrogen, Carlsbad, CA, USA) were used as bead-bound capture antibody or detection antibody, respectively. 20 µL of beads (2,000 per well) were incubated with protein lysates or GST-β-catenin overnight at 4°C in a 96-well microtiter plate (non-binding

surface, Corning, New York, NY, USA) in a thermo mixer (Eppendorf, Hamburg, Germany) at 750 rpm. The assays were transferred to a blocked filter plate (Millipore, Billerica, MA, USA) and washed twice with PBS using a vacuum manifold (Millipore, Billerica, MA, USA). For the detection, 30 µL anti total β-catenin (Invitrogen, Carlsbad, CA, USA, 1:200 diluted with assay buffer) were added to the beads for 60 min at RT under rotation. Then 30 µL of 2.5 µg/mL donkey anti rabbit phycoerythrin-conjugated antibody dilution (Jackson ImmunoResearch, West Grove, PE, USA) were added for 45 min at RT. Each incubation step was finished with the removal of unbound antibody by washing with PBS as described above. Finally, beads were resuspended in 100 µL assay buffer and analyzed with a Luminex 100 IS system (Luminex Corp, Austin, TX, USA). Antibodies and beads were diluted in assay buffer, GST-β-catenin and samples were diluted in cell lysis buffer.

2.8 Molecular biological methods

2.8.1 Expression and purification of GST-ECT and GST-TCF4

The expression vector for the cytoplasmic tail of E-cadherin (GST-ECT) was previously described [68, 112, 113]. The GST-TCF4 fusion protein contains amino acids 1-80 from human TCF4. The fusion protein was prepared by inserting a cDNA fragment derived from pCS2+TCF4 [114] into the EcoRI and NotI restriction sites of pGEX2TK (GE Healthcare, Uppsala, Sweden). GST fusion proteins were expressed in *E.coli* BL21 or Top10F' cells and purified on glutathione sepharose as described previously [112]. Vectors and recombinant proteins were kindly provided by A. Hecht.

2.8.2 Expression and purification of GST-β-catenin

The construction of a full-length β-catenin expression construct pGEX-β-catenin was described by Aberle et al. [112] and provided kindly by R. Kemmler. Protocols of plasmid purification, amplification and transfection were depicted in [115].

E.coli BL21 cells (DE3) were cultured in autoclaved LB-medium (100 µg/mL Ampicillin, Carl Roth, Karlsruhe, Germany) at 30°C until they reached an optical density of 0.6 OD (λ 600 nm, Biophotometer Eppendorf, Hamburg, Germany). The overexpression of GST-β-catenin was induced by adding Isopropyl-β-D Thiogalactopyranosid (1 mM total concentration, Carl Roth, Karlsruhe, Germany) for 4 h. Cells were harvested by centrifugation (4000xg, 5 min, 4°C, 5810 Centrifuge Eppendorf, Hamburg, Germany). After removal of the supernatant the pellets were snapfrozen and stored at -70°C. Each pellet was lysed for 20 min at RT by adding 1 mg lysozyme (Biomol, Hamburg, Germany) and 1x Complete protease inhibitor (Roche Diagnotics, Mannheim, Germany) contained in a 10 fold pellet volume of PBS. The

lysate was first sonicated for several 10 s intervals (Ultrasonic Sonotex RK 31, Bandelin, Berlin, Germany). Subsequently Triton X-100 (Merck KGaA, Darmstadt, Germany) was added (final concentration 1%) and incubated for 20 min on ice. After centrifugation (10,000xg, 30 min, 4°C, 5810 Centrifuge Eppendorf, Hamburg, Germany) the supernatant was transferred for storage (-70°C).

GST-β-catenin was affinity-purified using an Äkta FPLC (GE Healthcare, Uppsala, Sweden) with a GST Hitrap FF 1 mL (GE Healthcare, Uppsala, Sweden) column. GST-β-catenin was eluted with 50 mM Tris HCl pH 8.5 containing 10 mM Glutathione (dissolved immediately before usage, Invitrogen, Carlsbad, CA, USA). NaCl (Merck KGaA, Darmstadt, Germany) was added to fractions containing eluted target protein (final concentration 150 mM NaCl). PBS was used for washing and equilibration of the column. Protein concentrations were determined using a photometer (Eppendorf, Hamburg, Germany).

2.9 Cell culture methods

2.9.1 Cell lines

Table 7 List of cell lines

Cell line	**source**	**Protein expression β-catenin**
HepG2	ATCC # HB-8065	Deletion aa 25-140 (increased) WT (low) [86]
FOCUS	P. Sorger, Harvard Medical School	normal
HEK293	ATCC # CRL-1573	normal

Human 293 embryonic kidney (HEK293) (ATCC # CRL-1573, [116]), FOCUS (kindly provided by P. Sorger, [117]) and HepG2 (ATCC # HB-8065, [118-120]) cells were cultured in DMEM (PAA Laboratories GmbH, Pasching, Austria) containing 2 mM L-glutamine (PAA Laboratories GmbH, Pasching, Austria), 1% penicillin/streptomycin (PAA Laboratories GmbH, Pasching, Austria) and 10% foetal bovine serum (PAA Laboratories GmbH, Pasching, Austria) at 37°C and 5% CO_2.

For subculturing, medium was aspirated and cells were rinsed with sterile PBS. 1 mL of Trypsin (PAA Laboratories GmbH, Pasching, Austria) was added to each T75 flask or to

each 10 cm cell culture dish. After incubation for 1-3 minutes at 37°C in the incubator, 9 mL medium were added to stop the dissociation. FOCUS and HEK293 cells were resuspended, diluted and plated as required. HepG2 needed to be separated carefully using a 10 mL syringe (BD Biosciences, Franklin Lakes, NJ, USA) and needle (Carl Roth, Karlsruhe, Germany, 18 G x 1 1/2 in.). Cell suspension was filtered using a cell strainer (BD Biosciences, Franklin Lakes, NJ, USA) to remove remaining cell clusters. Trypsinized cells were counted using with a particle counter (Casy TT, Innovatis AG, Reutlingen, Germany).

For the time-course experiments, cells were plated on 24-well plates, starved in serum-free medium for 24 h prior to the experiment and then treated with 200 ng/mL recombinant human Wnt3a (R&D Systems, Minneapolis, MN, USA), 200 ng/mL recombinant mouse Wnt5a (R&D Systems, Minneapolis, MN, USA) or 20 µM GSK-3 inhibitor SB216763 (Sigma-Aldrich, St. Louis, MO, USA). The perturbation steps were performed gradually to enable the lysis of all wells at the same time point.

Additionally, the cell culture protocol was adapted to the 96-well cell culture format. 2x 10^4 beads HepG2 cells or 1x 10^4 cells of FOCUS were plated on 96-well plate (Greiner Bio-One, Frickenhausen, Germany), starved for 24 h with serum-free medium and treated gradually with 200 ng/mL rWnt3a or 200 ng/mL rWnt5a. Liquid was removed using a multichannel adapter Vacuboy (INTEGRA Biosciences, Fernwald, Germany). Reagents for treatment were diluted to the concentration used in the experiment in serum-free medium before the treatment and added with a multichannel pipette (Eppendorf, Hamburg, Germany). Cell-free wells of the 96-well plate were blocked in parallel with medium during the cell culture experiment.

2.9.2 Primary mouse hepatocytes

Primary mouse hepatocytes were isolated and cultured at the Universitätsklinikum Freiburg according to the Hepatosys standard protocol [121]. Cell culture experiments were performed and the corresponding cell lysates were prepared by the group of Prof. A. Hecht, Institute of Molecular Medicine and Cell Research, University of Freiburg. Primary mouse hepatocytes were treated with either 200 ng/mL recombinant Wnt3a (R&D Systems, Minneapolis, MN, USA)) or 80 µM GSK-3 inhibitor SB216763 (Sigma-Aldrich, St. Louis, MO, USA).

2.9.3 TCF reporter assay

For the validation of the β-catenin bead array panel, reporter assays were performed in the lab of Prof. A. Hecht. Human 293 embryonic kidney (HEK293) cells (ATCC # CRL-1573) were cultured as previously described [114]. Reporter gene experiments involved 1 x 10^5 cells per well (24-well plates). The cells were transfected with 100 ng of the TOP-flash

reporter [122] and 20 ng of the *Renilla* luciferase expression vector pRL-TK (Promega, Madison, WI, USA) for normalization purposes using the FuGENE6 (Roche Diagnostics, Mannheim, Germany) reagent [123]. Luciferase activities were determined 48 h after transfection [123].

2.10 Biochemical methods

2.10.1 Sample preparation for the β-catenin bead array panel

For this purpose, the cells were rinsed twice with PBS after the treatment and then lysed using 100 µL (for each well of a 24-well plate), 1 mL (for each 10 cm dish) or 50 µL (for each well of a 96-well plate) of cell lysis buffer for 30 min at 4°C under shaking. Cell debris was removed by centrifugation at 15,000xg at 4°C for 30 minutes. The total protein concentration was determined as described in 2.10.2. The samples were stored at -70°C until analysis was performed.

Regarding the protocol for a 96-well cell culture experiment, the samples were directly used for analysis without centrifugation or protein quantification after lysis. Here, the prepared beads (2000 per set/well) were directly added to the cell lysates or controls in the cell culture plate, respectively, and incubated overnight at 4°C under rotation (750 rpm). Then, the assays were manually transferred to a pre-blocked PCR plate and processed as described before (2.7.3).

2.10.2 Protein quantification

Total protein concentrations were determined using the DC Protein Assay (BioRad Laboratories, Hercules, CA, USA) which is a colorimetric assay for protein determination similar to the well-documented Lowry assay [124]. The assay was performed according to the manufacturer's protocol. For the standard dilution series BSA (Thermo Fisher Scientific, Waltham, MA, USA) was diluted in the appropriate lysis buffer. The absorption was read out at 650 nm on an ELISA reader (FLUOstar Optima, BMG Labtechnologies, Offenburg, Germany).

2.10.3 β-catenin fishing (GST-pulldown)

For the validation of the suspension bead array, protein extracts were prepared by lyzing the cells in ice-cold IPN150 buffer for 30 min on ice with occasional mixing. After cell lysis, the samples were centrifuged at 20,000xg for 10 min and the protein concentration of cleared supernatant was determined (2.10.2). For affinity purification of free β-catenin, 2 µg GST-ECT, 5 µL bed volume of glutathione sepharose beads (already washed with PBS and

equilibrated with sample dilution buffer) and cell lysates with a protein content of 350 µg were combined [125]. The total volume was adjusted to 500 µL. GSH-beads and lysates were incubated over night at 4°C under rotation (Thermomixer, Eppendorff, Hamburg, Germany). Then, beads were washed 3 times with 1 mL of cell lysis buffer and centrifuged at 500xg for 5 min. The supernatant was removed and the beads were resuspended in 25 µL 4x LDS sample buffer (Invitrogen, Carlsbad, CA, USA). After 5 min at 95°C (GeneAmp PCR System 2400, Applied Biosystems, Foster City, USA), beads were centrifuged for 3 min at 15,000xg. The supernatant war stored for further analysis by Western blotting.

2.10.4 LDS-Polyacrylamide gel electrophoresis

In a PCR tube (Biozyme Scientific, Oldendorf, Germany) a defined amount of protein lysate was mixed with 2 µL of 10x Reducing Reagent (Invitrogen, Carlsbad, CA, USA), with 5 µL of 4x LDS sample buffer (Invitrogen, Carlsbad, CA, USA) and with x µL water ending with a total volume of 20 µL. The samples were denaturated for 10 min at 95°C, cooled down to 4°C (GeneAmp PCR System 2400, Applied Biosystems, Foster City, USA) and loaded on a pre-cast Nupage 4-12% Bis/Tris Gel (Invitrogen, Carlsbad, CA, USA). In principal, LDS denaturated proteins possess identical charge per unit mass resulting in fractionation by size. The elecrophoresis was run in an XCell SureLock MiniCell (Invitrogen, Carlsbad, CA, USA) for 50 min under a voltage of 200 V using Nupage MOPS Running Buffer containing 500 µL Nupage Antioxidant (Invitrogen, Carlsbad, CA, USA).

2.10.5 Coomassie staining

Electrophoretically separated proteins were visualized by staining with Coomassie staining solution for 1 h at RT under rotation. Excessive staining solution was removed by washing the gel for 1 h with destaining solution I followed by an overnight washing step in destaining solution II. The gel was photographed using Kodak photo imager (Kodak, Rochester, NY, USA).

2.10.6 Western blot

Proteins were transferred from the gel onto a nitrocellulose membrane using Nupage blotting system (Invitrogen, Carlsbad, CA, USA) with the following parameters: 75 min transfer time at 160 mA and 25 V. The membrane was incubated with Ponceau staining solution to control the transfer. For the detection of specific proteins, the membrane was first blocked with 3% BSA in TBST and then incubated over night at 4°C under rotation with a primary antibody (diluted in TBST containing 1% BSA). The unbound antibody was removed by 3 times washing with TBST. The appropriate species-specific HRP-labeled secondary antibody

(diluted in TBST containing 1% BSA) was applied for 60 min followed by a repetition of the washing step. Finally, 4 mL of freshly mixed ECL Plus Western Blot detection System (Thermo Fisher Scientific, Waltham, MA, USA) was added for 5 min. The chemiluminescence signal was visualized by the Kodak photo imager (Kodak, Rochester, NY, USA).

3 Results

3.1 β-catenin bead array panel

3.1.1 Assay development - β-catenin bead array panel

For the monitoring of different β-catenin characteristics, a suspension bead array panel was developed. Here, for the first time three biochemical methods – sandwich immunoassay, co-immunoprecipitation and protein-protein interaction assay – were combined in a suspension bead array panel. Figure 7 summarizes for all of the targeted forms of β-catenin their cellular function as well as the appropriate assay set up. Sandwich immunoassays targeting N-terminally phosphorylated β-catenin as well as the miniaturized co-immuniprecipitation were developed and described in Poetz 2005 [115]. The miniaturized GST-pulldown as well as the sandwich immunoassays specific for pan- and C-terminally phosphorylated β-catenin were developed within this thesis.

Function	**Pathway regulation**	**Transcription co-factor**	**Cell adhesion**
Status	phosphorylated	transcriptionally active “free”	complexed by cadherins
Assay system Multiplex	sandwich immunoassay 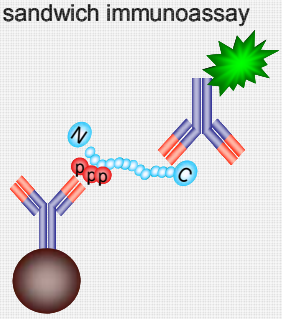	protein-protein interaction assay 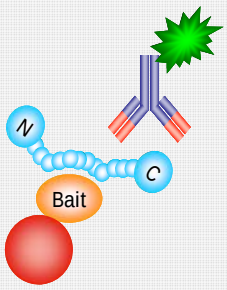	µco-immunoprecipitation 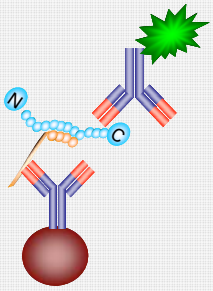
Capture molecule	anti-β-catenin anti-phospho β-catenin • pS33/pS37/pT41 • pS45 • pS675 • pS552	GST-TCF4 GST-ECT	anti-E-cadherin
Detector molecule	anti-β-catenin (C-term)		

Figure 7 Overview β-catenin bead array panel.

The figure summarizes biological function, localization and posttranslational modification of the different investigated forms of β-catenin. For each function and form of β-catenin the appropriate miniaturized assay set up is shown. The β-catenin bead array panel combines 5 sandwich immunoassays, 2 GST-pulldown assays and a co-immunoprecipitation in a miniaturized format.

First, 5 different sandwich immunoassays were built for the detection of total and several phosphorylated β-catenin forms. One antibody pan-specific for β-catenin and antibodies specific for different β-catenin phosphorylation sites including the pS33/pS37/pT41 and pS45 residues at the N-terminus as well as pS675 and pS552 at the C-terminus of β-catenin were used as capture molecules to determine the total and modified β-catenin levels (Figure 7).

For the detection of the E-cadherin/β-catenin complex, a co-immunoprecipitation protocol was adapted to the miniaturized, bead-based assay format [126]. Here, an E-cadherin-specific antibody was used to capture the E-cadherin/β-catenin complex localized at the membrane (Figure 7).

Beside total, phosphorylated and complexed fractions of β-catenin, it is necessarily required to quantitate a biologically active form of β-catenin. During the activation of the Wnt pathway, β-catenin accumulates in the cytosol and translocates in the nucleus functioning as a transcription co-factor. This transcriptionally active form of β-catenin is unbound and termed “free β-catenin” below. For the detection of free β-catenin a miniaturized protein-protein interaction assay was developed following previously proposed pulldown assays [41, 55]. This µ-fishing enables the measurement of free cytosolic β-catenin which reflects the activated status of the canonical Wnt pathway. Recombinantly expressed binding partners - E-cadherin cytosolic tail (ECT) and TCF4 - were used as capture molecules (bait) for the analysis of free β-catenin (prey) (Figure 7).

The above described assays were parallelized and combined within one bead array panel. In Figure 8 the established workflow is shown. Pan- and phospho-specific antibodies and recombinant ECT and TCF4 were immobilized on different color-coded beads (Luminex Corp., Austin, TX). Magnetic beads were used to take advantage of a magnetic bead handler which allows processing of the bead array in a semi-automated manner. Cell culture experiments were performed as described (Figure 8, step 1). The mixed beads were incubated in cell lysates either in assay plates or directly in 96-well cell culture plates (Figure 8, step 2). All washing and transfer steps during incubation and detection were performed on the kingfisher system (Thermo Fisher Scientific, Waltham, MA, USA). Captured analytes were visualized in a Luminex 100 system (Luminex Corp., Austin, TX) using a β-catenin-specific detection antibody and a fluorescently labeled reporter molecule (Figure 8, step 3 and 4).

In summary, the established cell culture and bead array protocols allow sample preparing and processing as well as data gaining of 96 independent cell culture experiments within 2 days only. The protocol enables for the first time the simultaneous analysis of protein abundance, phosphorylation, complexation as well as activity of β-catenin in 96 samples for instance.

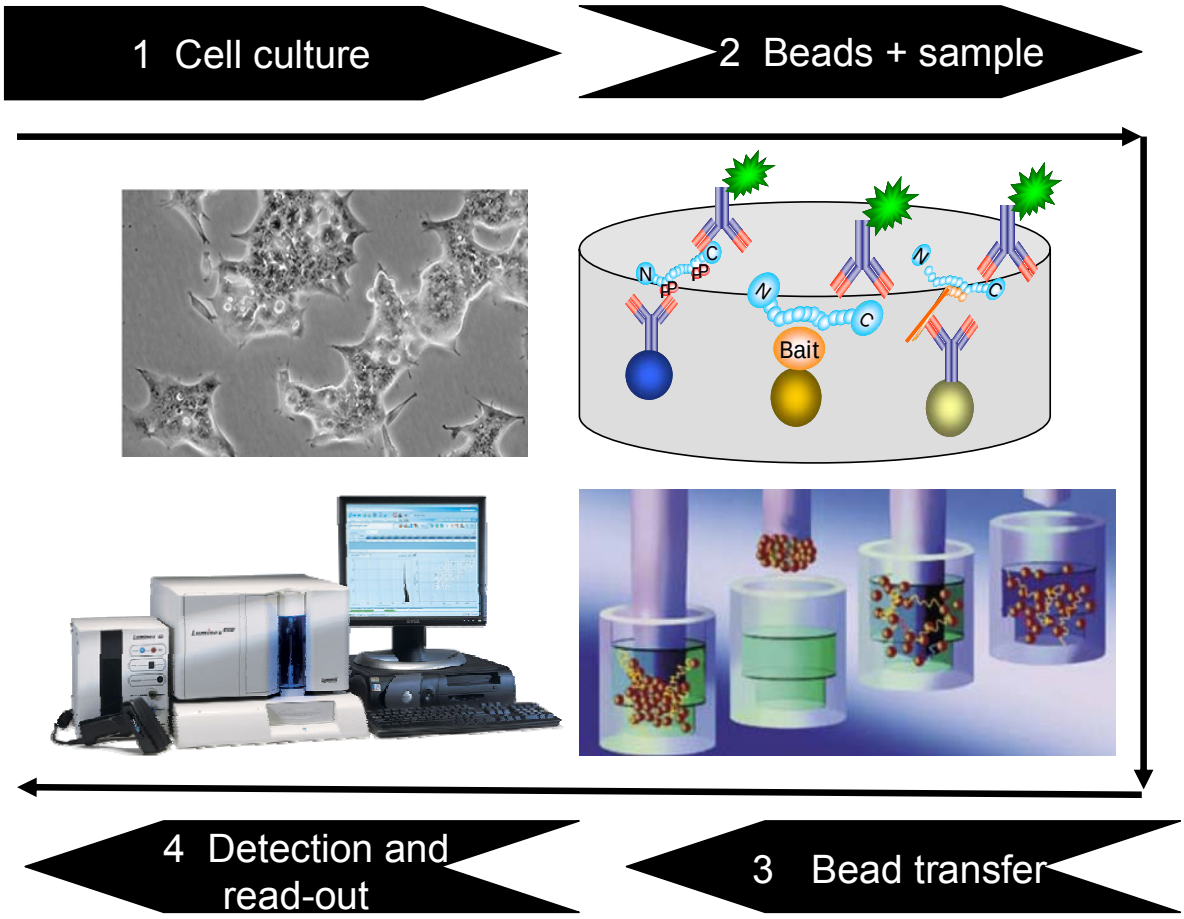

Figure 8 Workflow of the analysis of β-catenin using the β-catenin bead array panel.

Cells (here HEK293) are stimulated, collected and subsequently lysed for analysis (step 1). Cell lysates and mixed bead populations are incubated in a microtiter plate over night (step 2). The color-coded magnetic beads are transferred from the incubation plate to the assay plate. All detection and washing steps are performed in a semi-automated manner (step 3). Captured analytes are read out using a Luminex 100 system (step 4). Source: www.atcc.com (1), www.thermo.com (3) and www.luminexcorp.com (4).

In order to demonstrate the capability of the β-catenin bead array panel for the detailed analysis of the different forms of β-catenin, HEK293 cells and primary mouse hepatocytes were treated with Wnt pathway-activating components for 3 h: recombinant Wnt3a (rWnt3a) was used to activate the pathway *via* the Wnt receptor and a GSK-3 inhibitor (SB216763) [127] was used to induce the accumulation of free β-catenin at the level of the destruction complex. Both samples sets were kindly provided by Prof. A. Hecht, University of Freiburg. Each cell culture experiment was performed in biological triplicates. 25 µg of differently treated cell lysates were analyzed for the different functions of β-catenin using the described β-catenin bead array panel.

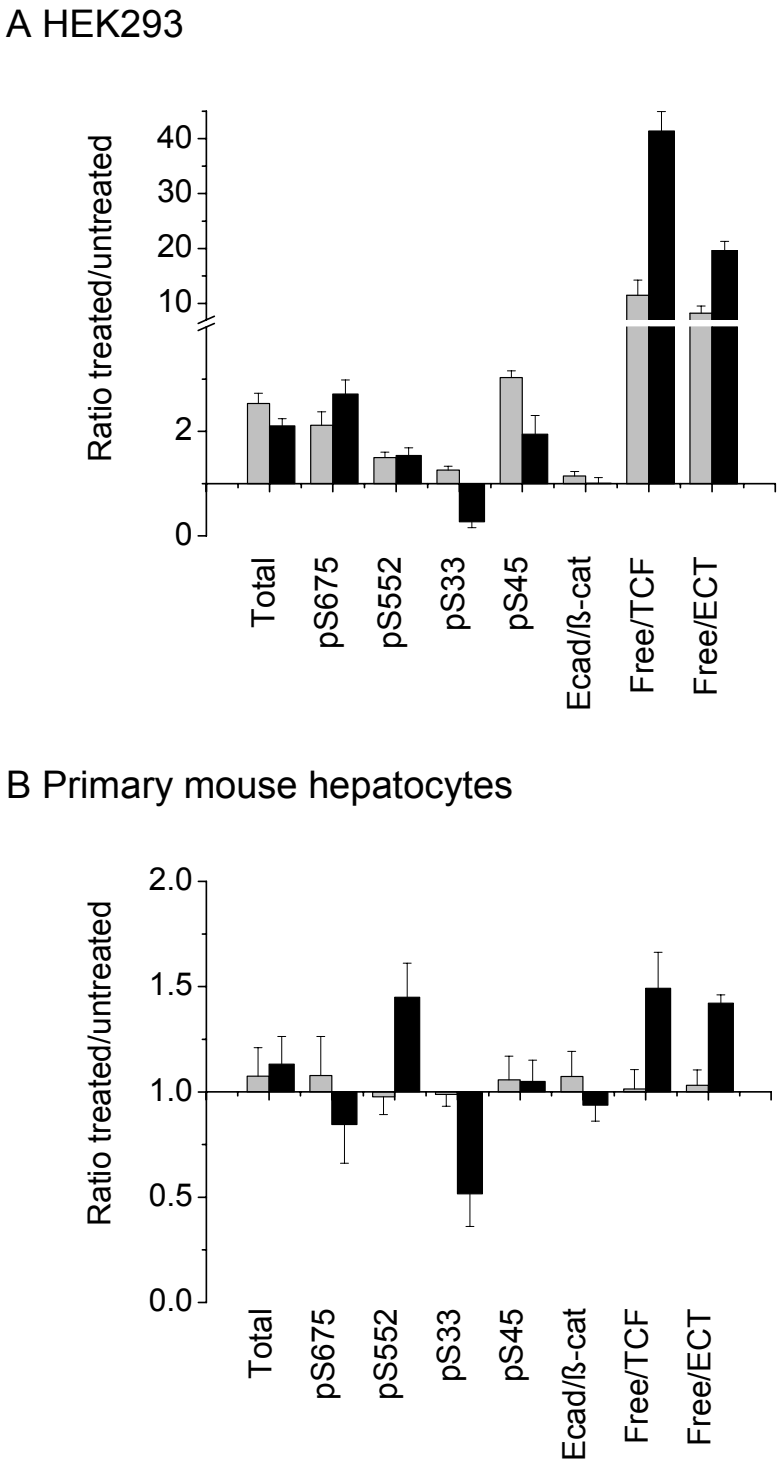

Figure 9 Validation of the β-catenin bead array panel.

HEK293 cells (A) or primary mouse hepatocytes (B) were treated with 200 ng/mL rWnt3a or SB216763 (A 20 µM or B 80 µM) for 3 h. Control cells received PBS or DMSO as solvent control. The cell culture experiments were performed in biological triplicates. 25 µg cell lysate of each sample (biological triplicates) were analyzed with the β-catenin bead array panel. Signal intensities are displayed as ratios treated/untreated including error propagation. Results are indicated in grey and black for the rWnt3a and inhibitor treated cells, respectively.

As shown in Figure 9, following the addition of rWnt3a or SB216763 in HEK293 (A) the total amount of β-catenin increased 2- to 3-fold compared to non-activated cells. Also elevated amounts of all phosphorylated β-catenin forms were observed after Wnt pathway activation. The application of the GSK-3 inhibitor led to an increase of pS675, pS552, and pS45 β-catenin, whereas pS33/pS37/pT41 β-catenin decreased at the respective time point. The E-cadherin/β-catenin complex did not show any significant changes after the activation of the Wnt signaling pathway. Finally, cytosolic β-catenin able to bind to GST-ECT and GST-TCF4 was present at a low basal level in non-activated cells and did increase significantly upon treatment of cells with rWnt3a or GSK-3 inhibitor. The µ-fishing assay revealed differences between the two bait proteins in the detectable levels of free β-catenin after GSK-3 inhibition, but not after treatment with Wnt3a.

However, the response to the activating reagents in primary mouse hepatocytes (Figure 9B) did not resemble the detected degree of activation compared to HEK293 (Figure 9A). Although all analytes were measured in primary mouse hepatocytes, the Wnt3a treatment did not induce observable changes at the respective time point. With respect to the GSK-3 inhibition, an increase in free β-catenin and pS552 β-catenin was observed, while reduced levels of pS33/pS37/pT41 β-catenin were shown.

Taken together, using a sample set composed of two different cell types both treated with the same Wnt activating reagents, the β-catenin bead array panel allowed the simultaneous detection of different forms of β-catenin in single bead array panel. It needs to be pointed out that only 25 µg lysates of each sample corresponding to extracts from 10^5 cells were required. However, the results between the investigated β-catenin forms in two cell types differed primarily in the detection of free β-catenin. Therefore, this µ-fishing assay was further validated as described in 3.1.3.

3.1.2 Technical reproducibility of the β-catenin bead array panel

In order to demonstrate the technical reproducibility of the β-catenin bead array panel, HEK293 cells were treated with DMSO (solvent control) or SB216763 (inhibitor) for 3 h and lysed as described in 2.10.1. The reproducibility of the bead array panel was demonstrated by performing four technical replicates either on one day to determine the intra-assay variability or on 4 days to show the inter-assay variability. Table 8 lists the intra- and inter-assay variability for all 8 analytes separately. Intra-assay variation was below 15%, whereas an average inter-assay variation of 20% was calculated.

Table 8 Inter- and intra-assay variances of the β-catenin bead array panel

HEK293 cells were treated with DMSO (solvent control) or 20 µM SB216763 (inhibitor) for 3 h and lysed as described in 2.10.1. 25 µg of each samples was analyzed in four technical replicates either on one day to determine the intra-assay variability or on 4 days to show the inter-assay variability.

Intra-assay variances	**Control**		**Solvent control**		**Inhibitor**	
	Mean (n=4)	CV [%]	Mean (n=4)	CV [%]	Mean (n=4)	CV [%]
Total	644	3	568	4	1118	5
pS675	392	3	320	4	686	7
pS552	70	5	64	4	140	5
pS33/pS37/pT41	169	4	138	2	182	2
pS45	216	5	177	1	706	3
E-cadherin/β-catenin	4370	1	3929	1	4248	2
Free/TCF	47	5	28	8	379	1
Free/ECT	26	10	22	15	219	11
Inter-assay variances	**Control**		**Solvent control**		**Inhibitor**	
	Mean (n=4)	CV [%]	Mean (n=4)	CV [%]	Mean (n=4)	CV [%]
Total	753	12	722	17	1307	12
pS675	450	11	411	19	814	14
pS552	80	11	78	13	163	11
pS33/pS37/pT41	174	8	149	5	195	7
pS45	224	6	198	13	744	11
E-cadherin/β-catenin	4481	3	4245	6	4527	6
Free/TCF	45	27	37	33	421	30
Free/ECT	26	17	23	19	231	9

3.1.3 Cross-validation of the µ-fishing assay

To demonstrate the selectivity and sensitivity of the data obtained by bead-based µ-fishing, cell lysates of HEK293 or primary mouse hepatocytes were analyzed using conventional biochemical methods including quantitative Western blots, a GST-pulldown assay (β-catenin fishing), and TOPflash luciferase reporter assays. A cross-validation of the µ-fishing assay with conventional methods was required to prove whether the miniaturized GST-pulldown assay is capable of capturing biologically active forms of β-catenin. The present total amount of β-catenin in activated and non-activated HEK293 cells was quantified by Western blot (Figure 10). GST-ECT was used as bait molecule in the pulldown assay to capture free β-catenin from the cell extracts [41, 55]. β-catenin captured in the pulldown assay was visualized in a Western blot (Figure 10). Using both miniaturized and conventional pulldown assays, elevated levels of β-catenin were detected in cells exposed to rWnt3a or GSK-3 inhibitor SB216763 (Figure 10). In parallel, a TOPflash luciferase reporter assay was used to visualize β-catenin/TCF-mediated gene expression (Figure 10). Since elevated levels of free β-catenin in cells exposed to rWnt3a or SB216763 were expected to promote luciferase expression, the detected increase in luciferase activity confirms that the free β-catenin monitored using conventional and miniaturized assays is transcriptionally active.

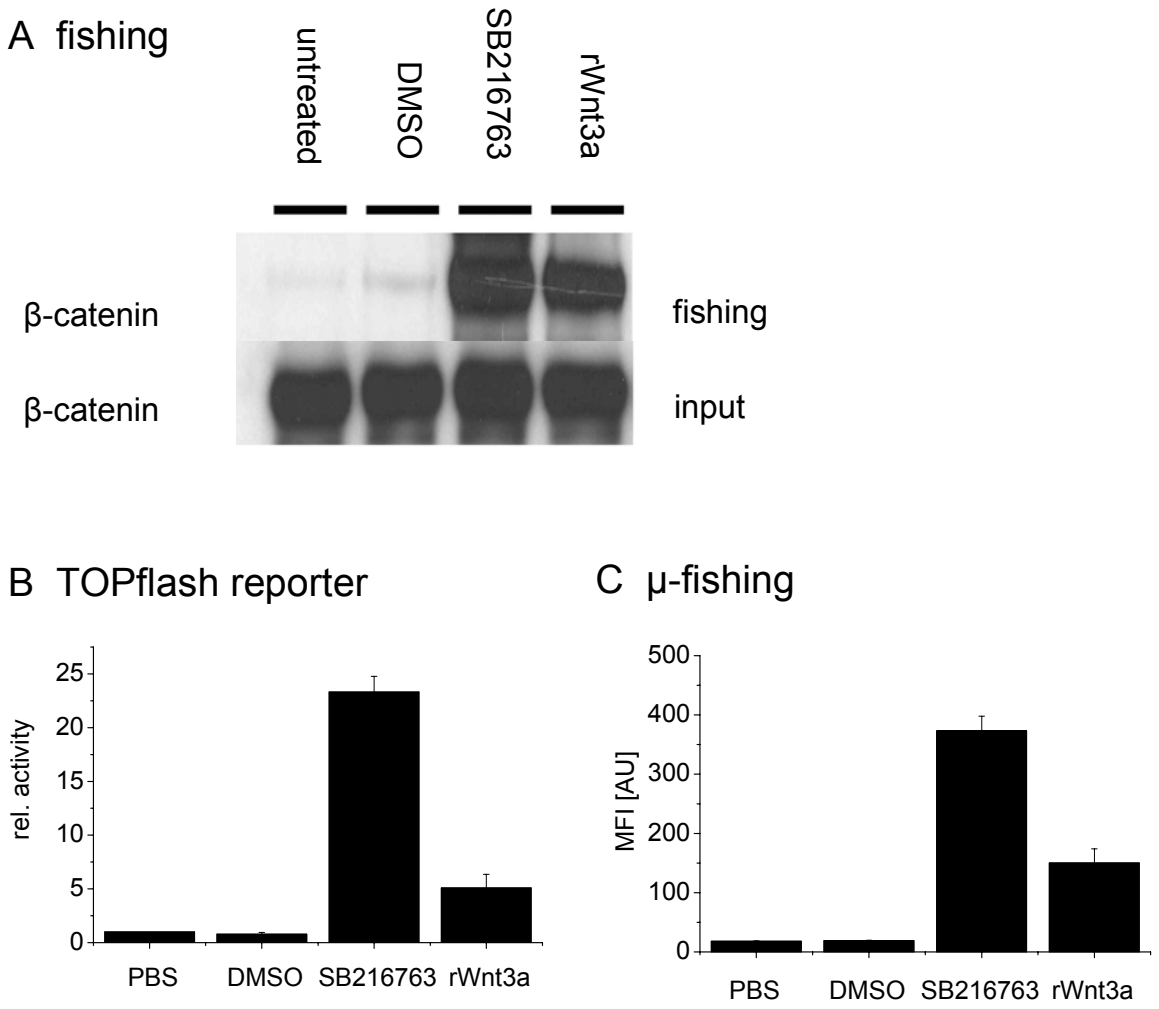

Figure 10 Cross-validation of the µ-fishing assay with HEK293 lysates.

HEK293 cells were treated with 200 ng/mL rWnt3a or 20 µM SB216763 for 3 h. Control cells received PBS or DMSO as solvent control. Samples were analyzed using either a β-catenin fishing and subsequent Western blot analysis (A) or the miniaturized β-catenin µ-fishing assay (C). TOPflash luciferase reporter assay measuring of β-catenin activity was done in separate experiments (B). (A) Upon harvest and preparation of cell lysates, the free cytosolic, signaling-competent pool of β-catenin was recovered by supplementing each cell lysate with glutathione sepharose beads and the GST-ECT fusion protein as indicated. After the binding reaction and extensive washing, proteins bound to the glutathione sepharose matrix were eluted with SDS-PAGE loading buffer. Samples were separated by SDS-PAGE and analyzed by Western blot with an antibody recognizing β-catenin. As input control, a fraction of each cell lysate was analyzed in parallel. Cellular β-catenin was detected by Western blot with an anti-β-catenin antibody. (B) HEK293 cells were transfected with the Wnt/β-catenin-inducible TOPflash luciferase reporter and the constitutively active Renilla luciferase reporter pRL-CMV, which was used for normalization purposes. Values shown represent average activities and the corresponding standard deviations derived from at least three independent transfection experiments. (C) 25 µg cell lysate of each sample (technical triplicates) were analyzed using the µ-fishing assay. Bead-bound GST-ECT was used to capture free β-catenin. The average values and the corresponding standard deviations are displayed.

In summary, the changes in free β-catenin levels in HEK293 induced by exposure to rWnt3a and SB216763 measured using bead-based µ-fishing assay were similar in magnitude to those measured using conventional methods (Figure 10). Table 9 summarizes the results of the validation experiments in HEK293 and displays the recorded fold changes in active β-catenin signaling for the purpose of comparison.

Table 9 Comparison of recorded changes in active β-catenin signaling in HEK293.

treatment	**fishing**	**TOPflash reporter**	**µ-fishing**
SB216763	45 fold	23 fold	20 fold
rWnt3a	20 fold	5 fold	8 fold

In a second experiment, primary mouse hepatocytes were stimulated with GSK-3 inhibitor SB216763 for 3 h and afterwards analyzed using both fishing and µ-fishing assay as described above. In line with the validation experiment of the whole β-catenin bead array panel (Figure 9), treatment-induced changes in free β-catenin were relatively small in hepatocytes (Figure11) compared to the changes in HEK293 (Figure 10). While Western blot analysis of the input lysates did not elucidate a significant activation of the Wnt pathway, samples pre-fractionated with GST-ECT (fishing) or directly analyzed using the µ-fishing assay showed a measurable increase in free β-catenin (Figure 11).

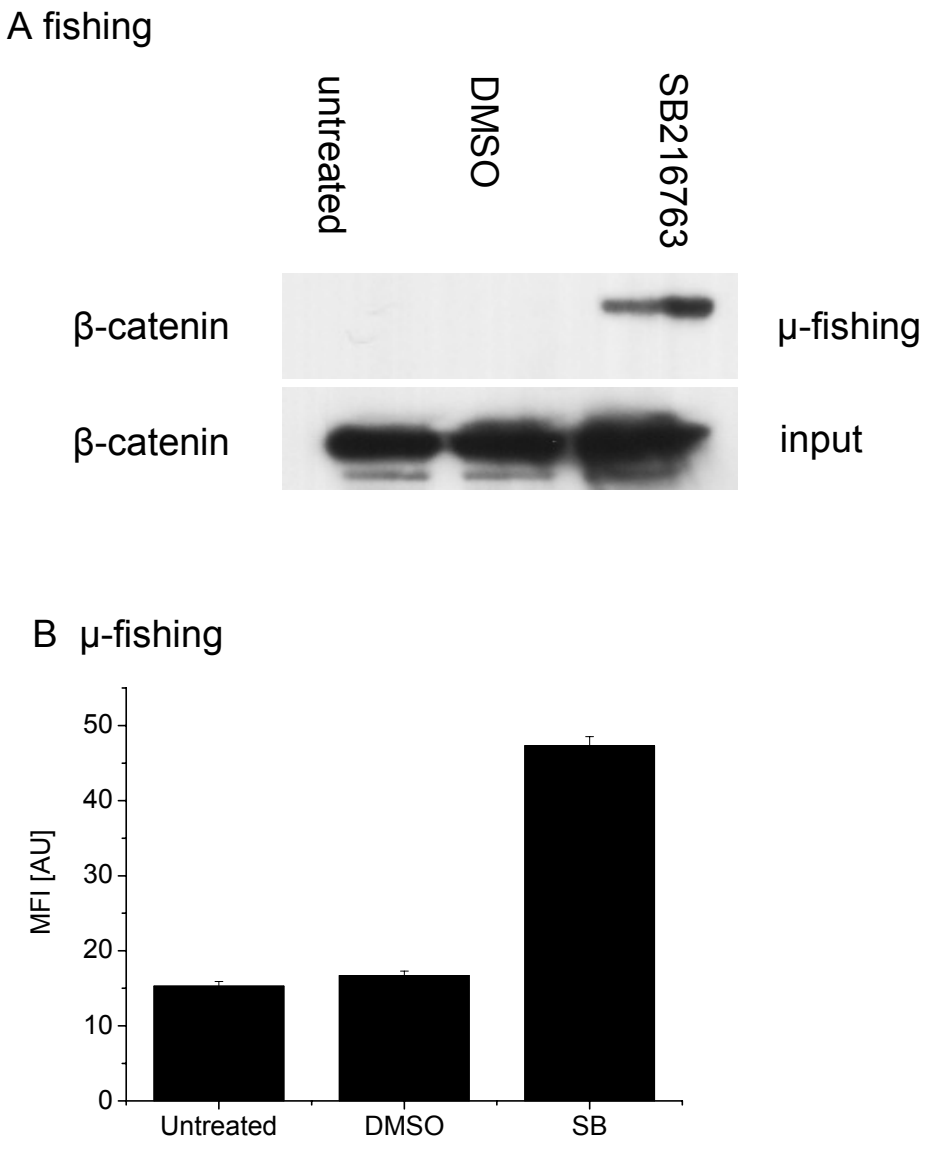

Figure 11 Cross-validation of the μ-fishing assay with lysates of primary mouse hepatocytes.

Primary mouse hepatocytes were starved for 24 h and treated with 80 μM SB216763 for 3 h. Control cells received PBS or DMSO as solvent control. Samples were analyzed using either β-catenin fishing and Western blot analysis (A) or the miniaturized β-catenin μ-fishing assay (B). (A) Upon harvest and preparation of cell lysates, free β-catenin was recovered by supplementing each cell lysate with glutathione sepharose beads and the GST-ECT fusion protein. After the binding reaction and extensive washing, proteins bound to the glutathione sepharose matrix were eluted with SDS-PAGE loading buffer. Samples were separated by SDS-PAGE and analyzed by Western blot with an antibody recognizing β-catenin. As input control, a fraction of each cell lysate was analyzed in parallel. Cellular β-catenin was detected by Western blotting with an anti-β-catenin antibody (BD Biosciences). (B) 25 μg cell lysate of each sample (technical triplicates) were analyzed using the μ-fishing assay. Bead-bound GST-ECT was used to capture free β-catenin. The average values and the corresponding standard deviations are displayed.

3.1.4 Linearity of µ-fishing assay for active β-catenin

Both assay controls and a standard curve are needed for a reliable multiplexed measurement of analytes in a complex sample. Assay controls itself could easily be generated in a huge batch parallel to the main cell culture experiment. In search of an appropriate recombinant β-catenin as a standard protein, His-tagged β-catenin was expressed in *E.coli*, but the purification of a native form failed. GST-β-catenin was available, but not useful since bait proteins also carry a GST-tag. Due to the lack of a pure standard protein for the detection of free β-catenin, a reference curve using activated cell lysates was established. To obtain a correlation between the amount of activated cell lysate and the corresponding detectable activation (termed as x-fold change), lysates of stimulated and non-stimulated HEK293 cells were mixed in a distinct ratio ending with a total amount of 50 µg lysates and analyzed with the µ-fishing assay. In Figure 12, the x-fold changes corresponding to the amount of activated lysates are plotted on the y-axis. The experiment revealed linear range of the µ-fishing assay between 20 and 40 µg activated cell lysate.

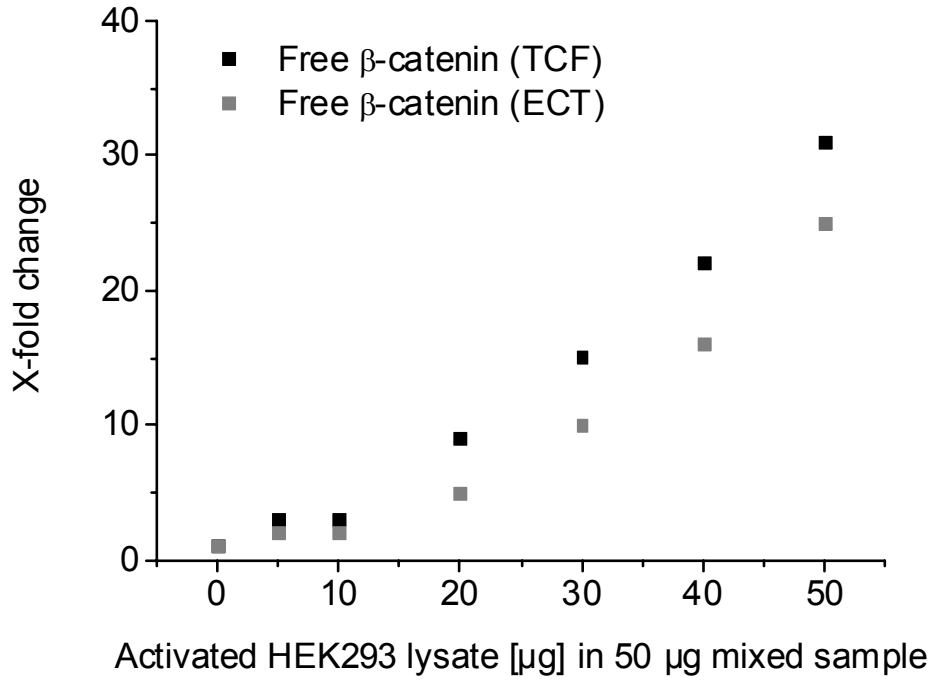

Figure 12 Linearity of µ-fishing assay for active β-catenin.

Lysates of activated and non-activated HEK293 cells (exposed to GSK-3 inhibitor SB216763 for 3 h and control treatments, respectively) were mixed containing a total amount of 50 µg protein. The mixed samples were analyzed with the µ-fishing assay. Relative changes in free β-catenin captured by GST-TCF4 and GST-ECT are displayed in black and grey, respectively. No technical replicates were performed.

3.1.5 Specificity and linearity of phospho-specific β-catenin sandwich immunoassays

In order to prove the specificity of the antibodies targeting phosphorylated species of β-catenin, dilution series of recombinantly expressed GST-β-catenin lacking post-translational modifications were analyzed with the pan- and phospho-specific sandwich immunoassays of the β-catenin bead array panel. As displayed in Figure 13, only the sandwich immunoassays targeting total β-catenin showed signals correlating to the amount of recombinant β-catenin. Therefore, unspecific binding of non-phosphorylated forms of β-catenin could be excluded.

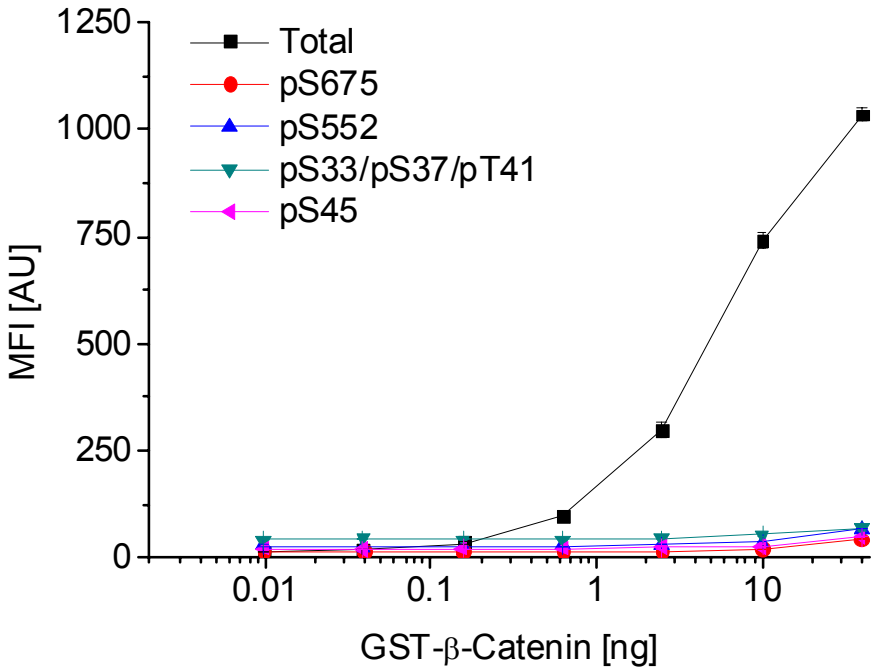

Figure 13 Validation of sandwich immunoassays specific for phosphorylated β-catenin.

GST-β-catenin was diluted with lysis buffer (40 to 0.01 ng protein) and analyzed with the five sandwich immunoassays contained in the β-catenin bead array panel. Technical replicates were performed. Only total β-catenin (black squares) was quantified. No unspecific signals were recorded by the phospho-specific β-catenin capture antibodies.

3.2 β-catenin/Wnt signaling in HEK293

3.2.1 Time-dependent Wnt signaling in HEK293

Comprehensive information on the dynamics of cell signaling is a prerequisite for detailed analysis and computational modeling. With regard to the Wnt signaling pathway, time-resolved data are required to create new or to verify existing models. Time-course experiments were therefore performed by treating HEK293 cells with either rWnt3a or SB216763 in biological triplicates. Cell lysates were collected at specific time points between 0-10 h in order to visualize changes that occurred immediately after the addition of rWnt3a or SB216763 (5 min) and monitor the effects of long-term treatment (10 h). Stimulation of the HEK293 cells with rWnt3a led to an increase in the overall levels of β-catenin (Figure 14) which is a hallmark of canonical Wnt signaling. Free β-catenin, a measure of activated Wnt signaling, accumulated transiently after exposure of the cells to rWnt3a whereas the amount of membrane-associated β-catenin did not change (Figure 14). With respect to the phosphorylated β-catenin forms, differently shaped response curves were monitored (Figure 14): an increase of phosphorylated β-catenin pS675, pS552 or pS45, starting 60 min after treatment and reaching a peak at t = 180 (pS675 and pS552) or 300 min (pS45), respectively. In contrast, β-catenin phosphorylated at S33/S37/T41 had a relatively high initial concentration and then fell 3-fold, reaching a minimum at t = 60 min, subsequently increasing and returning to its basal level. The decrease of pS33/pS37/pT41 β-catenin within the first 60 min of rWnt3a treatment was determined as a characteristic feature of β-catenin phosphorylated at the GSK-3 casette.

Exposure of cells to SB216763 led to a steady increase (starting at t = 60 min) in total β-catenin levels (Figure 15), while the levels of membrane-associated protein did not change either during rWnt3a treatment or SB216763 treatment. In comparison to what was observed in rWnt3a-treated cells, the amount of free β-catenin increased steadily after t = 60 min (Figure 15). An increase in phosphorylated β-catenin pS675, pS552 as well as pS45 was observed. In contrast, the inhibition of GSK-3 resulted in a strong decrease in the amount of phosphorylated β-catenin pS33/pS37/pT41 by t = 5 min. This rapid decrease is expected since S33/S37/T41 are direct substrates of GSK-3β. By 10 h, the level of phosphorylation returned to basal levels.

In summary, both treatments led to changes in the modification status and the accumulation of free β-catenin consistent with Wnt pathway activation described in literature [76], but the detailed dynamics differed in the two cases.

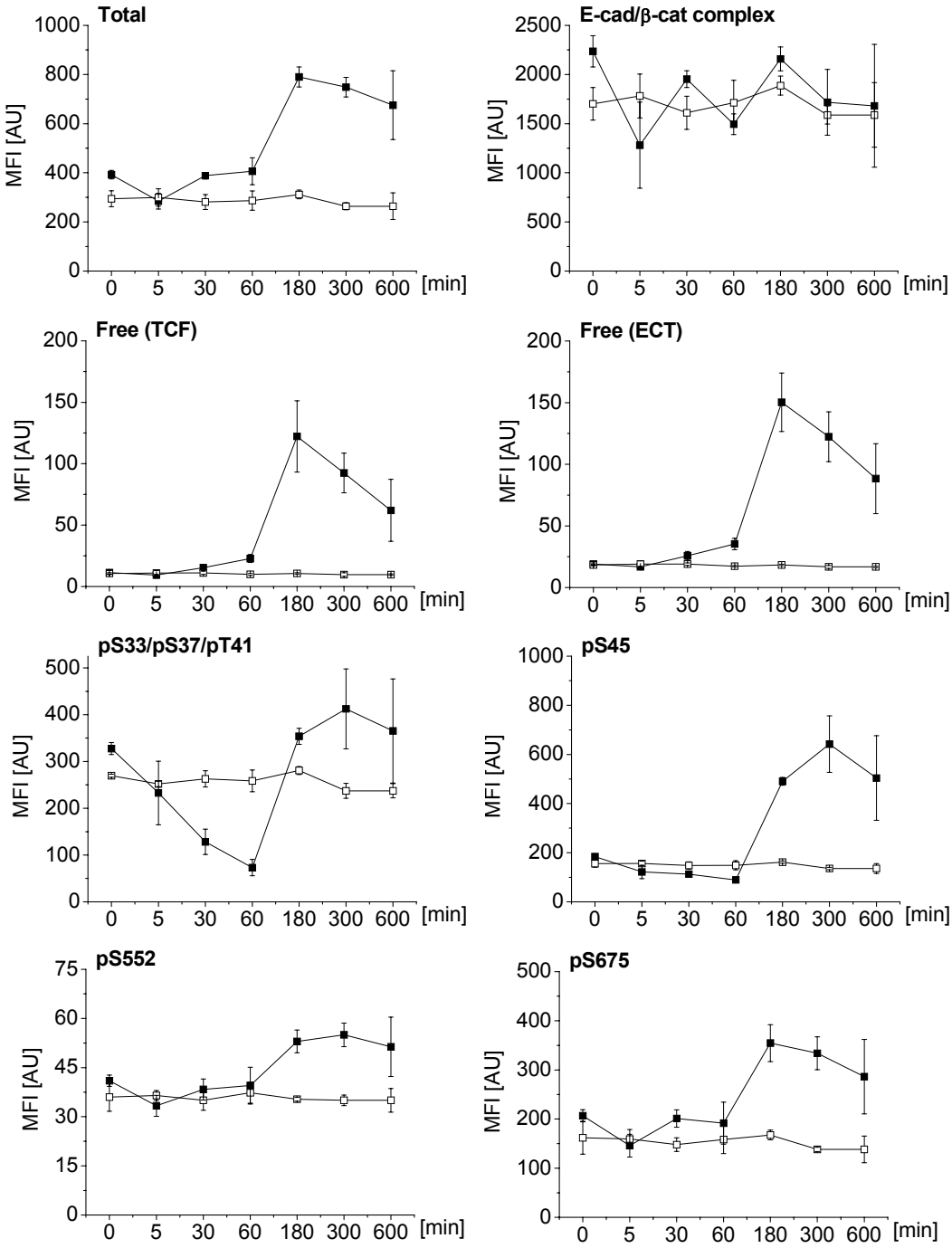

Figure 14 Time-dependent Wnt activation in HEK293 by rWnt3a.

HEK293 cells were starved for 24 h and then treated with 200 ng/mL rWnt3a (■) or PBS (□) for 5, 30, 60, 180, 300 and 600 minutes. Each data point represents the average of independent results from 3 cell culture wells. 25 µg of each sample were analyzed using the β-catenin bead array panel. The result is displayed in median fluorescence intensities. A transient increase in the amount of total, free β-catenin captured by GST-TCF4 or GST-ECT and phosphorylated β-catenin pS45, pS552 or pS675 was detected. β-catenin pS33/pS37/pT41 decreased within the first 60 min of rWnt3a treatment. The amount of the E-cadherin/β-catenin complex did not change under the treatment. Cells treated with PBS did not show alterations regarding all analytes.

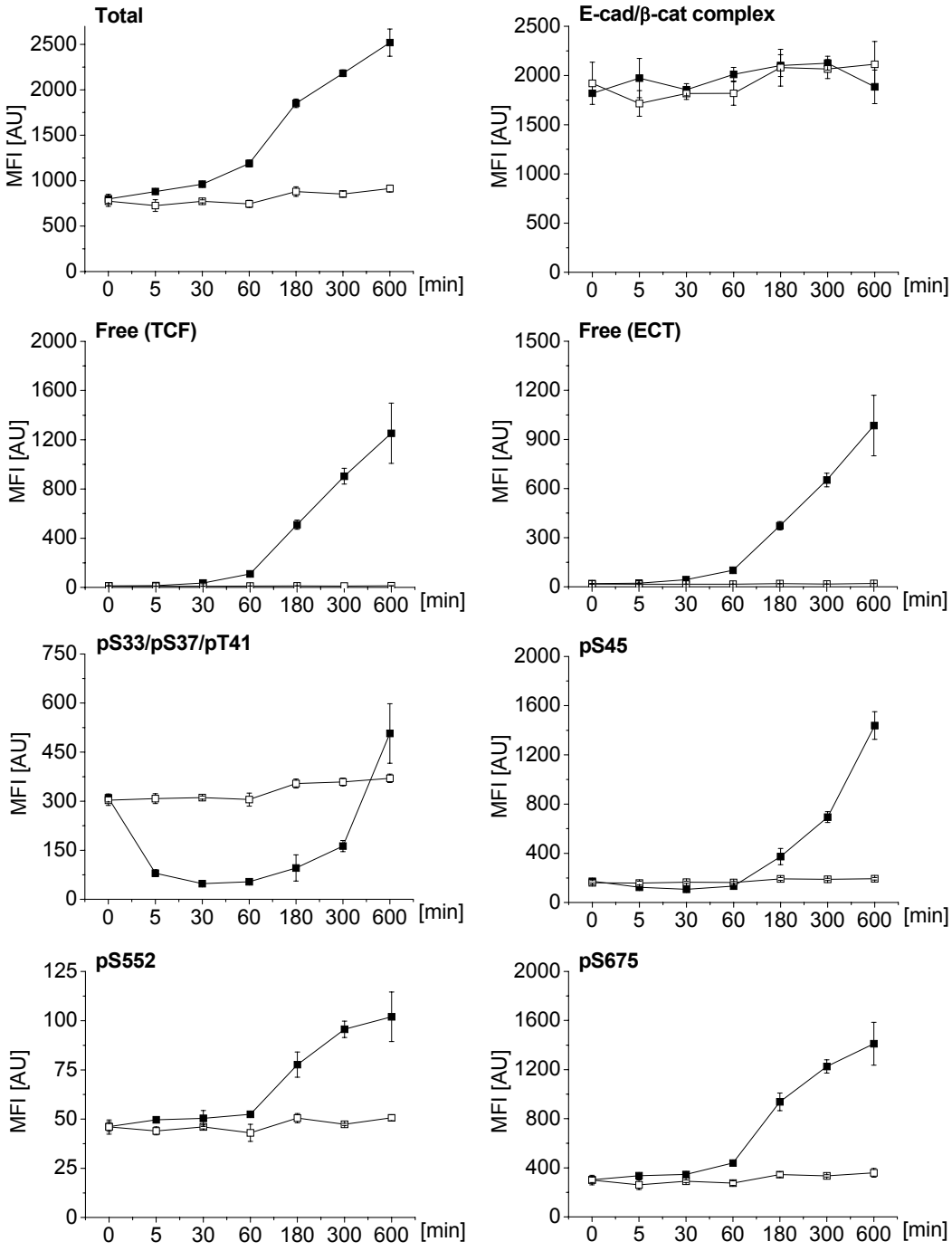

Figure 15 Time-dependent Wnt activation in HEK293 cells through GSK-3 inhibition.

HEK293 cells were starved for 24 h and then treated with 20 µM SB216763 (■) or DMSO (□) for 5, 30, 60, 180, 300, and 600 minutes. Each data point represents the average of independent results from 3 cell culture wells. 25 µg of each sample were analyzed using the β-catenin bead array panel. The result is displayed in median fluorescence intensities. An increase in the concentration of total and phosphorylated β-catenin pS45, pS552 or pS675 was detected, whereas pS33/pS37/pT41 β-catenin reached an interim low and leveled off at the base level. The amount of E-cadherin/β-catenin complex did not change under the treatment. The treatment of the cells with SB216763 led to the accumulation of free β-catenin captured by GST-TCF4 or GST-ECT. DMSO treatment did not have any effect on the cells.

3.2.2 Origin and characteristics of active β-catenin signaling in HEK293

After a detailed time profile of active β-catenin signaling in response to Wnt pathway activation (3.2.1) was obtained, questions concerning the characteristics of the monitored inducible pool of β-catenin remained. Several groups reported a Wnt–inducible increase of the overall levels of β-catenin detected both at the membrane and in the cytosol using conventional methods [128, 129]. In contrast, the detailed β-catenin kinetic (3.2.1) only confirmed an increase in the overall levels of β-catenin, but did not reveal a change in the levels of the E-cadherin/β-catenin complex. Furthermore, experiments aiming to resolve the origin of free β-catenin were previously performed [125] in the group of A. Hecht and hint on an inducible pool of free β-catenin which is dependent from biosynthesis.

The following experiment aimed to show whether activated β-catenin is released from the membrane or originates from *de-novo* biosynthesis. Therefore, HEK293 cells were pre-treated with cycloheximide [130] for 30 min to block the eukaryotic *de-novo* biosynthesis. Cells were then exposed to rWnt3a or SB216763 to induce active β-catenin signaling. Cell lysates were prepared in the group of A. Hecht, University of Freiburg and provided for analysis. The samples were analyzed in technical replicates with the β-catenin bead array panel.

In line with the time-resolved description of β-catenin dynamics in HEK293 (3.2.1), activated β-catenin signaling was detected in the cycloheximide-free stimulation (Figure 16). By the inhibition of biosynthesis, this activation was neither observed using the ligand nor the small molecule. Here, the signal levels resembled the control treatments. Simple inspection of the data show that the sequential treatment with cycloheximide and rWnt3a or SB216763 respectively (Figure 16), completely prevents the increase in the overall levels of β-catenin as well as the accumulation of free, active β-catenin. Furthermore phosphorylated forms of β-catenin which were found to be increased in the case of pathway activation (pS45, pS552 and pS675) did not show changed concentrations when cells were perturbed with cycloheximide. The amount of the E-cadherin/β-catenin complex remained unchanged within the two treatment groups (with or without cycloheximide). When protein biosynthesis was inhibited, the levels of the E-cadherin/β-catenin complex were reduced in general, but did not change after Wnt activation.

In summary, this experiment demonstrated that active β-catenin signaling depends on *de-novo* biosynthesis in HEK293 cells. The signaling active pool of β-catenin comprises free β-catenin as well as β-catenin phosphorylated at S45, S552 and S675 since ligand and inhibitor inducible increase of these forms of β-catenin was completely repressed by the inhibition of *de-novo* biosynthesis.

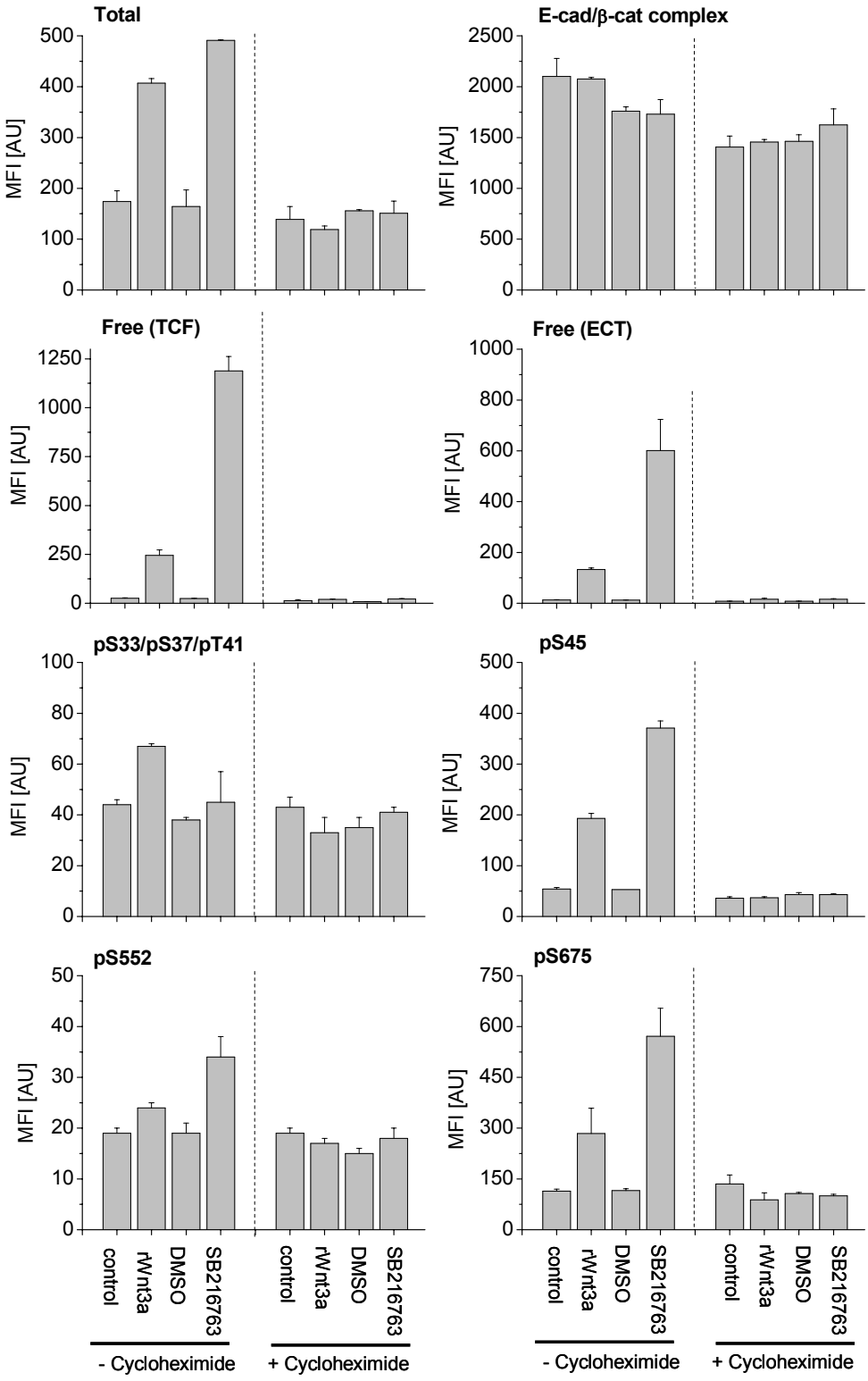

Figure 16 Origin and characteristics of active β-catenin signaling in HEK293 cells.

HEK293 cells were pre-treated with 10 µg/mL cycloheximide for 30 min in 4 of 8 experiments (right). To activate the Wnt/β-catenin pathway, cells were then treated with 20 µM SB216763 or 200 ng/mL rWnt3a for 3 h. Control cells received DMSO or remained untreated. 50 µg lysate of each sample were analyzed in technical replicates with the β-catenin bead array panel. The recorded signal intensities (MFI) are plotted separately for each analyte.

3.3 β-catenin/Wnt signaling in primary mouse hepatocytes

3.3.1 Time-dependent Wnt signaling in primary mouse hepatocytes

Wnt signaling in primary mouse hepatocytes (3.1.1 and 3.1.3) differed from signaling measured in HEK293 since only weak effects were detected under similar cell culture conditions. To obtain a complete description of dynamic β-catenin signaling in primary mouse hepatocytes, cells were starved for 24 h and then treated with either rWnt3a or SB216763 for 5, 30, 60, 180, 300 and 600 minutes. PBS and DMSO were used as solvent controls. The cell culture experiment and the sample preparation were performed by the group of A. Hecht, University of Freiburg. The sample sets (biological triplicates) were analyzed with the β-catenin bead array panel.

Basically the detected x-fold changes in response to both activation mechanism – ligand or inhibitor - were relatively small in hepatocytes compared to HEK293 cells (3.2). Nevertheless, activation profiles for the signaling pool of β-catenin were detected thereby uncovering differences between the two applied activation mechanisms.

First, an increase in the overall levels of β-catenin as a hallmark for active Wnt signaling was measured only after long-term treatment (10 h) with rWnt 3a (Figure 17). Treatment with the GSK-3 inhibitor did not significantly alter the overall levels of β-catenin (Figure 18).

The amount of the E-cadherin/β-catenin complex remained stable under all perturbed conditions (Figure 17 and Figure 18). Although measured with very low signal intensity, free β-catenin was found to increase after both treatments. Compared to the inhibitor treatment, treatment with rWnt3a led to a more sustained response (Figure 17and Figure 18). In line with the result obtained in HEK293 cells, free β-catenin captured by GST-ECT or GST-TCF4 showed similar time- or treatment-dependently altered levels.

Regarding the phosphorylated species of β-catenin, the experiment illustrates a cellular scenario which seems to be more complicated and diverse as observed in HEK293 (Figure 14 and Figure 15): The amount of β-catenin marked for proteasomal degradation (pS33/pS37/pT41) was temporarily decreased by the GSK-3 inhibitor (Figure 18) during the first hour and after 5 h of treatment, whereas rWnt3a did not lead to significant changes (Figure 17). Both ligand and inhibitor treatment led only to minor changes in pS45, pS552 and pS675 β-catenin. Nevertheless, the detection of these phosphorylated forms of β-catenin denoted differences concerning the shape of the response curve (Figure 17 and Figure 18).

In summary, the measurement of β-catenin signaling in primary mouse hepatocytes revealed remarkable cell-type specific differences compared to HEK293 cells. In hepatocytes, only weak effects in response to both rWnt3a and GSK-3 inhibitor were monitored.

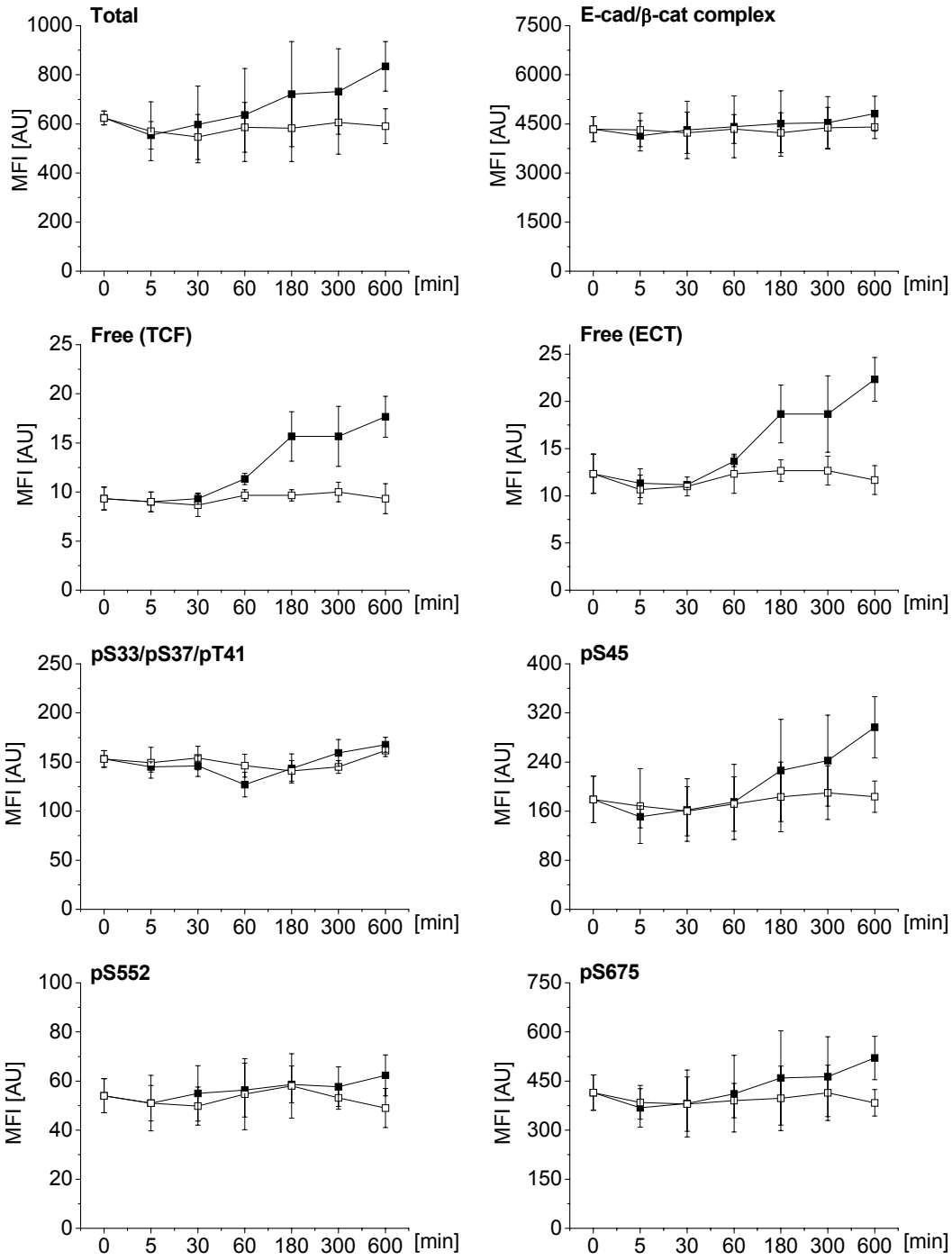

Figure 17 Time-dependent Wnt activation in primary mouse hepatocytes with rWnt3a.

Primary mouse hepatocytes were starved for 24 h and then treated with 200 ng/mL rWnt3a (■) or PBS (□) for 5, 30, 60, 180, 300 and 600 minutes. Each data point represents the average of independent results from 3 cell culture wells performed on 3 different days. 25 µg of each sample were analyzed using the β-catenin bead array panel. The result is displayed in median fluorescence intensities. An increase in the amount of free β-catenin captured by GST-TCF4 or GST-ECT was measured after rWnt3a treatment. The amount of E-cadherin/β-catenin complex did not change under the treatment. Cells treated with PBS did not show alterations regarding all analytes.

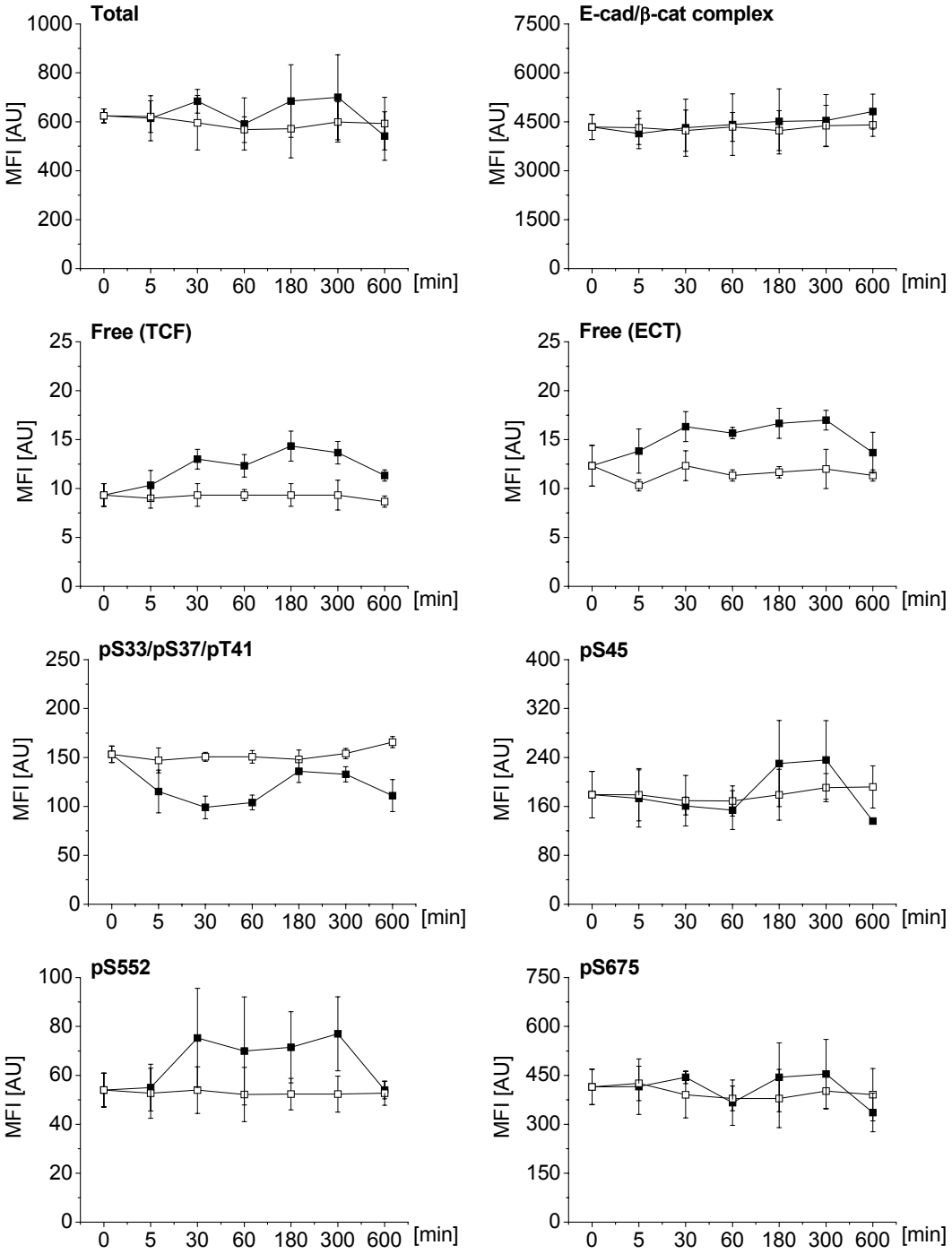

Figure 18 Time-dependent Wnt activation in primary mouse hepatocytes through GSK-3 inhibition.

Primary mouse hepatocytes were starved for 24 h and then treated with 80 µM SB216763 (■) or DMSO (□) for 5, 30, 60, 180, 300 and 600 minutes. Each data point represents the average of independent results from 3 cell culture wells performed on 3 different days. 25 µg of each sample were analyzed using the β-catenin bead array panel. The result is displayed in median fluorescence intensities. An increase of free β-catenin and a transient decrease of β-catenin pS33/pS37/pT41 levels were detected upon GSK-3 inhibition. The amount of E-cadherin/ β-catenin complex did not change under the treatment.

3.3.2 Origin and characteristics of active β-catenin signaling in primary mouse hepatocytes

The time-resolved activation profile of β-catenin signaling (3.3.1) raised the question about the origin of a Wnt-inducible signaling-competent pool of β-catenin. According to the experiment in HEK293 (3.2.2), serum-starved primary mouse hepatocytes were pre-treated with cycloheximide to block protein biosynthesis and afterwards stimulated with rWnt3a or SB216763 to activate the Wnt pathway.

In Figure 19 the detected levels of all analytes after sequential stimulation are displayed. A ligand and inhibitor-mediated increase at the respective time point could only be monitored in the case of free β-catenin in the control group (without cycloheximide).

In line with the dynamics of active β-catenin signaling (3.3.1) at time point t = 180 min, the phosphorylated forms of β-catenin did not show altered levels (Figure 17 and Figure 19). Ambigous results were obtained regarding the overall levels of β-catenin. The E-cadherin/β-catenin complex signal fluctuated to a certain extent which did not allow to draw a conclusion. As already shown in 3.3.1, the amount of the E-cadherin/β-catenin complex remained stable over a longer time period under the same treatments. When cells were pre-incubated with cycloheximide, a ligand or inhibitor-mediated increase in free β-catenin was blocked. Here, signal levels were similar to the control levels. Due to the missing activation signal, no result was obtained concerning the phosphorylated forms of β-catenin.

In summary, albeit the detected signals were relatively low, the data identified two inducible forms of active β-catenin (captured by either GST-ECT or GST-TCF4) in primary mouse hepatocytes. It could be demonstrated that the ligand or inhibitor-mediated increase was blocked by the inhibition of *de-novo* biosynthesis. Furthermore, data sets gained in HEK293 (3.2.2) and primary mouse hepatocytes (3.3.2) correlate well concerning the origin of a Wnt-inducible free β-catenin pool.

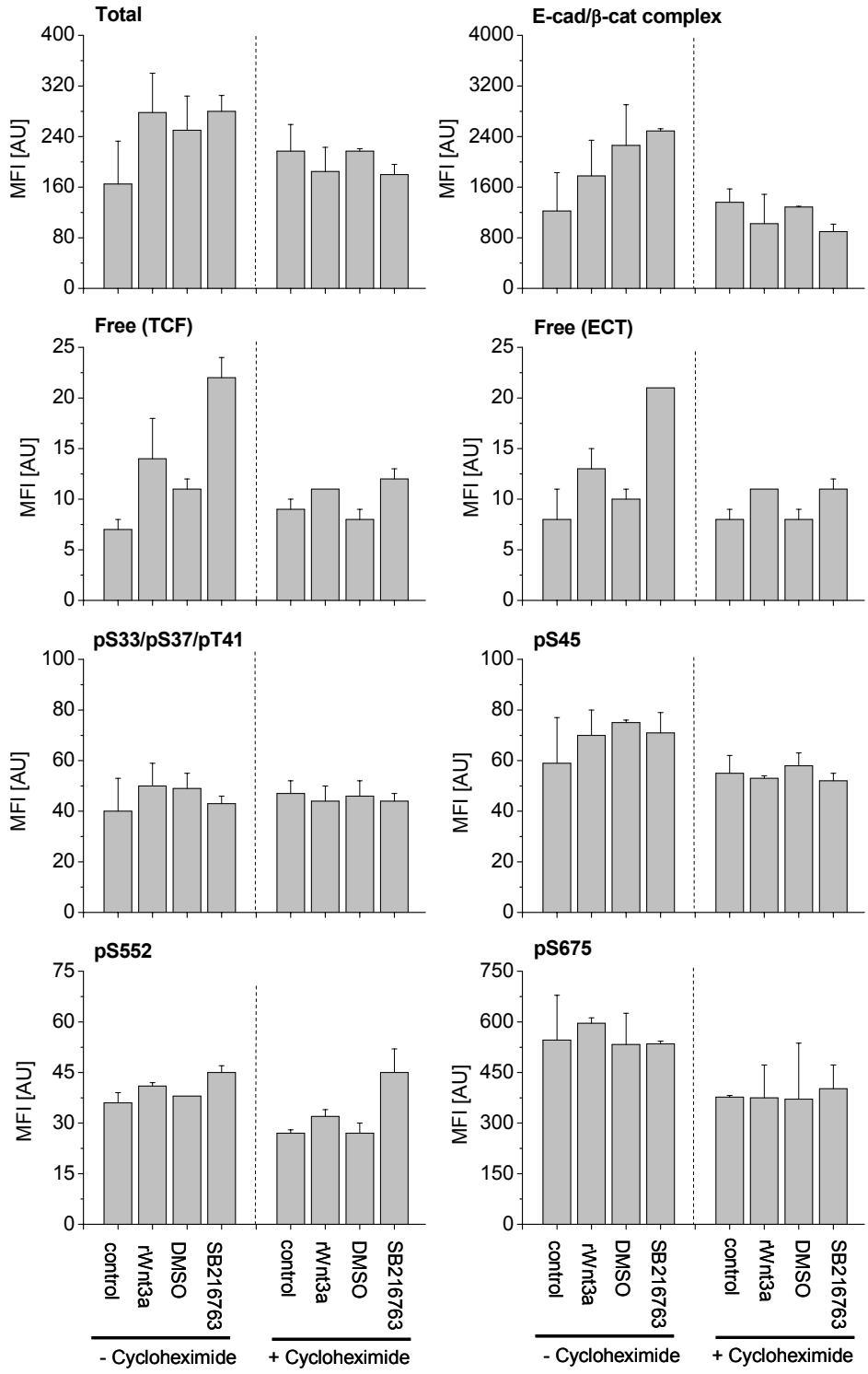

Figure 19 Origin and characteristics of active β-catenin signaling in primary mouse hepatocytes.

Primary mouse hepatocytes were serum-starved for 24 h. As a pre-treatment, 4 of 8 experiments received 10 µg/mL cycloheximide for 30 min. To activate the Wnt/β-catenin pathway, cells were then treated with 80 µM SB216763 or 200 ng/mL rWnt3a for 3 h. Control cells were treated with DMSO or remained untreated. 50 µg lysate of each sample were analyzed in technical replicates with the β-catenin bead array panel. The recorded signal intensities (MFI) are plotted separately for each analyte.

3.4 β-catenin/Wnt signaling in human HCC derived cell lines HepG2 and FOCUS

The cell lines HepG2 and FOCUS were used to analyze β-catenin/Wnt signaling in transformed hepatocytes. These cell lines were characterized with respect to morphology, growth rate, production of albumin, anchorage independent growth in soft agar and tumor formation in nude mice [117-119] and were categorized as poorly differentiated (FOCUS) or well-differentiated (HepG2) [131, 132]. Both cell lines harbor abnormalities concerning β-catenin or E-cadherin. HepG2 cells express a strongly increased truncated form of β-catenin lacking aa 25-140 as well as a small pool of wild type β-catenin [86, 133]. FOCUS cells constitute a model system for HCC cells undergoing epithelial to mesenchymal transition (EMT) since very low levels of E-cadherin were found. In general, EMT [134] is a normal developmental process or implicated in tumor progression leading to enhanced motility or invasiveness, respectively. The loss of E-cadherin is considered as a hallmark of EMT [135].

3.4.1 HepG2 – model system for hepatocytes harboring an activating β-catenin mutation

The analysis of time-resolved β-catenin signaling in HepG2 revealed dynamics of β-catenin as a sum of changes occurring in the wild type and the truncated pool of β-catenin regarding all analytes except N-terminally phosphorylated β-catenin. Since truncated β-catenin lacks aa 25-140 and therewith the N-terminal regulation sites for degradation, only the detection of pS33/pS37/pT41 and pS45 β-catenin captures exclusively the wild type pool of β-catenin.

First, the overall levels of β-catenin remained unchanged during ligand and control treatment (Figure 20). Albeit levels at t = 0 min differed between control and treatment series, a comparable time-course was detected. Just as total β-catenin, the amount of the E-cadherin/β-catenin complex did not change (Figure 20). As expected, a high basal level of free β-catenin was observed in unperturbed HepG2 cells originating from the deleted N-terminal regulatory site. Interestingly, a comparable increase in free β-catenin was detected with both bait proteins after exposure to rWnt3a for 20 h (Figure 20). In the case of C-terminally phosphorylated forms of β-catenin, a comparably high basal level was monitored (Figure 20). A Wnt3a-mediated change was not detected.

Results presented so far based on the detection of a sum signal of wild type and truncated β-catenin which was not differentiable into the two distinct pools. However, the measurement of pS33/pS37/pT41 and pS45 β-catenin in HepG2 demonstrated the presence of the wild type pool revealing a relatively high signal from pS33/pS37/pT41 β-catenin and a comparably low level of pS45 β-catenin. Both analytes remained unchanged under the rWnt3a treatment.

Thus, both expression of the wild type pool and the associated regulation machinery modulating this fraction was shown.

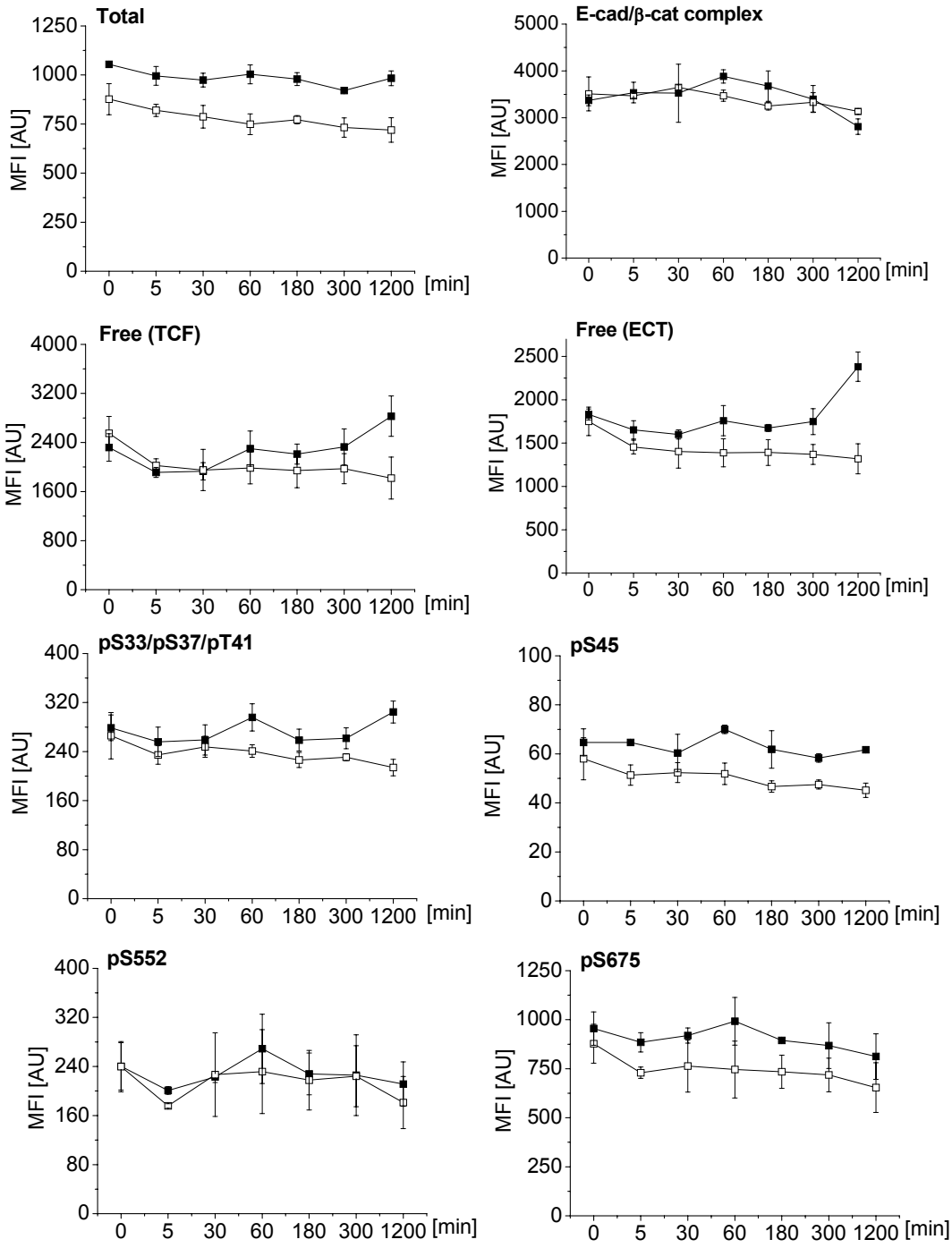

Figure 20 Time-dependent Wnt activation in HepG2 using rWnt3a.

HepG2 cells were starved for 24 h and then treated with 200 ng/mL rWnt3a (■) or PBS (□) for 5, 30, 60, 180, 300 and 1200 minutes. Each data point represents the average of independent results from 3 cell culture wells. 20 µg of each sample were analyzed using the β-catenin bead array panel. The result is displayed in median fluorescence intensities. Changes in the detected forms of β-catenin only occurred in free β-catenin after 20 h of treatment. All other analytes did not show treatment-mediated alterations. Cells treated with PBS did not show any concentration changes regarding all analytes.

3.4.2 FOCUS - model system for hepatocytes undergoing EMT

To investigate how FOCUS as a model system for enhanced tumor grade reacts to the canonical Wnt3a ligand, serum-starved FOCUS cells were treated with rWnt3a from 0 to 20 h and analyzed using the β-catenin bead array panel. In Figure 21, the recorded dynamic changes of all analytes are displayed. Focusing first on the overall levels of β-catenin, a sustained increase in total β-catenin concentration was found starting at t = 60 min and reaching a maximum after 20 h of treatment. A low amount of the E-cadherin/β-catenin complex was measured in unperturbed FOCUS cells. When perturbed with rWnt3a, the signal fluctuated marginally, but did not reveal significant changes in the amount of the E-cadherin/β-catenin complex. For clarity how Wnt signaling in FOCUS is transduced, levels of free and phosphorylated β-catenin need to be taken into account for the analysis. With respect to free β-catenin, an accumulation of free, active β-catenin was monitored over time. This treatment-induced increase occurred simultaneously to the changes in the overall levels of β-catenin only differing in the time point of reaching the respective maximum. The occurrence of free β-catenin is accompanied at the same time by augmented levels of β-catenin phosphorylated at S45, S552 and S675. In FOCUS β-catenin marked for proteasomal degradation exhibited comparable dynamics as observed in HEK293: pS33/pS37/pT41 β-catenin had a relatively high initial concentration and then fell 2-fold, reaching a minimum at t = 60 min, subsequently increasing and returning to its basal level. Thus, this characteristic rWnt3a-inducible drop could be confirmed in 2 cell lines.

In summary, all forms of β-catenin were monitored and treatment-induced expression profiles were recorded except for the E-cadherin/β-catenin complex (Figure 21). Thus, the susceptibility of FOCUS cells as a poorly differentiated cell line to the canonical Wnt3a ligand was demonstrated. Furthermore, for the first time the dynamics of β-catenin-mediated Wnt signaling in FOCUS were assembled by the detected changes in the different forms of β-catenin.

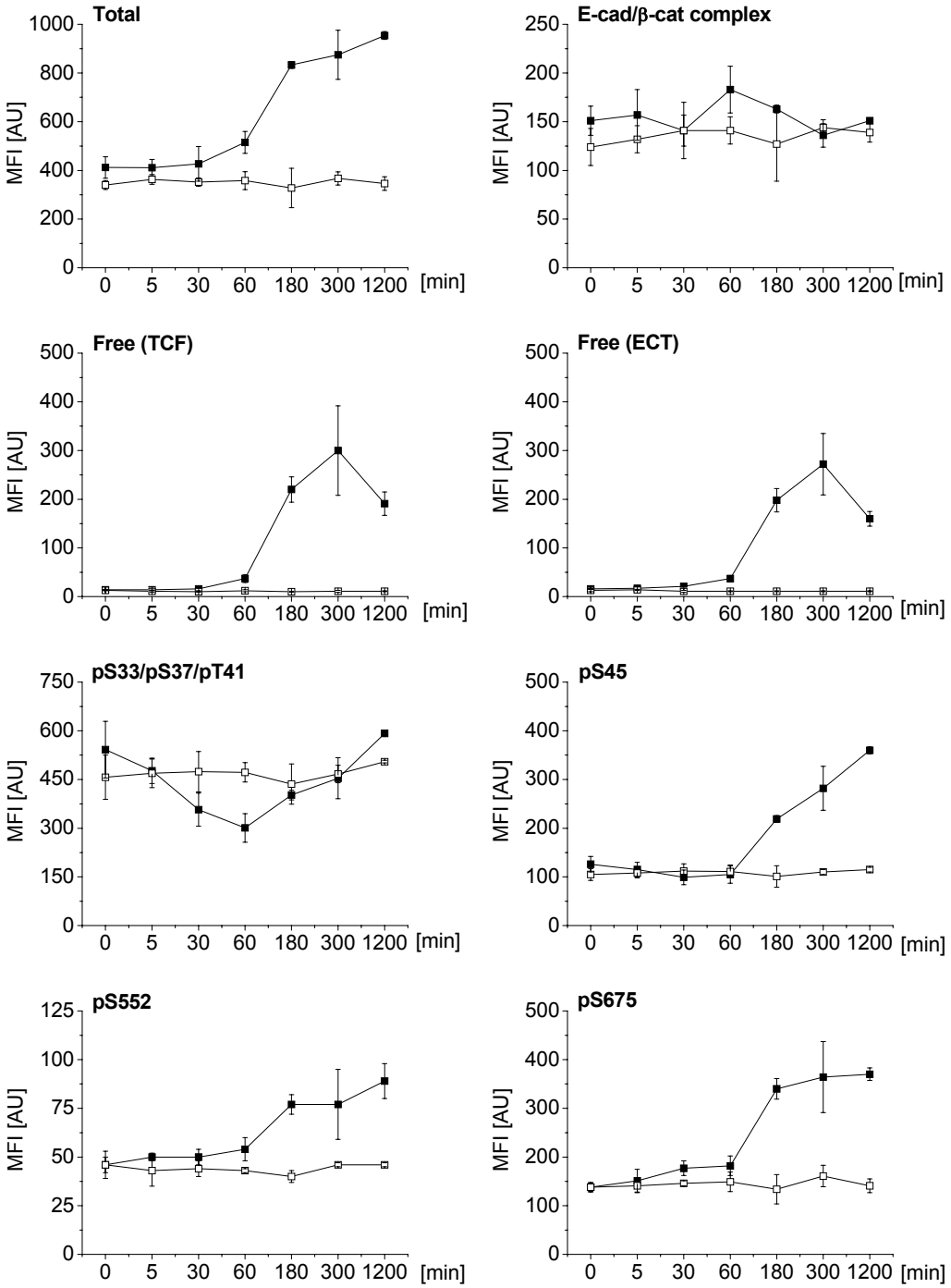

Figure 21 Time-dependent Wnt signaling in FOCUS using rWnt3a.

FOCUS cells were starved for 24 h and then treated with 200 ng/mL rWnt3a (■) or PBS (□) for 5, 30, 60, 180, 300 and 1200 minutes. Each data point represents the average of independent results from 3 cell culture wells. 25 µg of each sample were analyzed using the β-catenin bead array panel. The result is displayed in median fluorescence intensities. An increase of total, free β-catenin captured by GST-TCF4 or GST-ECT and phosphorylated β-catenin pS45, pS552 and pS675 was detected, whereas the amount of β-catenin pS33/pS37/pT41was decreasing within the first 60 min of treatment. The E-cadherin/β-catenin complex did not change under the treatment. Cells treated with PBS did not show alterations regarding all analytes.

3.5 Non-canonical and canonical Wnt signaling in HCC cell lines

The response of HCC cell lines FOCUS and HepG2 to rWnt3a was analyzed as described in 3.4. Beside canonical Wnt signaling, non-canonical Wnt signaling was analyzed in these cell lines on the level of β-catenin (3.5.1) and compared to canonical β-catenin signaling. Subsequent experiments aiming to solve a direct influence between the pathways are shown in 3.5.2.

In contrast to the aforementioned experiments, both cell culture experiments and subsequent assay processing (incubation of beads and sample) were performed in a 96-well cell culture plate. The assays were transferred and further processed as described in 2.7.3 using the KingFisher system. The adaptation of the cell culture experiments to a smaller format and the capability of directly processing the β-catenin bead array panel from cell culture plate to the semi-automated assay protocol allowed to increase the number of biological replicates, to test more perturbations and to simplify and fasten the analysis.

3.5.1 Time-dependent β-catenin signaling in response to Wnt5a

To investigate the response of the HCC cell lines FOCUS and HepG2 to the non-canonical ligand Wnt5a, both cell lines were serum-starved and then treated for 1 h with rWnt5a or rWnt3a. After 1 h of treatment, the cells gradually received control treatments (medium). The samples were analyzed with the β-catenin bead array panel. Detected changes in FOCUS cells are displayed in Figure 22 (●). Since HepG2 cells showed only minor changes, data are not shown.

The already described and characterized canonical Wnt3a-mediated β-catenin signaling in FOCUS and HepG2 constitutes the basis for comparison with the non-canonical rWnt5a-induced response. In general, activation of β-catenin signaling shaped by the accumulation of free β-catenin and characteristic changes in the phosphorylation pattern (see 3.2.1 and 3.4.2) were neither observed in HepG2 nor in FOCUS after rWnt5a treatment. The analysis indeed revealed only minor changes within the range of 0.7 to 1.5 fold changes with reference to the untreated control at t = 0 min. The overall levels of β-catenin did not change notably and E-cadherin-complexed β-catenin remained stable under the treatment in both cell lines.

Nevertheless, for distinct analytes distinguishable trends were monitored on the level of phosphorylation. A slight increase in N-terminally phosphorylated β-catenin pS33/pS37/pT41 was detected in FOCUS. In contrast to the other phosphorylated forms of β-catenin, pS33/pS37/pT41 β-catenin showed enhanced levels after 1 h of rWnt5a treatment.in FOCUS (Figure 22, “0h kinetic”). Furthermore, slightly enhanced levels of pS33/pS37/pT41 β-catenin were detected in HepG2 (data not shown). The recorded pS33/pS37/pT41 levels correlate

well with the non-appearance of free β-catenin in FOCUS. In HepG2, the high level of free β-catenin was not impaired by the rWnt5a treatment (data not shown). In addition, C-terminally modified β-catenin pS675 was found decreased in comparison to the overall levels of β-catenin in FOCUS, while in HepG2 the tendency was implied only (data not shown).

Summing up, it needs to be pointed out that rWnt5a did not induce an active Wnt/β-catenin dynamic comparable to the rWnt3a-mediated response. Levels of pS33/pS37/pT41 as well as pS675 β-catenin showed directly opposing trends in FOCUS (Figure 22) compared to the rWnt3a-induced activation profile measured in HEK293 (3.2.1) or FOCUS (3.4.2), while this trend is identifiable but less pronounced in HepG2 (data not shown).

3.5.2 Does non-canonical Wnt5a impair Wnt3a-mediated activation of canonical β-catenin/Wnt signaling?

Separately performed kinetic experiments revealed differentially shaped responses of β-catenin to Wnt ligands classified as canonical (Wnt3a) and non-canonical (Wnt5a) (3.5.1). Yuzugullu et al. [132] recently proposed that autocrinely expressed non-canonical Wnt5a antagonizes canonical Wnt signaling in HCC cell lines. Since rWnt5a did not activate β-catenin/Wnt signaling on protein level (3.5.1), the question rose whether non-canonical Wnt5a impairs or even abolishes Wnt3a-mediated activation of β-catenin signaling.

Thus, the interference of Wnt5a on Wnt3a-mediated signaling on protein level should be proven with the following experimental set up: FOCUS and HepG2 cells received sequentially rWnt3a for 1 h followed by a time-course treatment with rWnt5a (1/3/5 h) or the other way round. Consistent with separately performed experiments using canonical and non-canonical Wnt ligands, significant changes in β-catenin signaling were only detectable in FOCUS but not in HepG2 (3.5.1). Therefore, results described below are referred to the response measured in FOCUS cells (Figure 22 and Figure 23).

First, pre-treatment with rWnt3a for 1 h did not lead to changes in total β-catenin concentration (Figure 22, 0 h kinetic) which is in line with the kinetic data at the respective time point (Figure 21 and 3.4.2). However, the further treatment with either rWnt5a or medium control showed an increase in total, free and pS45 β-catenin over time. The regarded analytes reached a peak after 3 h of rWnt5a or control treatment, thus 4 h after the initial pulse with rWnt3a. Hence, the rWnt3a pulse led to a detectable activation of β-catenin although the rWnt3a ligand was removed and substituted by either medium only (control) or medium supplemented with rWnt5a. Since signals of control and rWnt5a treatment resembled each other, these data led to the conclusion that rWnt5a does not down regulate an already existing Wnt3a activation signal on the level of β-catenin under the chosen experimental conditions. Regarding pS675 β-catenin, the pulse of rWnt3a did not lead to

enhanced pS675 β-catenin concentration; whereas the Wnt5a pulse (Figure 22) denoted a decrease. Due to the very low signal levels of pS552 β-catenin, no significant changes could be determined.

The second part of the experiment aimed to resolve whether a rWnt5a pulse completely blocks a subsequent rWnt3a-mediated activation of β-catenin signaling or modulates the activation of β-catenin to a certain extent. Basically, FOCUS cells retained their susceptibility to fully activate β-catenin signaling although they were exposed to rWnt5a before (Figure 23). Increased levels of total, free, pS45 and pS675 β-catenin were detected (Figure 23). For all analytes, the maximal concentration was detected after 5 h exposure to rWnt3a. The detected temporal activation profile composed of elevated levels of total, free and the before mentioned phosphorylated forms of β-catenin is consistent with rWnt3a kinetic experiments shown before in 3.4.2. Signal levels of all analytes remained unchanged after the Wnt5a pulse and subsequent medium treatment except pS675 β-catenin denoted a slight decrease (3.5.1). Thus, the pre-treatment with rWnt 5a did not block an activation of the characteristic β-catenin signaling.

Taken together, both experiments demonstrated that canonical Wnt3a signaling was not blocked on the level of β-catenin by the non-canonical Wnt5a in FOCUS cells. An antagonizing effect of Wnt5a on β-catenin and its modifications could not be measured.

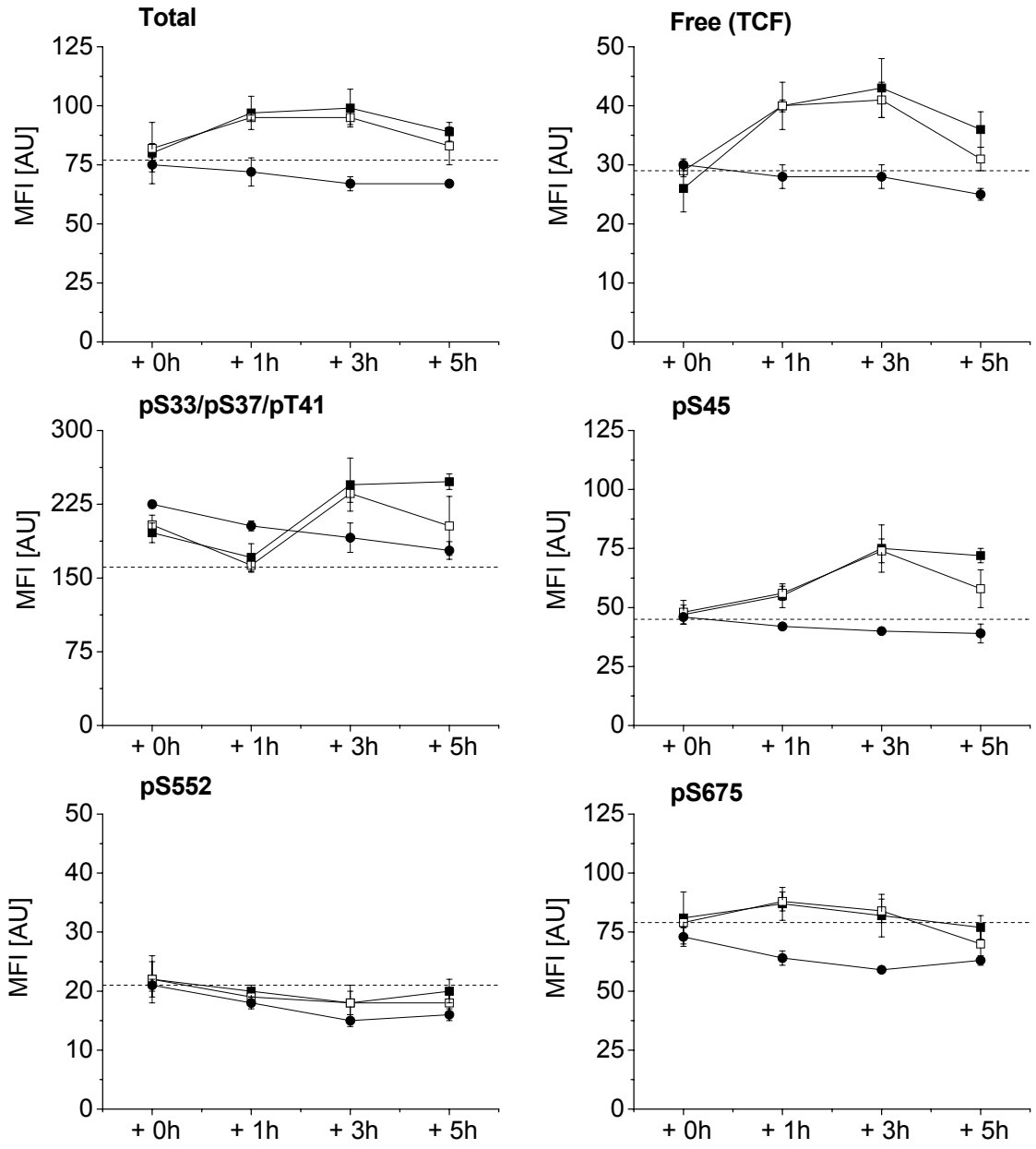

Figure 22 Impact of Wnt5a on Wnt3a-mediated activation of β-catenin signaling in FOCUS.

FOCUS cells were cultured in a 96-well cell culture plate and serum-starved for 24 h. After 1 h of treatment with 200 ng/mL rWnt3a, the medium was removed and cells were gradually exposed to 200 ng/mL rWnt5a (■) or medium as a control (□) for 1, 3 or 5 h. In parallel, cells were pre-treated with 200 ng/mL rWnt5a and then gradually exposed to medium as a control for 1, 3 or 5 h (●). Untreated controls received medium only (dashed line). Each data point represents the average of independent results from at least 3 cell culture wells. Cell lysates were analyzed using the β-catenin bead array panel. Increased levels of total, free (captured by GST-TCF4) and pS45 β-catenin were detected after 1 h of rWnt3a pre-treatment independent of further Wnt5a (■) or control treatment (□). Exposure of rWnt5a as a pre-treatment followed by control treatment (●) did not lead to detectable changes on protein level except pS675 β-catenin. The E-cadherin/β-catenin complex did not change (not shown).

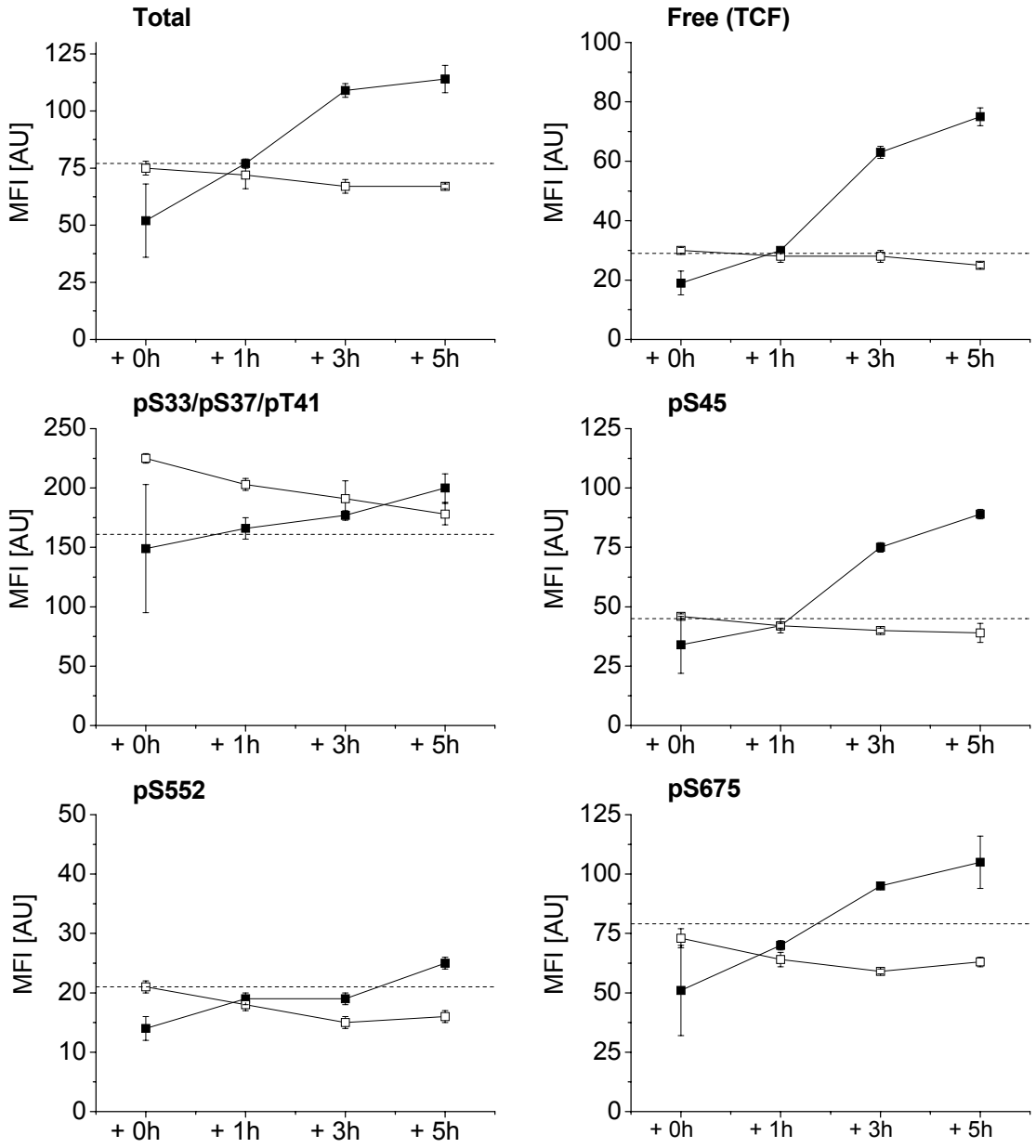

Figure 23 Impact of Wnt5a on Wnt3a-mediated activation of β-catenin signaling in FOCUS.

FOCUS cells were cultured in a 96-well cell culture plate and serum-starved for 24 h. After 1 h of treatment with 200 ng/mL rWnt5a, the medium was removed and cells were gradually exposed to 200 ng/mL rWnt3a (■) or medium as a control (□) for 1, 3 or 5 h. Untreated controls received medium only (dashed line). Each data point represents the average of independent results from at least 3 cell culture wells. Cell lysates were analyzed using the β-catenin bead array panel. Increased levels of total, free (captured by GST-TCF4) and pS45 β-catenin were detected after gradual exposure to rWnt3a, but not after gradual control treatment. The rWnt5a pulse did not block an activation of β-catenin signaling by rWnt3a. The E-cadherin/β-catenin complex did not change (not shown).

4 Discussion

4.1 Development and validation of the β-catenin bead array panel

Assay development

β-catenin is one of the central molecules in Wnt signaling. Its diverse cellular roles are determined by its state of phosphorylation, intracellular localization and extent of binding to proteins such as cadherins [45, 78]. Thus, determining the role played by β-catenin activity in cell adhesion or transcription requires a multi-factorial analysis of its biochemical state. This is usually accomplished using a combination of Western blots, transcription reporter assays and immunohistochemistry. In this thesis a suspension bead array panel was developed capable of measuring simultaneously eight β-catenin issues including four distinct phosphorylated sites, levels of the E-cadherin/β-catenin complex and the amount of free transcriptionally active and total protein requiring sample material in the low µg range. The technical innovation in this work, relative to other suspension bead arrays described previously, is the combination of different assays formats – sandwich immunoassays, co-immunoprecipitation and GST-pulldown – in one array panel. The novel array type is composed of three distinct types of affinity capture (Figure 7): (i) capture of β-catenin with pan- and phospho-specific antibodies (ii) capture of a protein complex using antibodies against E-cadherin and (iii) capture of unbound β-catenin using two biologically relevant binding partners. The detection of transcriptionally active β-catenin was made possible by the adaptation of previously described protein-protein interaction assays [41, 55] to the miniaturized bead-based format using recombinant GST-TCF or GST-ECT as capture molecules.

Assay validation

Several experiments were performed to validate the separate assays. A dilution series of GST-β-catenin lacking posttranslational modifications was performed to test the phospho-specific sandwich immunoassays for unspecific binding and to show the dynamic range of the sandwich immunoassay targeting total β-catenin (3.2.3). Detailed description of the miniaturized co-ip and the accompanying validation protocols are depicted in Poetz et al. [126]. By the cross-validation with conventional methods it was demonstrated that free β-catenin captured by the µ-fishing assay correlated with the fishing experiment and the detected TCF reporter activity (3.2.3 and 3.2.4). In addition, the dynamic range of the µ-fishing assay was demonstrated using a dilution series of activated cell lysates (3.2.4).

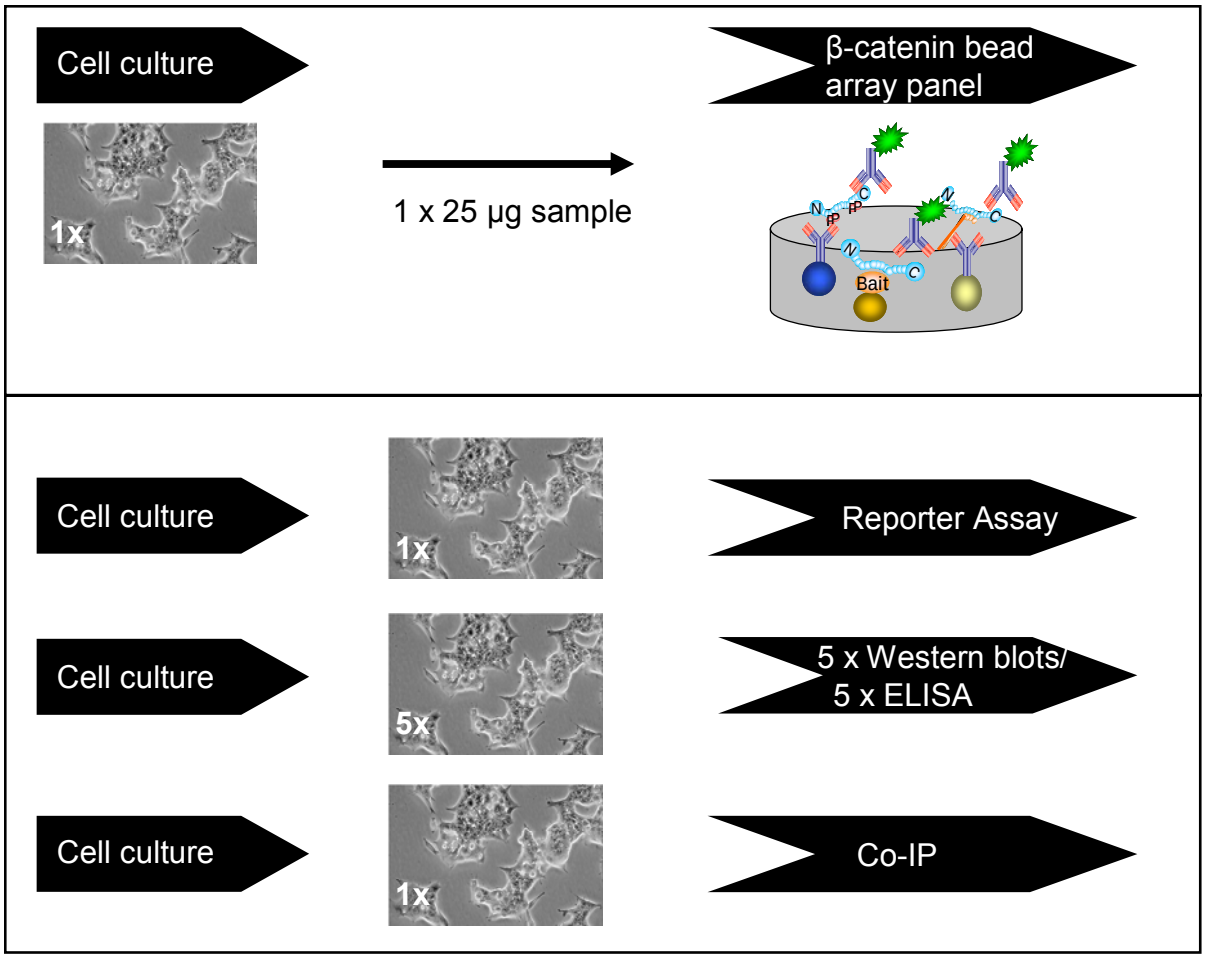

Figure 24 Workflow - from the cell culture experiment to the analysis of β-catenin.

Using conventional methods, separate cell culture experiments of identical conditions need to be performed for each analytical platform. Here, the required amount of sample ranges from 10 – 500 µg cell lysates for each analytical platform and parameter to analyze. For the β-catenin bead array panel, one cell culture experiment is sufficient for the detection of all described parameters requiring only 25 µg of cell lysates of each sample.

Novel type of bead array

The established β-catenin bead array panel for the first time combines the detection of protein abundance, complexation and posttranslational modification of one molecule. Following Ekin's "Ambient analyte theory" [104], the capture molecules of a microarray do not capture analytes from the sample allowing to set up multiplex measurements regardless whether different proteins or different features of one protein are analyzed. Thus, based on the fundamental principle of microarray technology, the simultaneous detection of different features of a protein such as abundance, complexation and posttranslational modification is feasible. As a case study, different forms and functions of β-catenin could be analyzed using the novel type of bead array. In line with the presented novel bead array, Poetz et al. (submitted 2010, *Sequential Multiplex Analyte Capturing for Phospho-Protein Profiling*)

demonstrated previously that different analytes and features including protein abundance and modifications can be measured in a sequential multiplex assay protocol.

Advantages

The multiplex nature of the β-catenin bead array panel eliminates the need to perform separate cell culture experiments and to prepare material for different analytical procedures. Using conventional methods, multiple separate or large scale cell cultures are needed in order to carry out a Western blot, a reporter and a co-immunoprecipitation assay (Figure 24). This leads to the potential for great variability with respect to culturing, the different sample preparation methods and the different read-out systems. These potential sources of error are eliminated in the presented β-catenin bead array panel resulting in comparable data free from biological variability, since all parameters are measured within the same sample. Measurements using the β-catenin bead array panel were highly reproducible (Table 8). The measurement of three independent cell culture wells led to a variability that was below 30%, which includes the variability due to technical and biological issues and sample preparation.

Moreover, low sample consumption (10^5 cells) and minimal hands-on time increased sample throughput compared to standard methods. Multiple time points, stimuli or inhibitor concentrations can be examined using material from 24-well or even 96-well cultured materials. Applied as a screening tool for chemical compounds perturbing the Wnt pathway, for example, the proposed assay could minimize the work load compared to the standard reporter assays and Western blots as previously performed by Huang et al. [136]. Furthermore, indirect visualization of active Wnt signaling *via* green fluorescent protein (GFP) tagged β-catenin or luciferase activity [137] rely on transfection of reporter constructs. Using the β-catenin bead array panel these transfection steps are omitted since endogenous proteins levels and modifications serve directly as indicators for activity.

4.2 β-catenin/Wnt signaling in HEK293

Within this section of the discussion, results generated with HEK293 cells are discussed concurrently with fundamental β-catenin and canonical Wnt signaling dynamics, respectively. Cell type-specific differences and corresponding mechanism detected in hepatocytes and HCC cell lines are further argued basing on the model system HEK293 which is widely used for the investigation of Wnt signaling.

4.2.1 Time-dependent β-catenin/Wnt signaling in HEK293

The analysis of time-dependent rWnt3a treatment and GSK-3 inhibition in HEK293 cells using the established bead array panel revealed novel insights into the dynamics of β-catenin.

Although the detailed mechanism of β-catenin phosphorylation inhibition is still unclear, the data confirm that receptor activation and inhibition of β-catenin destruction machinery leads to an increase in the total amount of β-catenin which is in accordance with literature (current models discussed and reviewed in [138]). For the first time, signaling activity of the β-catenin/Wnt pathway was monitored by the detection of different forms of a single protein, here β-catenin. Detailed time-resolved studies revealed a dynamic phosphorylation pattern of β-catenin after Wnt activation. Furthermore, this thesis demonstrated for the first time that Wnt signaling activity can be measured on protein level using established µ-fishing assay instead of conventional DNA-based reporter assay.

The role of phosphorylated β-catenin within canonical Wnt signaling

For the first time, dynamics of different phosphorylations of β-catenin were monitored simultaneously revealing definite time-courses for inhibitory and activating phosphorylation sites. In Figure 25, the investigated 4 phospho-acceptor sites as well as the corresponding enzymes are depicted according to the current literature.

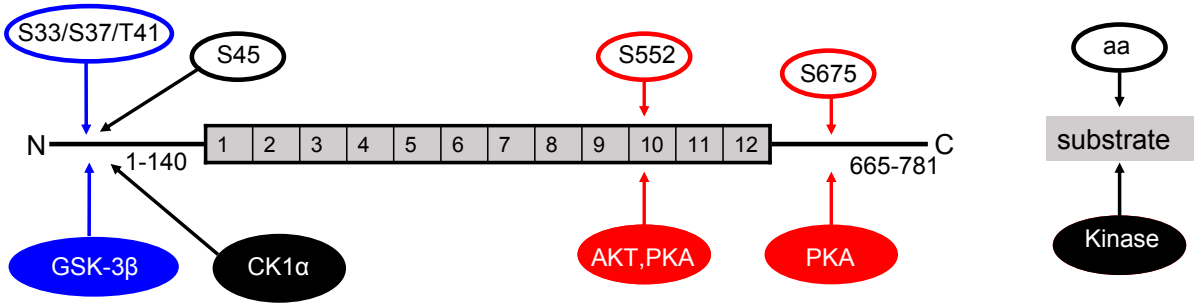

Figure 25 Investigated phospho acceptor sites and the corresponding protein kinase.

Full-length β-catenin is schematically displayed. The four investigated phosphorylation sites as well as their position and the corresponding protein kinases are highlighted. On the right, a legend for the scheme is shown.

Focusing on the inhibitory phosphorylation of β-catenin, both rWnt3a exposure and GSK-3 inhibition transiently reduced the amount of phosphorylated β-catenin pS33/pS37/pT41 (Figure 14 and Figure 15). However, the two stimuli induced differently shaped response curves: A more efficient and enduring reduction of pS33/pS37/pT41 β-catenin was mediated by the organic compound than by the ligand. The strongly decreased amount of S33/S37/T41 phosphorylated β-catenin triggered by the activation of the Wnt pathway at the receptor level or by specific GSK-3 inhibition fits perfectly into the postulated models of the destruction machinery, since GSK-3β mediates the key steps that target β-catenin for proteasomal degradation [54, 56].

Of greater interest is the discovery that levels of β-catenin phosphorylated at S45, S552 and S675 increased concomitantly with a rise in total β-catenin and free β-catenin levels during

both GSK-3 inhibitor and rWnt3a treatment (Figure 14 and Figure 15). Following classical models of the Wnt pathway, S45 phosphorylation by CK1α is performed within the destruction complex and is considered to be a priming event that enhances the affinity of GSK-3β for binding to β-catenin [53, 139]. In contrast to the classical description, Maher and colleagues [140] suggested recently a spatially uncoupled phosphorylation process from the GSK-3 cassette (S33/S37/T41) and S45. Furthermore, they allocated pS45 a potential role of β-catenin being targeted for the nucleus. Using the β-catenin bead array panel, the decrease of pS33/pS37/pT41 β-catenin within the first 60 min of rWnt3a treatment was determined as a characteristic feature of β-catenin phosphorylated at the GSK-3 casette. In contrast rWnt3a-induced changes in pS45 β-catenin occurred not until 1 h of treatment. Thus this data set suits perfectly into the novel model proposed by the Gottardi group. Additionally, similar temporal dynamics of pS45 and free β-catenin were recorded indicating a potential signaling-related or even signaling-promoting role of pS45 β-catenin. But it needs to be pointed out here that this study was focused on a temporal, but not a spatial resolution of β-catenin signaling dynamics. The increase of S45 phosphorylation raises the question of further functions aside from its priming activity as recently discussed [141-143].

The phospho-acceptor sites S45, S552 and S675 of β-catenin are less well characterized and further investigations are needed to precisely determine their regulatory functions. Furthermore, it needs to be investigated whether the observed activation-related phosphorylation events occur in the context of the destruction complex or whether they are spatially or temporally separated. While Taurin et al. [77] propose a PKA-dependent phosphorylation of β-catenin at S675 leading to enhanced transcriptional activity without stabilization of β-catenin, Hino and colleagues [144] showed additionally a stabilizing effect. S552 β-catenin was described as a substrate of AKT [145]. The S552 phosphorylation of β-catenin resulted in stabilization and enhanced transcriptional activity of β-catenin. For the first time, the data generated with the β-catenin bead array panel indicated a link from the modification sites S675 and S552 to canonical β-catenin signaling. After ligand and small molecule induced activation of the pathway these modified forms of β-catenin were found increased over time. Based on the microarray data a stabilizing effect cannot be excluded since both transcriptionally active and C-terminally modified β-catenin levels enhanced concurrently. However, assuming an activation-induced stop of the degradation machinery, the observed increase could merely be due to the accumulation of β-catenin. Thus, it needs to be further investigated whether β-catenin is constitutively phosphorylated at the respective sites after synthesis.

β-catenin and its role as a cell adhesion molecule

In contrast to the alterations detected at the posttranslational modification level, the cell adhesion complex remained unaffected by the treatments over time (Figure 14 and Figure

15). These data suggest that membrane-associated β-catenin is not released from the membrane to function as a transcription co-factor. This issue is discussed in detail in 4.2.2.

Active β-catenin/Wnt signaling and its regulation

Finally, free cytosolic β-catenin, which correlates with transcriptionally active β-catenin, accumulated transiently or linearly over time, depending on the treatment with either rWnt3a or the GSK-3 inhibitor, respectively (Figure 14 and Figure 15). Staal et al. [146] provided evidence that the pivotal event leading to β-catenin/TCF-mediated transcription is not enhanced β-catenin stability, but a signaling-induced β-catenin dephosphorylated at S37 and T41. Consequently, data generated in the context of this thesis are consistent with that model: Here, after Wnt activation augmented concentrations of free β-catenin and concurrently transiently reduced levels of pS33/pS37/pT41 β-catenin were measured. Interestingly, the induction of free β-catenin is temporally delayed compared to the drop of pS33/pS37/pT41 β-catenin levels. This result suggests that the inhibition of the inhibitory machinery is the initial step of the Wnt pathway activation triggering increased concentrations of active β-catenin.

Differences in the kinetics were observed when comparing the time-resolved responses to inhibitor or natural ligand. For instance, after 3 h of inhibitor treatment, the level of free β-catenin was still increasing (Figure 15) whereas for the natural ligand, a steady state had already been reached and the levels were on the decline (Figure 14). In a separate experiment, it could be shown that this signal decrease after 3 h is not due to degradation of the Wnt3a ligand during the time of stimulation (data not shown).

These findings suggest that there are fundamental differences between the mechanisms which control β-catenin levels and dynamics in response to rWnt3a and the GSK-3 inhibitor. Axin2 is a target of the Wnt pathway and is classically reported to be a negative feedback regulator of β-catenin turnover [73, 74]. Gujral and MacBeath [147] further investigated the transcriptional regulation of the Wnt pathway in HEK293 cells and suggested a regulation mechanism divided into an early phase (positive feedback) and a late phase (negative feedback) including the classical Axin-2 feedback. According to their mRNA expression data, the early phase (1-3 h after Wnt3a exposure) is characterized by the up regulation of mediators of active Wnt signaling including β-catenin which is consistent with this study (Figure 14). The involvement of feedback loops might be responsible for the differences between the dynamic changes caused by the small molecule inhibitor and rWnt3a treatment. In the case of rWnt3a stimulation, up regulation of antagonists on the level of the receptor or the intracellular cascade may restore the activity of the destruction complex and trigger a return to the starting equilibrium of β-catenin turnover. In contrast, the usage of a GSK-3 inhibitor does not activate components upstream of the destruction complex, but only

releases β-catenin as one component of active Wnt signaling which might not be powerful enough to induce the complete feedback response.

In summary, time-resolved dynamics of β-catenin/Wnt signaling in HEK293 were recorded for the first time in a multiparametric assay set up providing insights into the mechanism of Wnt signal transduction by detected accumulation of free active β-catenin as well as a sophisticated phosphorylation pattern of β-catenin. Apart from well-investigated modifications C-terminal phospho-acceptor sites S552 and S675 were recorded and found to increase in concurrently with active β-catenin signaling.

4.2.2 Origin and characteristics of active β-catenin signaling in HEK293

The interplay between E-cadherin/β-catenin-mediated cell adhesion and β-catenin-dependent Wnt signaling is still controversially discussed since both intersection and separation of the two pathways have been shown up to now. Birchmaier and Heuberger addressed this complicated issue currently in a comprehensive review [51].

Results generated using the β-catenin bead array panel contributed to this discussion on the one hand by providing evidence that the E-cadherin/β-catenin complex remains stable upon Wnt activation even if protein biosynthesis was blocked by cycloheximide. Reduction of the amount of the E-cadherin/β-catenin complex was not monitored. Therefore the E-cadherin-bound fraction of β-catenin was neither impaired nor released from the membrane or recruited for signaling (Figure 16).

On the other hand, it could be demonstrated that activated Wnt signaling is mediated by a signaling inducible pool of β-catenin which comprises free β-catenin as well as β-catenin phosphorylated at S45, S552 and S675. The ligand or enzyme inhibitor triggered activation of β-catenin signaling was completely blocked by the inhibition of protein synthesis. In this case the abovementioned forms of β-catenin were absent (free β-catenin) or remained unchanged (phosphorylated β-catenin). For the first time, a panel of active β-catenin forms could be defined by the time-resolved studies and further verified by the cycloheximide experiment.

However, the experimental set up does not allow to conclude about potential posttranslational modifications of transcriptionally active β-catenin. Enhanced transcriptional activity of β-catenin was recently linked to β-catenin phosphorylated at S675 and S552 induced by Forskolin treatment [77]. Data generated in the context of this thesis provide evidence for a direct link between activation of the Wnt pathway and the occurrence or increase of pS675 and pS552. Although the distinct roles of β-catenin pS675 and pS552 as well as the conducting enzymes remain unclear, their involvement in mediating active Wnt signaling could be stressed by the cycloheximide experiment.

In contrast to this data set, several groups reported about a Wnt-inducible membrane association of β-catenin. Yokoyama et al. [129] presented Western blots of subcellular fractions after Wnt activation which contained an increased amount of total β-catenin in the membrane fraction. Using reporter assays and immunofluorescence-based techniques Hendriksen et al. [128] proposed that a dephosphorylated fraction of β-catenin is recruited to the membrane after Wnt activation to generate a signaling active form there. It needs to point out here that within this thesis the membrane-bound fraction of β-catenin was directly measured by the detection of the E-cadherin/β-catenin complex. During all experiments in HEK293 cells, the levels of this complex remained unchanged. In contrast to the described direct complex detection, the abovementioned approaches used the membrane staining or subcellular fractionation analyzed by Western blotting to analyze the membrane fraction of β-catenin, but no co-immunoprecipitation.

In contrast, Gottardi and co-workers proposed a model of two independent pools of β-catenin. Following this model, Wnt activation generates an active form of β-catenin which is targeted for signaling by a molecular fold-back mechanism [41]. This active form favorably binds TCF, but not ECT. Using the μ-fishing assay, the suggested Wnt3a-induced differences in the detection of free β-catenin captured by GST-ECT and GST-TCF4 could not be confirmed. The amount of free β-catenin (Figure 14 and Figure 15) captured by either GST-ECT or GST-TCF4 was in a comparable range. Differences between the detected signal intensities by the two bait proteins GST-ECT and GST-TCF4 after GSK-3 inhibition were found in the microarray validation experiment (Figure 9). Taken together, the data sets did neither clearly confirm nor negate the proposed model. It needs to be further investigated whether these differences are due to the different activation mechanisms.

Furthermore, the same group recently reported about a link between posttranslational modification and regulation of signaling activity of β-catenin [140]. According to that model, only β-catenin dephosphorylated at S33/S37/T41 and S45 is able to bind ECT, but not β-catenin carrying the respective modifications. The second model of the Gottardi group [140] does not contradict the microarray data; it rather explains with respect to the GSK-3 phosphorylation sites that a comparable increase in free β-catenin was captured by both GST-ECT and GST-TCF4. If an active form of β-catenin is rescued from the destruction complex after Wnt activation, it consequently lacks phosphorylation at S33/S37/T41 and can be detected by both capture proteins equally. However, basing on the microarray data a signaling-related function of pS45 β-catenin can not be excluded since similar dynamics of free and pS45 β-catenin were detected.

The E-cadherin/β-catenin interaction was found to be under the control of tyrosine kinases and phosphatases (reviewed in [44]). For instance, β-catenin phosphorylated at Y142 strengthens Wnt signaling activity and at the same time permits the binding of α-catenin [50].

The Y654 phosphorylation of β-catenin reduces cadherin binding and adhesive function [49], but could not be linked to active β-catenin signaling. Due to a lack of a suitable antibody directed against pY654 β-catenin, this modified form of β-catenin could not be analyzed with the β-catenin bead array panel. A suitable capture antibody for pY142 β-catenin was available and tested within the β-catenin bead array panel, but only low signal levels were obtained. In summary, the monitoring of β-catenin phosphorylated at pY142 and pY654 might provide novel insights into the regulation of the E-cadherin/β-catenin complex on the level of posttranslational modification.

4.3 β-catenin/Wnt signaling in primary mouse hepatocytes

4.3.1 Time-dependent β-catenin/Wnt signaling in primary mouse hepatocytes

Experiments aiming to monitor Wnt signaling activity and to resolve the origin of a signaling active pool of β-catenin in primary mouse hepatocytes revealed an attenuated, less pronounced response to rWnt3a and to the GSK-3 inhibitor compared to HEK293 or FOCUS, respectively.

In Figure 26, selected results of the rWnt3a treatment of HEK293 (3.2.1), FOCUS (3.4.2) and primary mouse hepatocytes (3.3.1) are displayed as x-fold changes (treated/untreated at t = 0 min) over time. Note that different time points for the analysis of the long-term effect were chosen for FOCUS (20 h) and hepatocytes/HEK293 (10 h). HepG2 data were omitted since only minor changes were detected. Strikingly different fold changes were recorded regarding free β-catenin (Figure 26A). Both FOCUS and HEK293 responded transiently in a comparably shaped activation curve, while hepatocytes lack a ligand induced definite pulse of detectable free β-catenin. Recorded dynamics of β-catenin targeted for proteasomal degradation uncovered the strongest response in HEK293 which correlated temporarily with changes detected in FOCUS (Figure 26B). In hepatocytes the transient decrease was only weakly denoted. However, changes in total β-catenin revealed smaller differences between the analyzed cell types (Figure 26C). Taken together, the comparison of relative changes over time underlined that conserved molecular mechanisms are involved in active β-catenin signaling. Differences between primary cells and cell lines need to be further investigated.

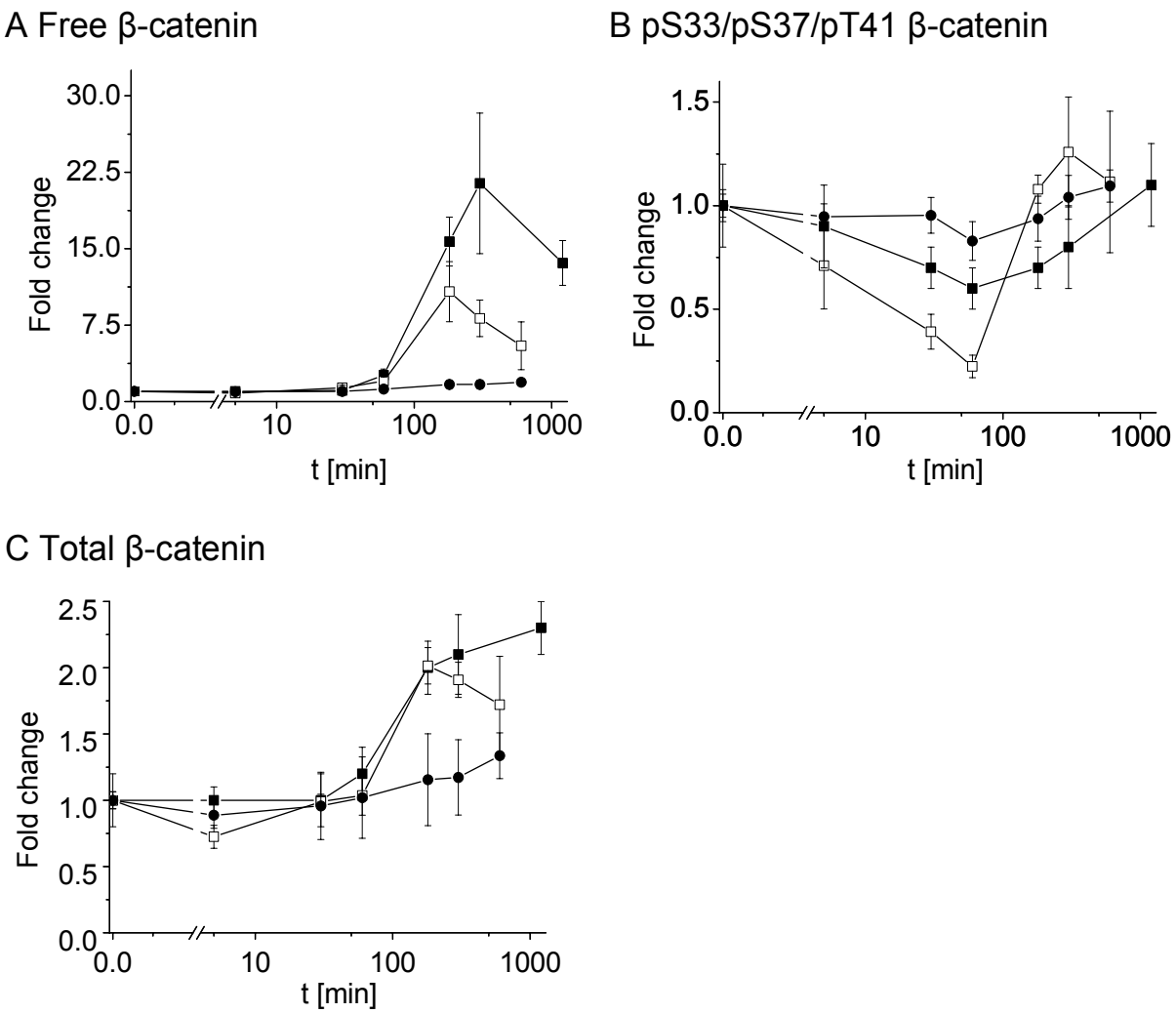

Figure 26 Comparison of rWnt3a-induced β-catenin signaling in different cell types.

The responses of HEK293 (□) and FOCUS (■) cells as well as primary mouse hepatocytes (●) to rWnt3a were analyzed as shown in 3.2.1, 3.3.1 and 3.4.2. The average of 3 independent experiments was calculated and displayed as ratios (treated/untreated at time = 0 min). The relative changes are displayed for (A) free, (B) pS33/pS37/pT41 and (C) total β-catenin. Note that different time points for the analysis of the long-term effect were chosen for FOCUS (20 h) and hepatocytes/HEK293 (10 h).

Since hepatocytes express a relatively high amount of total β-catenin, the question was raised why only a small amount of free β-catenin was detectable after pathway activation either by rWnt3a treatment or GSK-3 inhibition. On the one hand, the absence of a detectable strong pulse of free β-catenin might be due to the binding properties of the bait proteins GST-ECT and GST-TCF4. It is conceivable that the used bait proteins could capture instead of β-catenin another Armadillo protein such as γ-catenin (plakoglobin) in primary mouse hepatocytes only, but not in the cell lines. This could be due to potential differences in expression, complexation and posttranslational modification. Although the contribution of plakoglobin to the Wnt pathway is not yet clear, plakoglobin was found to be implicated in

Wnt signaling acting as a transcriptional activator together with TCF/LEF factors in HEK293 cells [148] or as a competitor of β-catenin/TCF4 mediated signaling transcription [149].

Furthermore, spatial and temporal differences in complex formation with proteins involved in Wnt signaling could result in a reduced amount of free β-catenin being released after activation in hepatocytes compared to the cell lines. In general, cell type specific protein abundance and posttranslational modification play a role in protein complex formation and thus, might cause significantly different levels of detectable free β-catenin independent of the presence or absence of a Wnt trigger. It is known, for instance, that after Wnt activation various transcriptional regulators bind to C-terminal β-catenin in the nucleus (reviewed in [59]). To improve the detection of free β-catenin in hepatocytes, primary mouse hepatocytes were stimulated with the GSK-3 inhibitor SB216763 and were lysed under different conditions in order to release proteins potentially bound to β-catenin (Supplementary material 8.3). Thus the experiment aimed to resolve whether β-catenin's association to further interaction partners after activation might cause the low signals. In summary, different lysis conditions did neither improve the detection nor provide further indications of a masked free β-catenin in hepatocytes.

With respect to the expected phosphorylation patterns observed in activated or non-activated cells, the detected low basal level of pS33/pS37/pT41 β-catenin compared to FOCUS or HEK293 (3.2.1 and 3.4.2) is worth to discuss. Higher levels of E-cadherin-complexed β-catenin (Supplementary material 8.2) were coincidentally measured with low basal levels of pS33/pS37/pT41 β-catenin in normal hepatocytes. This result is directly opposed to the low detectable amount of E-cadherin/β-catenin complex (Supplementary material 8.1 and 8.2) and high pS33/pS37/pT41 β-catenin levels monitored in FOCUS and HEK293 cells. Thus, the result suggests that a high basal level of pS33/pS37/pT41 β-catenin (FOCUS and HEK293) supports a fast and more pronounced induction of free β-catenin since a single inhibition step (GSK-3) might be sufficient. In hepatocytes, pS33/pS37/pT41 β-catenin was detected in lower concentrations. Consequently these cells lack a pool of β-catenin for fast pathway activation. This activation was rather performed in an attenuated manner indicating a more complex multi-parametric β-catenin signaling in hepatocytes. Taken together, hepatocytes show a similar response compared to the cell lines, albeit differing with respect to the extent of activation (free β-catenin) and inhibition of degradation (pS33/pS37/pT41 β-catenin levels).

With respect to the other phosphorylated forms of β-catenin, basal levels detected in primary mouse hepatocytes did not differ significantly compared to HEK293 and FOCUS cells, but the measurement revealed only minor changes after treatment. Interestingly, the differences between the activation profiles generated by either ligand or inhibitor treatment differed more strongly than observed in HEK293. Ligand-mediated activation denoted a sustained

response in hepatocytes even after 10 h of treatment, while the GSK-3 inhibition indicated a transient activation curve.

Apart from the activation mechanism (ligand or inhibitor), differences in duration and dynamics of active β-catenin signaling might also be caused by liver specific drug metabolism targeting small molecules such as the GSK-3 inhibitor SB216763. The hepatocyte is specialized for the s metabolism of xenobiotics and thus could dramatically influence the detected Wnt response by metabolizing the activation trigger. Additionally, as recently shown the GSK-3 inhibitor itself affected the expression of drug metabolizing enzymes [150]. Thus, the application of small molecules could induce unexpected changes in the liver metabolism beyond Wnt signaling affecting indirectly GSK-3 as a central enzyme of various pathways (reviewed in [139]).

4.3.2 Origin and characteristics of active β-catenin signaling in primary mouse hepatocytes

In line with the HEK293 data, cycloheximide pre-treatment abolished a ligand or inhibitor mediated increase in free β-catenin in primary mouse hepatocytes. Thus, it was shown that the investigated primary and transformed cells exhibit a comparable activation mechanism which depends in both cases on *de-novo* synthesis of β-catenin. Although fluctuating signals of the E-cadherin/β-catenin complex were detected in this experiment, the stability of the E-cadherin/β-catenin complex was reliably shown in the time-course experiments (3.3.1).

In contrast to the signaling active pool observed in HEK293, the detected activation in hepatocytes is limited to free β-catenin since only minor changes in phosphorylated β-catenin were found. Ambigous results were gained regarding total β-catenin which did not allow to draw a conclusion. These observations are consistent with the time-course experiment (3.3.1) which manifested only minor x-fold changes at the respective time point of 3 h. Thus, it was not possible to draw a conclusion whether the investigated phosphorylated forms of β-catenin can be allocated to the panel of β-catenin activated forms which mediate the activation dependent of biosynthesis in hepatocytes.

4.4 β-catenin/Wnt signaling in human HCC cell lines

4.4.1 HepG2 – model system for hepatocytes harboring an activating β-catenin mutation

The analysis of β-catenin signaling in HepG2 cells offered the opportunity to use a model system of HCC harboring an activating mutation in the *CTNNB1* gene. HepG2 cells express a small pool of wild type β-catenin and a huge fraction of truncated β-catenin ([151] and Figure 27). The β-catenin bead array panel was used to investigate the two pools separately thereby taking advantage of the different methods included in the array panel.

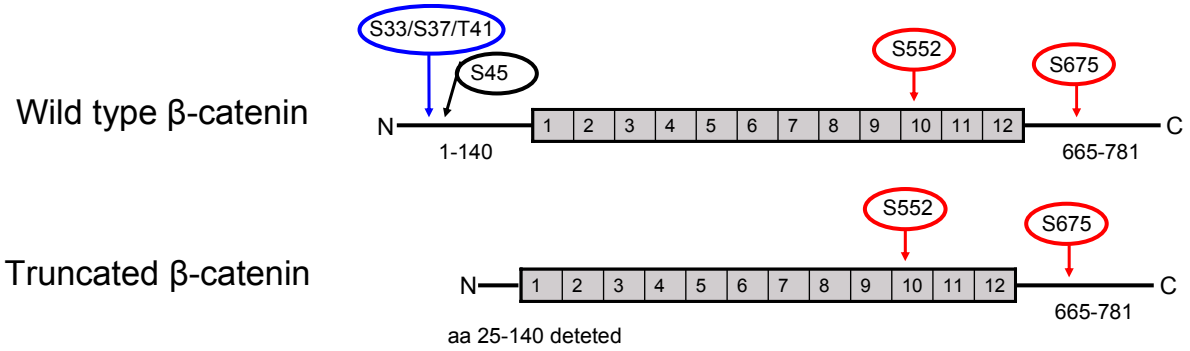

Figure 27 Wild type and truncated β-catenin in HepG2.

Both wild type and truncated β-catenin are displayed including the analyzed phosphorylations sites. Truncated β-catenin lacks the N-terminal regulation sites (GSK-3 casette S33/S37/T41).

First taking advantage of the properties of the µ-fishing assay, the assumed high basal level of accumulated free β-catenin was clearly demonstrated in unperturbed HepG2 cells (Figure 20). Detected basal levels of free β-catenin were 100 to 200 fold higher compared to FOCUS or HEK293 cells. The truncated form of β-catenin was expected to accumulate in the cytosol as the N-terminal regulation sites are missing. Interestingly, this high cytosolic pool of β-catenin seems to be mainly non-complexed since high signals were monitored with the µ-fishing assay. The GST-pulldown-related µ-fishing allows to detect exclusively the unbound form of a protein (here the active form of β-catenin), while conventional, average based methods such as Western blots and sandwich immunoassays measure the overall levels of a protein in a complex sample. For the first time, the constitutive accumulation of an active form of β-catenin resulting from the deletion of the regulatory site could be confirmed on protein level using the µ-fishing assay. The result is consistent with previous studies showing constitutive activation of the Wnt pathway on transcriptional level *via* TCF reporter activity in HepG2 [152]. Zeng et al. further demonstrated that the observed constitutive reporter activity can be downregulated by siRNA-mediated knockdown of the *CTNNB1* gene in HepG2 cells.

Since HepG2 express normal total β-catenin levels but enhanced free β-catenin, the μ-fishing data underlines that free, but not total β-catenin is correlated with enhanced transcriptional activity. By the detection of free β-catenin in a time-course experiment, it was demonstrated that HepG2 cells are still susceptible to rWnt3a. As a long-term response an increase in free β-catenin was monitored (Figure 20). But it needs to be pointed out that free, wild type β-catenin potentially induced by the rWnt3a treatment cannot be distinguished from the constitutively present truncated form of β-catenin here.

Apart from the accumulated free β-catenin, a relatively high basal level of C-terminally phosphorylated β-catenin was detected in HepG2 (Figure 20). Although direct evidence is lacking, this indicates that truncated free β-catenin might be constitutively phosphorylated at the regarded C-terminal phosphorylation sites. Otherwise, changes in distribution or complexation of β-catenin due to the constitutively active β-catenin could lead to a higher level of pS552 and especially pS675 β-catenin. Using the established assay set up, an experimental verification was not possible.

The measurement of pS45 and pS33/pS37/pT41 β-catenin on the one hand provided evidence of the presence of a wild type pool and on the other hand underlined that a functional degradation machinery is present in HepG2 (Figure 20). Thus, although the pathway is constitutively activated by the mutation in the *CTNNB1* gene, the remaining wild type pool was shown to be regulated. A high level of pS33/pS37/pT41 β-catenin and low amount of pS45 β-catenin led to the assumption that the wild type pool of β-catenin is down regulated constantly and does not react to the extracellular canonical activation signal – here the rWnt3a ligand. It cannot be excluded that wild-type β-catenin signaling HepG2 cells is kept low by additional regulation mechanisms independent of GSK-3.

In summary, the analysis of β-catenin signaling in HepG2 provided snapshots of canonical β-catenin-mediated Wnt signaling as a model system for HCC cells with a hyper-activated Wnt pathway. However, measurements of different forms of β-catenin revealed an idea of altered cellular signaling due to a *CTNNB1* mutation, but they do not provide insights into feedback loops or target gene expression probably differing between cells exhibiting a normal or hyper-activated Wnt signaling. To obtain a complete description of this prototypic cancer cell transcriptional activity and the associated phenotypic responses such as migration or proliferation need to be measured and added to the protein data set of this thesis.

4.4.2 FOCUS - model system for hepatocytes undergoing EMT

In principle, rWnt3a-activated FOCUS cells exhibited dynamic changes comparable to HEK293 cells: the response to rWnt3a comprised the same panel of altered β-catenin forms – a signaling active pool. Taken together, an exact match of activated forms of β-catenin was

demonstrated by monitoring of time-resolved β-catenin activation in two cell lines harboring wild type β-catenin. To be precise an enhanced amount of active free β-catenin as well as increased levels of pS45, pS552 and pS675 and total β-catenin were found concordantly.

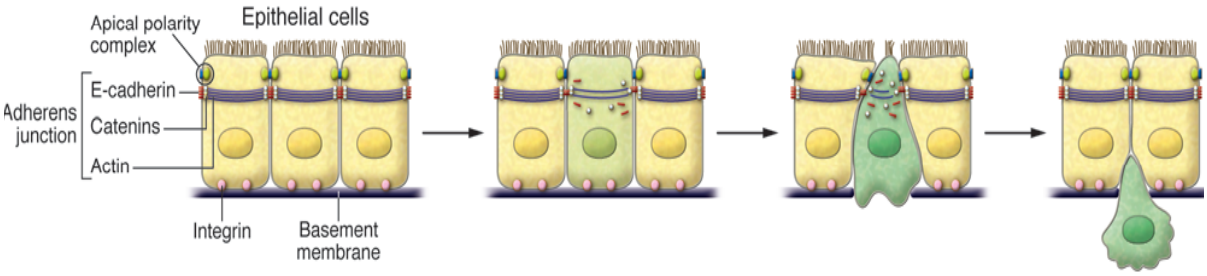

Figure 28 Cellular rearrangements during EMT.

(1) Normal epithelial cells are polarized and form cell adhesion complexes. (2) The loss of adhesive properties is induced by the reduction of E-cadherin levels. (3) Cytoskeleton remodeling causes changes in cellular structure and induces changes in the cell layer. (4) The cells gain invasive properties and leave the cell layer. Source: [153]

The cell line FOCUS was used as a model system of HCC cells having lost normal E-cadherin expression and concurrently undergoing EMT [154]. According to literature the HCC cell lines were characterized as mesenchymal (FOCUS) or epithelial (HepG2) cell types based on their expression of E-cadherin and vimentin [132, 154]. EMT is considered as an early step in cancer metastasis, since cancer cells need to separate from the tumor to invade the circulatory systems and afterwards the healthy tissue [155]. Cells discard their E-cadherin-mediated cell-adhesion properties and gain at the same time altered contact properties and motility.

Consistent with the current literature [154], low E-cadherin expression was confirmed by the measurement of the E-cadherin/β-catenin complex (3.4.2 and 8.2). Since the overall levels of β-catenin in FOCUS cells were not found augmented in unperturbed cells (3.4.2 and 8.1), the cells need presumably to compensate the reduced amount of membrane anchor by differences in the turnover of β-catenin compared to normal cells. In this study it could be demonstrated on protein level that the mere loss of E-cadherin does neither rearrange the distribution of β-catenin nor activate Wnt signaling in FOCUS cells. Although no subcellular fractionation experiments were perfomed, the analysis using the β-catenin bead array panel allows indirectly to analyze β-catenin`s cellular distribution. The E-cadherin/β-catenin was detected over time. The data suggested a low, but stable E-cadherin/β-catenin complex in FOCUS. Free β-catenin was measured in untreated and treated cells as an indicator for active β-catenin in the cytosol. However, free β-catenin was only found in Wnt-activated FOCUS cells. Consistent with this data, among others Kuphal and Behrens [156] demonstrated that loss of E-cadherin only enhanced transcriptional activity when cells

additionally harbor an activating mutation in one component of the Wnt pathway. Regarding FOCUS cells, a mutation in genes directly involved in the Wnt pathways is currently not known.

In general, EMT is characterized by the loss of E-cadherin-mediated cell adhesion and concurrently by an enhanced expression of mesenchymal markers such as N-cadherin [155]. Since β-catenin is able to bind both E- and N-cadherin, membrane-binding of β-catenin is maintained when cells undergo EMT. This change between the membrane anchors of β-catenin was described as “cadherin switch” in the context of melanoma [157]. In order to obtain a complete picture of E- and N-cadherin abundance in the investigated cell types, N-cadherin/β-catenin complexes were measured additionally in the cell lines (Supplementary material 8.2). All 3 cell lines revealed a low amount of N-cadherin/β-catenin complex. Thus, although FOCUS was classified as a mesenchymal cell line, an enhanced N-cadherin/β-catenin complex formation could not be detected. The involvement of Wnt signaling in the process of E-cadherin down regulation is topic of current research [158].

Due to the low basal level of free β-catenin and the high amount of phosphorylated β-catenin at S33/S37/T41 in the non-activated FOCUS cell (Figure 21), this data suggests a hypothetic scenario of an enhanced β-catenin turnover compared to normal cells in order to keep the cytosolic level low. When the pathway is activated by a canonical Wnt ligand, the destruction machinery seems to be inhibited in a comparable manner as detected in HEK293 (Figure 14).

The monitored time-resolved β-catenin signaling demonstrates that FOCUS as a model system for poorly differentiated HCC cells with enhanced EMT status maintained its susceptibility for the canonical Wnt3a ligand and the activation of the Wnt pathway on the level of β-catenin.

4.5 Non-canonical canonical Wnt signaling in HCC cell lines

Time-resolved Wnt/β-catenin signaling in response to the canonical Wnt3a ligand was monitored in FOCUS using the β-catenin bead array panel. Yuzugullu et al. [132] proposed a selective activation or repression of canonical Wnt signaling dependent on the absence or presence of autocrinely expressed non-canonical ligands in well-differentiated or poorly differentiated cell lines, respectively. Thus before discussing the detected Wnt signaling activity in FOCUS and HepG2, both cell lines were proven for expression of basic components involved in Wnt signaling. On mRNA level Wnt5a was shown to be autocrinely expressed by FOCUS cells, while HepG2 lack this prototypic non-canonical ligand (Supplementary material 8.4, unpublished data provided by Taranjit Gujral, Harvard Medical School, [132]). Thus, it needs to be taken into account that differentially expressed Wnt ligands might influence Wnt signaling in unperturbed cells as well as in activated cells.

Furthermore, the expression of Wnt receptors and co-receptors as a pre-requisite for Wnt signaling was shown (Supplementary material 8.4 and [132]). Here, the 2 cell lines differed only significantly in the expression of *FZD2,* which was found several hundred fold higher expressed in FOCUS compared to HepG2 (Supplementary material 8.4). With regard to *FZD2*, Boutros et al. [159] reported about the importance of *FZD2* in Drosophila regarding active β-catenin signaling.

Focusing first on the unperturbed β-catenin signaling in HCC cells, low β-catenin signaling activity was measured in FOCUS and a high amount of free β-catenin monitored in HepG2 (3.4.1 and 3.4.2). Here, profiled β-catenin status on protein level correlate well. However, the status of β-catenin signaling in unperturbed FOCUS and HepG2 cells seems to be caused by the mutation status regarding *CTNNB1*, but not by distinct autocrinely-mediated Wnt signaling depending on the differentiation state of the HCC cell lines [132].

In contrast to their hypothesis [132], indeed a response of FOCUS cells exposed to rWnt3a was measured on the level of β-catenin. Thus, it could be demonstrated that the autocrine expression of Wnt5a itself did not impair Wnt signaling on the level of β-catenin (4.4.2). The signaling activity measured on protein level reflects in both cell lines rather the mutation status regarding *CTNNB1* than allows to draw conclusions about repression of Wnt activity by differently expressed autocrine Wnt ligands. Beside this ligand-based view of Wnt signaling transduction, a favorable receptor expression might support the fast response to rWnt 3a in FOCUS independent of their autocrine Wnt 5a expression.

In order to elucidate a Wnt5a involvement in β-catenin signaling in FOCUS and HepG2, first the effect of Wnt5a on protein level was investigated. A second approach focused on the resolution of a direct interference of Wnt3a and Wnt5a signaling impinging on β-catenin in the regarded cell lines.

4.5.1 Time-dependent β-catenin signaling in response to Wnt5a

The effect of rWnt5a on β-catenin signaling in FOCUS and HepG2 was recorded revealing cell type-specific responses. The different forms of β-catenin in HepG2 remained mainly unchanged or slightly changed only, while alterations in the phosphorylation pattern of β-catenin were observed in FOCUS (3.5.1).

First, rWnt5a failed to change the overall levels of β–catenin. rWnt5a did neither lead to an increase of total β-catenin similar to a rWnt3a-mediated response, nor reduced the overall levels as an opposed cellular response. It was reported that Wnt5a promotes a GSK-3 independent degradation mechanism which regulates β-catenin stability under APC and Siah involvement [95]. This model is in contrast to data sets generated with FOCUS and HepG2

cells which both show stable overall levels of β-catenin. In HepG2, even levels of truncated free β-catenin remained unchanged.

Second, β-catenin marked for proteasomal degradation (pS33/pS37/pT41) was modestly enhanced in FOCUS (Figure 22). Regarding this posttranslational modification of β-catenin, rWnt3a and rWnt5a respectively induced a directly opposed response on the level of posttranslational modification. While rWnt3a led to a transient decrease of pS33/pS37/pT41 β-catenin, rWnt5a induced a slight transient increase (1h treatment). Furthermore, the absence of free β-catenin in FOCUS is in line with the enhanced pS33/pS37/pT41 levels. This result led to the assumption that an antagonizing effect might exist, albeit a direct or indirect involvement needs to be further discussed.

Third, levels of C-terminally phosphorylated β-catenin pS675 were transiently reduced in FOCUS cells after rWnt5a treatment (3.5.1). As shown in HEK293 (3.2.1), a correlation between active β-catenin and increased pS675 β-catenin levels after rWnt3a treatment was demonstrated. Furthermore, the regarded C-terminal modification was proposed to enhance transcriptional activity [77, 145].

Regarding the rWnt5a-induced decrease of pS675 β-catenin, an interference with transcriptional activity cannot be excluded. In addition, Ishitani et al. [94] demonstrated that Wnt5a negatively regulates TCF/β-catenin transcriptional activity *via* Wnt5a/Ca^{2+} pathway and the kinases TAK and NLK without impairing protein stability of β-catenin. A potential decrease of transcriptional activity after rWnt5a treatment was not detectable with the µfishing assay since basal levels of free β-catenin were per se low in unperturbed FOCUS cells. In order to connect results on protein level with pathway activity, TCF/β-catenin reporter assays are needed to underline or to reverse the detected indications.

4.5.2 Does non-canonical Wnt5a impair the Wnt3a-mediated activation of canonical β-catenin/Wnt signaling?

The rWnt5a mediated response in FOCUS and HepG2 was analyzed on the level of β-catenin and compared to the rWnt3a induced activation. The result did not indicate a single activated analyte, but changes in the phosphorylation pattern were detected. Thus, the question was raised whether Wnt 5a has a negative effect on active β-catenin signaling. To gain insights into a direct interference of Wnt5a in Wnt3a signaling, cell culture experiments were performed by sequential exposure of HepG2 and FOCUS cells with rWnt3a and rWnt5a. Effects on β-catenin signaling were analyzed on protein level using the β-catenin bead array panel.

As expected, only β-catenin signaling in FOCUS revealed significant changes. The first experiment aimed to show whether rWnt5a impairs or even down regulates an existing

activation of β-catenin. The pulse of rWnt3a led to a complete activation of all β-catenin features in FOCUS as described in 3.4.2. Here, it was clearly shown that rWnt5a does not block an ongoing activation process on protein level.

Taken together, separately recorded activation profiles of β-catenin in response to canonical and non-canonical Wnt signaling correlated well with the combined experiment in FOCUS. Levels of total, active and phosphorylated β-catenin – regardless of its role as an activating and inhibitory modification – support this model. The data set suggests that Wnt5a is not able to diminish existing β-catenin activation directly on protein level under the chosen experimental conditions. Interestingly, the rWnt5a pulse treatment (1 h pre-treatment) reduced pS675 β-catenin levels (Figure 22).

Additionally, inversely performed cell culture experiments demonstrated that rWnt5a exposure did not block a subsequent rWnt3a-mediated activation of β-catenin (Figure 23). Although pre-treated with the non-canonical rWnt5a, FOCUS cells exhibited a complete activation of β-catenin. Thus, neither a blockade nor a reduction of active β-catenin signaling was monitored. Taken together, neither autocrine Wnt5a expression nor rWnt5a treatment interferes detectably with β-catenin signaling. From the ligand-based view of Wnt signaling, it needs to be pointed out that a negative influence of the non-canonical Wnt5a ligand on β-catenin signaling could not be shown.

However, directly opposed changes in β-catenin pS33/pS37/pT41 and pS675 in response to rWnt3a and rWnt5a led to the assumption that there is a link between canonical and non-canonical Wnt signaling. The data does not clarify whether ligand-induced signals directly impinge on β-catenin or for instance influence transcriptional activity of β-catenin signaling *via* separate signaling pathways. Since modifications of β-catenin (pS675 and pS33/pS37/pT41) are slightly, but diametrically opposed changed, the data indicate that both pathways merge on β-catenin. How changes in the respective modifications occurred remained unclear.

Basing on TCF/β-catenin reporter assays, an antagonizing effect of Wnt5a onto Wnt3a signaling was measured in HepG2 directly [132]. Using the β-catenin bead array panel as a read-out system for active Wnt signaling, data gained on protein level contradict here. Interference downstream of β-catenin cannot be excluded.

The expression of Wnt ligands, receptors and important intracellular players in HepG2 and FOCUS was analyzed quantitatively on mRNA level by Taranit Gujral, Harvard Medical School (Supplementary material 8.4). Interestingly, *FZD2* was found to be drastically enhanced in FOCUS compared to HepG2 cells. From the recceptor-based view of Wnt signaling, this result suggests that differently expressed Wnt receptors could influence or even mediate the detected changes in β-catenin/Wnt signaling between HepG2 and FOCUS.

The distinct role of the different receptor expression in FOCUS and HepG2 need to be further analyzed in knockdown or overexpression experiments, respectively.

In general, recorded differences on protein level between FOCUS and HepG2 might contribute to the current discussion about the origin of fundamental differences in poorly and well-differentiated HCC cells. Several groups tried to classify subtypes of HCC using a panel of HCC cell lines by either global gene expression arrays [160], investigation of the EMT status [154] or the detection of autocrine expression of Wnt ligands or autocrine Wnt signaling respectively [132]. Mutations in the *CTNNB1* gene were found associated with low tumor grade [161]. Taken together, independent of the selected criteria the groupings correlated rather well and grouped FOCUS and HepG2 into different classes.

Finally, the role of Wnt5a in tumor development needs to be addressed since it is controversially discussed (reviewed in [93]). Published results indicate a cancer-specific or even cell-type specific role as a tumor suppressor [162] or a strong oncogenetic event [163]. In line with the current opinion, Wnt5a was not able to show transforming properties since increased β-catenin signaling was not observed in HepG2 and FOCUS. Interestingly, Medrek et al. [164] provided evidence that Wnt5a positively influences E-cadherin cell adhesion in breast cancer cells. In FOCUS and HepG2 the effect could not be shown; stable E-cadherin/β-catenin complex levels were measured over time (data not shown). With respect to its implication in HCC, only rare information is available [165] which does not allow a discussion. Yuzugullu et al. [132] referred to the differential expression of Wnt5a in poorly and well-differentiated HCC cell lines and suggested a role in manifesting cell invasiveness and motility.

4.6 The β-catenin bead array panel – a tool for a systems biology approach?

This thesis is embedded in the systems biology project Hepatosys and aimed to provide a novel tool for the analysis of Wnt signaling in primary mouse hepatocytes in the context of a systems biology approach. Here, a pivotal prerequisite of tools used for the generation of comprehensive data set is the ability of high throughput and fast assay procedure. Both criteria were fulfilled by the established β-catenin bead array panel. The multiplexed measurement of one sample substitutes at least the conduction of 8 conventional assays such as Western blots, reporter assay and co-immunoprecipitation for instance. Based on the semi-automated performance, a high sample throughput could be demonstrated.

The assay was used to generate necessarily required data describing multiparametric dynamic Wnt signaling. The experiments aimed to describe the time-resolved dynamic of β-

catenin signaling and were therefore designed to capture the response to a ligand or small molecule trigger from short time responses as well as long-term effects. The structure of the gained data sets fulfilled the criteria for computational modeling. Parts of the data were provided to the group of Jana Wolf, Max Delbrück Center in Berlin. The integration of the experimental microarray data gained in this thesis into their mathematical Wnt model is still ongoing.

5 Summary

β-catenin plays multiple roles in the canonical Wnt signaling pathway and in cell-cell adhesion complexes. In addition, β-catenin is a proto-oncogene and activating β-catenin mutations play a significant role in the genesis of colorectal, hepatocellular and other common cancers. Different functions of β-catenin as transcriptional co-activator or cell adhesion molecule are orchestrated by changes in concentration and phosphorylation as well as its ability to complex with proteins such as cadherins or transcription factors. Embedded in the liver systems biology project Hepatosys, the goal of this thesis was to prove the applicability of protein microarray-based assays to the quantitative and time-resolved study of signaling events and to further develop miniaturized and parallelized ligand binding assays for these purposes. In the context of this thesis a novel bead array panel for the analysis of β-catenin was developed, which is able to relatively quantify total β-catenin concentration, the extent of phosphorylation at multiple sites and the ratio of complexed and free cytoplasmic β-catenin. This is the first study to combine three biochemical methods – sandwich immunoassay, co-immunoprecipitation and protein-protein interaction assay – in one bead array panel.

The β-catenin bead array panel was used to study dynamic changes in the concentration of eight different β-catenin forms in primary mouse hepatocytes as well as in HEK293, FOCUS and HepG2 cells. For the first time, the time-resolved activity of the Wnt pathway could be measured directly on protein level using the µ-fishing assay and concurrently correlated with the characteristic phosphorylation pattern of β-catenin. This study could define a signaling–active pool of distinct forms of β-catenin (free β-catenin and pS45, pS552 and pS675 β-catenin) which mediates the canonical Wnt signaling on protein level in β-catenin wild type cells. It was demonstrated in HEK293 cells that this signaling active pool originates from *de-novo* protein biosynthesis only, but not from membrane release. In contrast to classical models of the Wnt pathway, phosphorylated β-catenin pS45 was found to increase after Wnt activation. Additionally, for the first time a link between Wnt signaling and β-catenin phosphorylated at S552 and S675 could be shown on protein level.

Moreover, in FOCUS and HepG2 the influence of non-canonical Wnt signaling on β-catenin-mediated canonical Wnt signaling was investigated. In contrast to recently published results, no inhibitory effect of non-canonical Wnt signaling was observed on the level of β-catenin.

Parts of the data sets describing dynamic β-catenin/Wnt signaling are currently used for mathematical modeling of the Wnt pathway.

6 Zusammenfassung

Das multifunktionelle Protein β-Catenin ist das zentrale Effektormolekül im Wnt Signalweg. Neben seiner Funktion als Adaptermolekül an der Zellmembran kann β-Catenin als Transkriptions-Co-Faktor und Protoonkogen die Expression von wachstumsfördernden Genen induzieren. In zelltypspezifischer Weise wird die Aktivität von β-Catenin über wechselnde Protein-Interaktionspartner, durch multiple Phosphorylierungen, durch Stabilisierung sowie durch seine intrazelluläre Lokalisation reguliert.

Um die Aktivität des Wnt Signalweges anhand seines zentralen Moleküls messen zu können, wurde im Rahmen dieser Doktorarbeit ein Mikrosphären-basiertes Arraysystem zur gleichzeitigen Bestimmung der Gesamtmenge, der Phosphorylierung, der Komplexierung sowie der Aktivität von β-Catenin entwickelt. Aus technischer Sicht gelang es erstmals, unterschiedliche technische und biochemische Methoden – GST-Pulldown, Sandwich Immunoassays und Co-immunopräzipitation – mit Hilfe einer miniaturisierten Array-Plattform in einem Testsystem zu kombinieren.

Das Arraysystem wurde eingesetzt um dynamisches β-Catenin-abhängiges Wnt Signaling in den Zellinien HEK293, HepG2 und FOCUS sowie in primären Hepatozyten zu untersuchen. Die Aktivität des Signalweges wurde auf Proteinebene mithilfe des miniaturisierten GST-Pulldowns erfasst. Parallel dazu konnte ein signall-induziertes Phosphorylierungsmuster von β-Catenin beschrieben werden. Darüberhinaus wurde gezeigt, dass Wnt-induzierbare Formen von β-Catenin (freies und phosphoryliertes β-Catenin pS45, pS552 und pS675) lediglich aus der *De-novo* Proteinbiosynthese stammen, jedoch nicht aus dem E-Cadherin/β-Catenin Komplex frei gesetzt werden können. Entgegen der klassischen Modellvorstellung deuten die vorliegenden Daten auf eine Beteiligung von pS45 β-Catenin an der Signalübertragung im Wnt Signalweg hin. Das Auftreten der C-terminalen Modifikationen (pS552 und pS675 β-Catenin) konnte erstmals in Zusammenhang mit der Aktivierung des Wnt Signalweges auf Proteinebene gezeigt werden.

Desweiteren wurde in den Zelllinien FOCUS und HepG2 untersucht, ob eine Verknüpfung zwischen kanonischem und nicht-kanonischem Wnt Signalweg auf der Ebene von β-Catenin stattfindet. Entgegen neuerer Erkenntnisse zeigte das Ergebnis eindeutig, dass kein inhibitorischer Einfluss des nicht-kanonischen Wnt Signalweges auf Proteinebene vorliegt.

Die im Rahmen dieser Arbeit generierten Daten stellen nun eine Grundlage zur Modellierung des Wnt Signalweges innerhalb des Systembiologie Projekts *Hepatosys* dar.

7 References

1. Lander, E.S., et al., *Initial sequencing and analysis of the human genome.* Nature, 2001. **409**(6822): p. 860-921.

2. Venter, J.C., et al., *The sequence of the human genome.* Science, 2001. **291**(5507): p. 1304-51.

3. Versteeg, R., et al., The human transcriptome map reveals extremes in gene density, intron length, GC content, and repeat pattern for domains of highly and weakly expressed genes. Genome Res, 2003. **13**(9): p. 1998-2004.

4. Yamada, K., et al., Empirical analysis of transcriptional activity in the Arabidopsis genome. Science, 2003. **302**(5646): p. 842-6.

5. Ideker, T., et al., Integrated genomic and proteomic analyses of a systematically perturbed metabolic network. Science, 2001. **292**(5518): p. 929-34.

6. Weintz, G., et al., The phosphoproteome of toll-like receptor-activated macrophages. Mol Syst Biol, 2010. **6**: p. 371.

7. Albeck, J.G., et al., *Collecting and organizing systematic sets of protein data.* Nat Rev Mol Cell Biol, 2006. **7**(11): p. 803-12.

8. Noble, D., *Biophysics and systems biology.* Philos Transact A Math Phys Eng Sci, 2010. **368**(1914): p. 1125-39.

9. Ewing, R.M., et al., Large-scale mapping of human protein-protein interactions by mass spectrometry. Mol Syst Biol, 2007. **3**: p. 89.

10. Rual, J.F., et al., Towards a proteome-scale map of the human protein-protein interaction network. Nature, 2005. **437**(7062): p. 1173-8.

11. Bauer-Mehren, A., L.I. Furlong, and F. Sanz, Pathway databases and tools for their exploitation: benefits, current limitations and challenges. Mol Syst Biol, 2009. **5**: p. 290.

12. Cusick, M.E., et al., *Literature-curated protein interaction datasets.* Nat Methods, 2009. **6**(1): p. 39-46.

13. Aldridge, B.B., et al., *Physicochemical modelling of cell signalling pathways.* Nat Cell Biol, 2006. **8**(11): p. 1195-203.

14. Gaudet, S., et al., A compendium of signals and responses triggered by prodeath and prosurvival cytokines. Mol Cell Proteomics, 2005. **4**(10): p. 1569-90.

15. Saez-Rodriguez, J., et al., Flexible informatics for linking experimental data to mathematical models via DataRail. Bioinformatics, 2008. **24**(6): p. 840-7.

16. Schilling, M., et al., Theoretical and experimental analysis links isoform-specific ERK signalling to cell fate decisions. Mol Syst Biol, 2009. **5**: p. 334.

17. Clevers, H., Wnt/beta-catenin signaling in development and disease. Cell, 2006. **127**(3): p. 469-80.

18. Logan, C.Y. and R. Nusse, *The Wnt signaling pathway in development and disease.* Annu Rev Cell Dev Biol, 2004. **20**: p. 781-810.

19. Nusse, R., *Wnt signaling in disease and in development.* Cell Res, 2005. **15**(1): p. 28-32.

20. Reya, T. and H. Clevers, *Wnt signalling in stem cells and cancer.* Nature, 2005. **434**(7035): p. 843-50.

21. Behrens, J. and B. Lustig, *The Wnt connection to tumorigenesis.* Int J Dev Biol, 2004. **48**(5-6): p. 477-87.

22. Moon, R.T., et al., *WNT and beta-catenin signalling: diseases and therapies.* Nat Rev Genet, 2004. **5**(9): p. 691-701.

23. Polakis, P., *Wnt signaling and cancer.* Genes Dev, 2000. **14**(15): p. 1837-51.

24. Mikels, A.J. and R. Nusse, *Wnts as ligands: processing, secretion and reception.* Oncogene, 2006. **25**(57): p. 7461-8.

25. Du, S.J., et al., Identification of distinct classes and functional domains of Wnts through expression of wild-type and chimeric proteins in Xenopus embryos. Mol Cell Biol, 1995. **15**(5): p. 2625-34.

26. Shimizu, H., et al., Transformation by Wnt family proteins correlates with regulation of beta-catenin. Cell Growth Differ, 1997. **8**(12): p. 1349-58.

27. van Amerongen, R., A. Mikels, and R. Nusse, *Alternative wnt signaling is initiated by distinct receptors.* Sci Signal, 2008. **1**(35): p. re9.

28. Cong, F., L. Schweizer, and H. Varmus, Wnt signals across the plasma membrane to activate the beta-catenin pathway by forming oligomers containing its receptors, Frizzled and LRP. Development, 2004. **131**(20): p. 5103-15.

29. Lu, W., et al., Mammalian Ryk is a Wnt coreceptor required for stimulation of neurite outgrowth. Cell, 2004. **119**(1): p. 97-108.

30. Mikels, A.J. and R. Nusse, Purified Wnt5a protein activates or inhibits beta-catenin-TCF signaling depending on receptor context. PLoS Biol, 2006. **4**(4): p. e115.

31. Schambony, A. and D. Wedlich, Wnt-5A/Ror2 regulate expression of XPAPC through an alternative noncanonical signaling pathway. Dev Cell, 2007. **12**(5): p. 779-92.

32. Peifer, M., S. Berg, and A.B. Reynolds, A repeating amino acid motif shared by proteins with diverse cellular roles. Cell, 1994. **76**(5): p. 789-91.

33. Huber, A.H., W.J. Nelson, and W.I. Weis, *Three-dimensional structure of the armadillo repeat region of beta-catenin.* Cell, 1997. **90**(5): p. 871-82.

34. Graham, T.A., et al., The crystal structure of the beta-catenin/ICAT complex reveals the inhibitory mechanism of ICAT. Mol Cell, 2002. **10**(3): p. 563-71.

35. Graham, T.A., et al., *Crystal structure of a beta-catenin/Tcf complex.* Cell, 2000. **103**(6): p. 885-96.

36. Huber, A.H. and W.I. Weis, The structure of the beta-catenin/E-cadherin complex and the molecular basis of diverse ligand recognition by beta-catenin. Cell, 2001. **105**(3): p. 391-402.

37. Xing, Y., et al., Crystal structure of a beta-catenin/axin complex suggests a mechanism for the beta-catenin destruction complex. Genes Dev, 2003. **17**(22): p. 2753-64.

38. Xing, Y., et al., Crystal structure of a beta-catenin/APC complex reveals a critical role for APC phosphorylation in APC function. Mol Cell, 2004. **15**(4): p. 523-33.

39. Mo, R., et al., The terminal region of beta-catenin promotes stability by shielding the Armadillo repeats from the axin-scaffold destruction complex. J Biol Chem, 2009. **284**(41): p. 28222-31.

40. Stadeli, R., R. Hoffmans, and K. Basler, *Transcription under the control of nuclear Arm/beta-catenin.* Curr Biol, 2006. **16**(10): p. R378-85.

41. Gottardi, C.J. and B.M. Gumbiner, Distinct molecular forms of beta-catenin are targeted to adhesive or transcriptional complexes. J Cell Biol, 2004. **167**(2): p. 339-49.

42. Gottardi, C.J. and M. Peifer, *Terminal regions of beta-catenin come into view.* Structure, 2008. **16**(3): p. 336-8.

43. Niessen, C.M. and C.J. Gottardi, *Molecular components of the adherens junction.* Biochim Biophys Acta, 2008. **1778**(3): p. 562-71.

44. Nelson, W.J. and R. Nusse, *Convergence of Wnt, beta-catenin, and cadherin pathways.* Science, 2004. **303**(5663): p. 1483-7.

45. Perez-Moreno, M., C. Jamora, and E. Fuchs, *Sticky business: orchestrating cellular signals at adherens junctions.* Cell, 2003. **112**(4): p. 535-48.

46. Drees, F., et al., Alpha-catenin is a molecular switch that binds E-cadherin-beta-catenin and regulates actin-filament assembly. Cell, 2005. **123**(5): p. 903-15.

47. Yamada, S., et al., *Deconstructing the cadherin-catenin-actin complex.* Cell, 2005. **123**(5): p. 889-901.

48. Piedra, J., et al., Regulation of beta-catenin structure and activity by tyrosine phosphorylation. J Biol Chem, 2001. **276**(23): p. 20436-43.

49. Roura, S., et al., Regulation of E-cadherin/Catenin association by tyrosine phosphorylation. J Biol Chem, 1999. **274**(51): p. 36734-40.

50. Brembeck, F.H., et al., Essential role of BCL9-2 in the switch between beta-catenin's adhesive and transcriptional functions. Genes Dev, 2004. **18**(18): p. 2225-30.

51. Heuberger, J. and W. Birchmeier, *Interplay of cadherin-mediated cell adhesion and canonical wnt signaling.* Cold Spring Harb Perspect Biol, 2010. **2**(2): p. a002915.

52. Amit, S., et al., Axin-mediated CKI phosphorylation of beta-catenin at Ser 45: a molecular switch for the Wnt pathway. Genes Dev, 2002. **16**(9): p. 1066-76.

53. Liu, C., et al., Control of beta-catenin phosphorylation/degradation by a dual-kinase mechanism. Cell, 2002. **108**(6): p. 837-47.

54. Liu, C., et al., beta-Trcp couples beta-catenin phosphorylation-degradation and regulates Xenopus axis formation. Proc Natl Acad Sci U S A, 1999. **96**(11): p. 6273-8.

55. Aberle, H., et al., beta-catenin is a target for the ubiquitin-proteasome pathway. EMBO J, 1997. **16**(13): p. 3797-804.

56. Hart, M., et al., The F-box protein beta-TrCP associates with phosphorylated beta-catenin and regulates its activity in the cell. Curr Biol, 1999. **9**(4): p. 207-10.

57. Kitagawa, M., et al., An F-box protein, FWD1, mediates ubiquitin-dependent proteolysis of beta-catenin. EMBO J, 1999. **18**(9): p. 2401-10.

58. Daniels, D.L. and W.I. Weis, Beta-catenin directly displaces Groucho/TLE repressors from Tcf/Lef in Wnt-mediated transcription activation. Nat Struct Mol Biol, 2005. **12**(4): p. 364-71.

59. Willert, K. and K.A. Jones, *Wnt signaling: is the party in the nucleus?* Genes Dev, 2006. **20**(11): p. 1394-404.

60. Davidson, G., et al., Casein kinase 1 gamma couples Wnt receptor activation to cytoplasmic signal transduction. Nature, 2005. **438**(7069): p. 867-72.

61. Tamai, K., et al., *A mechanism for Wnt coreceptor activation.* Mol Cell, 2004. **13**(1): p. 149-56.

62. Zeng, X., et al., A dual-kinase mechanism for Wnt co-receptor phosphorylation and activation. Nature, 2005. **438**(7069): p. 873-7.

63. MacDonald, B.T., et al., Wnt signal amplification via activity, cooperativity, and regulation of multiple intracellular PPPSP motifs in the Wnt co-receptor LRP6. J Biol Chem, 2008. **283**(23): p. 16115-23.

64. Willert, K., et al., Casein kinase 2 associates with and phosphorylates dishevelled. EMBO J, 1997. **16**(11): p. 3089-96.

65. Behrens, J., et al., Functional interaction of beta-catenin with the transcription factor LEF-1. Nature, 1996. **382**(6592): p. 638-42.

66. Brunner, E., et al., pangolin encodes a Lef-1 homologue that acts downstream of Armadillo to transduce the Wingless signal in Drosophila. Nature, 1997. **385**(6619): p. 829-33.

67. Molenaar, M., et al., XTcf-3 transcription factor mediates beta-catenin-induced axis formation in Xenopus embryos. Cell, 1996. **86**(3): p. 391-9.

68. Hecht, A., et al., Functional characterization of multiple transactivating elements in beta-catenin, some of which interact with the TATA-binding protein in vitro. J Biol Chem, 1999. **274**(25): p. 18017-25.

69. Hecht, A., et al., The p300/CBP acetyltransferases function as transcriptional coactivators of beta-catenin in vertebrates. EMBO J, 2000. **19**(8): p. 1839-50.

70. Tago, K., et al., Inhibition of Wnt signaling by ICAT, a novel beta-catenin-interacting protein. Genes Dev, 2000. **14**(14): p. 1741-9.

71. Takemaru, K., et al., Chibby, a nuclear beta-catenin-associated antagonist of the Wnt/Wingless pathway. Nature, 2003. **422**(6934): p. 905-9.

72. Daniels, D.L. and W.I. Weis, ICAT inhibits beta-catenin binding to Tcf/Lef-family transcription factors and the general coactivator p300 using independent structural modules. Mol Cell, 2002. **10**(3): p. 573-84.

73. Jho, E.H., et al., Wnt/beta-catenin/Tcf signaling induces the transcription of Axin2, a negative regulator of the signaling pathway. Mol Cell Biol, 2002. **22**(4): p. 1172-83.

74. Lustig, B., et al., Negative feedback loop of Wnt signaling through upregulation of conductin/axin2 in colorectal and liver tumors. Mol Cell Biol, 2002. **22**(4): p. 1184-93.

75. Yan, D., et al., Elevated expression of axin2 and hnkd mRNA provides evidence that Wnt/beta -catenin signaling is activated in human colon tumors. Proc Natl Acad Sci U S A, 2001. **98**(26): p. 14973-8.

76. Cadigan, K.M. and M. Peifer, *Wnt signaling from development to disease: insights from model systems.* Cold Spring Harbor Perspect Biol, 2009. **1**(2): p. a002881.

77. Taurin, S., et al., Phosphorylation of beta-catenin by cyclic AMP-dependent protein kinase. J Biol Chem, 2006. **281**(15): p. 9971-6.

78. Daugherty, R.L. and C.J. Gottardi, *Phospho-regulation of Beta-catenin adhesion and signaling functions.* Physiology (Bethesda), 2007. **22**: p. 303-9.

79. Hussain, S.Z., et al., Wnt impacts growth and differentiation in ex vivo liver development. Exp Cell Res, 2004. **292**(1): p. 157-69.

80. Monga, S.P., et al., Beta-catenin antisense studies in embryonic liver cultures: role in proliferation, apoptosis, and lineage specification. Gastroenterology, 2003. **124**(1): p. 202-16.

81. Nejak-Bowen, K. and S.P. Monga, *Wnt/beta-catenin signaling in hepatic organogenesis.* Organogenesis, 2008. **4**(2): p. 92-9.

82. Thompson, M.D. and S.P. Monga, *WNT/beta-catenin signaling in liver health and disease.* Hepatology, 2007. **45**(5): p. 1298-305.

83. Oda, H., et al., Somatic mutations of the APC gene in sporadic hepatoblastomas. Cancer Res, 1996. **56**(14): p. 3320-3.

84. Koch, A., et al., Childhood hepatoblastomas frequently carry a mutated degradation targeting box of the beta-catenin gene. Cancer Res, 1999. **59**(2): p. 269-73.

85. Taniguchi, K., et al., Mutational spectrum of beta-catenin, AXIN1, and AXIN2 in hepatocellular carcinomas and hepatoblastomas. Oncogene, 2002. **21**(31): p. 4863-71.

86. de La Coste, A., et al., Somatic mutations of the beta-catenin gene are frequent in mouse and human hepatocellular carcinomas. Proc Natl Acad Sci U S A, 1998. **95**(15): p. 8847-51.

87. Merle, P., et al., Functional consequences of frizzled-7 receptor overexpression in human hepatocellular carcinoma. Gastroenterology, 2004. **127**(4): p. 1110-22.

88. Ban, K.C., et al., GSK-3beta phosphorylation and alteration of beta-catenin in hepatocellular carcinoma. Cancer Lett, 2003. **199**(2): p. 201-8.

89. Fanto, M. and H. McNeill, *Planar polarity from flies to vertebrates.* J Cell Sci, 2004. **117**(Pt 4): p. 527-33.

90. Veeman, M.T., J.D. Axelrod, and R.T. Moon, A second canon. Functions and mechanisms of beta-catenin-independent Wnt signaling. Dev Cell, 2003. **5**(3): p. 367-77.

91. Kohn, A.D. and R.T. Moon, *Wnt and calcium signaling: beta-catenin-independent pathways.* Cell Calcium, 2005. **38**(3-4): p. 439-46.

92. van Amerongen, R. and R. Nusse, *Towards an integrated view of Wnt signaling in development.* Development, 2009. **136**(19): p. 3205-14.

93. McDonald, S.L. and A. Silver, *The opposing roles of Wnt-5a in cancer.* Br J Cancer, 2009. **101**(2): p. 209-14.

94. Ishitani, T., et al., The TAK1-NLK mitogen-activated protein kinase cascade functions in the Wnt-5a/Ca(2+) pathway to antagonize Wnt/beta-catenin signaling. Mol Cell Biol, 2003. **23**(1): p. 131-9.

95. Topol, L., et al., Wnt-5a inhibits the canonical Wnt pathway by promoting GSK-3-independent beta-catenin degradation. J Cell Biol, 2003. **162**(5): p. 899-908.

96. Torii, K., et al., Anti-apoptotic action of Wnt5a in dermal fibroblasts is mediated by the PKA signaling pathways. Cell Signal, 2008. **20**(7): p. 1256-66.

97. Hoheisel, J.D., Microarray technology: beyond transcript profiling and genotype analysis. Nat Rev Genet, 2006. **7**(3): p. 200-10.

98. Plomin, R. and L.C. Schalkwyk, *Microarrays.* Dev Sci, 2007. **10**(1): p. 19-23.

99. Punyadeera, C., et al., A biomarker panel to discriminate between systemic inflammatory response syndrome and sepsis and sepsis severity. J Emerg Trauma Shock, 2010. **3**(1): p. 26-35.

100. Yu, X., et al., Protein microarrays: effective tools for the study of inflammatory diseases. Methods Mol Biol, 2009. **577**: p. 199-214.

101. Schmohl, M., et al., Protein-protein-interactions in a multiplexed, miniaturized format a functional analysis of Rho GTPase activation and inhibition. Proteomics, 2010. **10**(8): p. 1716-1720.

102. Templin, M.F., et al., *Protein microarrays: promising tools for proteomic research.* Proteomics, 2003. **3**(11): p. 2155-66.

103. Uhlen, M. and S. Hober, Generation and validation of affinity reagents on a proteome-wide level. J Mol Recognit, 2009. **22**(2): p. 57-64.

104. Ekins, R.P., *Multi-analyte immunoassay.* J Pharm Biomed Anal, 1989. **7**(2): p. 155-68.

105. Hartmann, M., et al., *Protein microarrays for diagnostic assays.* Anal Bioanal Chem, 2009. **393**(5): p. 1407-16.

106. Poetz, O., et al., *Protein microarrays: catching the proteome.* Mech Ageing Dev, 2005. **126**(1): p. 161-70.

107. Dasso, J., et al., A comparison of ELISA and flow microsphere-based assays for quantification of immunoglobulins. J Immunol Methods, 2002. **263**(1-2): p. 23-33.

108. Dupont, N.C., et al., Validation and comparison of luminex multiplex cytokine analysis kits with ELISA: determinations of a panel of nine cytokines in clinical sample culture supernatants. J Reprod Immunol, 2005. **66**(2): p. 175-91.

109. Nielsen, U.B., et al., *Profiling receptor tyrosine kinase activation by using Ab microarrays.* Proc Natl Acad Sci U S A, 2003. **100**(16): p. 9330-5.

110. Ciaccio, M.F., et al., Systems analysis of EGF receptor signaling dynamics with microwestern arrays. Nat Methods, 2010. **7**(2): p. 148-55.

111. Du, J., et al., Bead-based profiling of tyrosine kinase phosphorylation identifies SRC as a potential target for glioblastoma therapy. Nat Biotechnol, 2009. **27**(1): p. 77-83.

112. Aberle, H., et al., Assembly of the cadherin-catenin complex in vitro with recombinant proteins. J Cell Sci, 1994. **107**(12): p. 3655-63.

113. Aberle, H., et al., Single amino acid substitutions in proteins of the armadillo gene family abolish their binding to alpha-catenin. J Biol Chem, 1996. **271**(3): p. 1520-6.

114. Hecht, A. and M.P. Stemmler, Identification of a promoter-specific transcriptional activation domain at the C terminus of the Wnt effector protein T-cell factor 4. J Biol Chem, 2003. **278**(6): p. 3776-85.

115. Poetz, O., Qualitative und quantitative Analyse von ß-Catenin in Catnb-mutierten hepatozellulären Tumoren der Maus mit Array-basierten Methoden. Dissertation, Tübingen, 2005.

116. Graham, F.L., et al., Characteristics of a human cell line transformed by DNA from human adenovirus type 5. J Gen Virol, 1977. **36**(1): p. 59-74.

117. He, L., et al., Establishment and characterization of a new human hepatocellular carcinoma cell line. In Vitro, 1984. **20**(6): p. 493-504.

118. Aden, D.P., et al., Controlled synthesis of HBsAg in a differentiated human liver carcinoma-derived cell line. Nature, 1979. **282**(5739): p. 615-6.

119. Darlington, G.J., J.H. Kelly, and G.J. Buffone, *Growth and hepatospecific gene expression of human hepatoma cells in a defined medium.* In Vitro Cell Dev Biol, 1987. **23**(5): p. 349-54.

120. Knowles, B.B., C.C. Howe, and D.P. Aden, Human hepatocellular carcinoma cell lines secrete the major plasma proteins and hepatitis B surface antigen. Science, 1980. **209**(4455): p. 497-9.

121. Klingmüller, U., et al., Primary mouse hepatocytes for systems biology approaches: a standardized in vitro system for modelling of signal transduction pathways. Syst Biol (Stevenage), 2006. **153**(6): p. 433-47.

122. Korinek, V., et al., Constitutive transcriptional activation by a beta-catenin-Tcf complex in APC-/- colon carcinoma. Science, 1997. **275**(5307): p. 1784-7.

123. Hirsch, C., et al., Canonical Wnt signaling transiently stimulates proliferation and enhances neurogenesis in neonatal neural progenitor cultures. Exp Cell Res, 2007. **313**(3): p. 572-87.

124. Lowry, O.H., et al., *Protein measurement with the Folin phenol reagent.* J Biol Chem, 1951. **193**(1): p. 265-75.

125. Goetschel, F., Zelltypspezifische Analyse dynamischer Prozesse des Wnt/β-Catenin Signalwegs mit Hilfe systembiologischer Verfahren. Dissertation, Freiburg, 2008.

126. Poetz, O., et al., Microsphere-based co-immunoprecipitation in multiplex. Anal

Biochem, 2009. **395**(2): p.244-8.

127. Coghlan, M.P., et al., Selective small molecule inhibitors of glycogen synthase kinase-3 modulate glycogen metabolism and gene transcription. Chem Biol, 2000. **7**(10): p. 793-803.

128. Hendriksen, J., et al., Plasma membrane recruitment of dephosphorylated beta-catenin upon activation of the Wnt pathway. J Cell Sci, 2008. **121**(Pt 11): p. 1793-802.

129. Yokoyama, N., D. Yin, and C.C. Malbon, Abundance, complexation, and trafficking of Wnt/beta-catenin signaling elements in response to Wnt3a. J Mol Signal, 2007. **2**: p. 11.

130. Obrig, T.G., et al., The mechanism by which cycloheximide and related glutarimide antibiotics inhibit peptide synthesis on reticulocyte ribosomes. J Biol Chem, 1971. **246**(1): p. 174-81.

131. Lee, J.S. and S.S. Thorgeirsson, *Comparative and integrative functional genomics of HCC.* Oncogene, 2006. **25**(27): p. 3801-9.

132. Yuzugullu, H., et al., Canonical Wnt signaling is antagonized by noncanonical Wnt5a in hepatocellular carcinoma cells. Mol Cancer, 2009. **8**: p. 90.

133. Cagatay, T. and M. Ozturk, P53 mutation as a source of aberrant beta-catenin accumulation in cancer cells. Oncogene, 2002. **21**(52): p. 7971-80.

134. Kang, Y. and J. Massague, Epithelial-mesenchymal transitions: twist in development and metastasis. Cell, 2004. **118**(3): p. 277-9.

135. Huber, M.A., N. Kraut, and H. Beug, *Molecular requirements for epithelial-mesenchymal transition during tumor progression.* Curr Opin Cell Biol, 2005. **17**(5): p. 548-58.

136. Huang, S.M., et al., Tankyrase inhibition stabilizes axin and antagonizes Wnt signalling. Nature, 2009. **461**(7264): p. 614-20.

137. Naik, S. and D. Piwnica-Worms, *Real-time imaging of beta-catenin dynamics in cells and living mice.* Proc Natl Acad Sci U S A, 2007. **104**(44): p. 17465-70.

138. MacDonald, B.T., K. Tamai, and X. He, *Wnt/beta-catenin signaling: components, mechanisms, and diseases.* Dev Cell, 2009. **17**(1): p. 9-26.

139. Doble, B.W. and J.R. Woodgett, *GSK-3: tricks of the trade for a multi-tasking kinase.* J Cell Sci, 2003. **116**(Pt 7): p. 1175-86.

140. Maher, M.T., et al., Beta-catenin phosphorylated at serine 45 is spatially uncoupled from beta-catenin phosphorylated in the GSK3 domain: implications for signaling. PLoS One, 2010. **5**(4): p. e10184.

141. Cselenyi, C.S., et al., LRP6 transduces a canonical Wnt signal independently of Axin degradation by inhibiting GSK3's phosphorylation of beta-catenin. Proc Natl Acad Sci U S A, 2008. **105**(23): p. 8032-7.

142. Merdek, K.D., N.T. Nguyen, and D. Toksoz, Distinct activities of the alpha-catenin family, alpha-catulin and alpha-catenin, on beta-catenin-mediated signaling. Mol Cell Biol, 2004. **24**(6): p. 2410-22.

143. Wu, G., et al., Inhibition of GSK3 phosphorylation of beta-catenin via phosphorylated PPPSPXS motifs of Wnt coreceptor LRP6. PLoS One, 2009. **4**(3): p. e4926.

144. Hino, S., et al., Phosphorylation of beta-catenin by cyclic AMP-dependent protein kinase stabilizes beta-catenin through inhibition of its ubiquitination. Mol Cell Biol, 2005. **25**(20): p. 9063-72.

145. Fang, D., et al., Phosphorylation of beta-catenin by AKT promotes beta-catenin transcriptional activity. J Biol Chem, 2007. **282**(15): p. 11221-9.

146. Staal, F.J., et al., Wnt signals are transmitted through N-terminally dephosphorylated beta-catenin. EMBO Rep, 2002. **3**(1): p. 63-8.

147. Gujral, T.S. and G. MacBeath, A system-wide investigation of the dynamics of Wnt signaling reveals novel phases of transcriptional regulation. PLoS One, 2010. **5**(4): p. e10024.

148. Williams, B.O., et al., A comparative evaluation of beta-catenin and plakoglobin signaling activity. Oncogene, 2000. **19**(50): p. 5720-8.

149. Miravet, S., et al., Tyrosine phosphorylation of plakoglobin causes contrary effects on its association with desmosomes and adherens junction components and modulates beta-catenin-mediated transcription. Mol Cell Biol, 2003. **23**(20): p. 7391-402.

150. Braeuning, A. and A. Buchmann, The glycogen synthase kinase inhibitor 3-(2,4-dichlorophenyl)-4-(1-methyl-1H-indol-3-yl)-1H-pyrrole-2,5-dione (SB216763) is a partial agonist of the aryl hydrocarbon receptor. Drug Metab Dispos, 2009. **37**(8): p. 1576-80.

151. Carruba, G., et al., Truncated form of beta-catenin and reduced expression of wild-type catenins feature HepG2 human liver cancer cells. Ann N Y Acad Sci, 1999. **886**: p. 212-6.

152. Zeng, G., et al., siRNA-mediated beta-catenin knockdown in human hepatoma cells results in decreased growth and survival. Neoplasia, 2007. **9**(11): p. 951-9.

153. Acloque, H., et al., Epithelial-mesenchymal transitions: the importance of changing cell state in development and disease. J Clin Invest, 2009. **119**(6): p. 1438-49.

154. Fuchs, B.C., et al., Epithelial-to-mesenchymal transition and integrin-linked kinase mediate sensitivity to epidermal growth factor receptor inhibition in human hepatoma cells. Cancer Res, 2008. **68**(7): p. 2391-9.

155. Thiery, J.P., et al., Epithelial-mesenchymal transitions in development and disease. Cell, 2009. **139**(5): p. 871-90.

156. Kuphal, F. and J. Behrens, E-cadherin modulates Wnt-dependent transcription in colorectal cancer cells but does not alter Wnt-independent gene expression in fibroblasts. Exp Cell Res, 2006. **312**(4): p. 457-67.

157. Cavallaro, U. and G. Christofori, *Cell adhesion and signalling by cadherins and Ig-CAMs in cancer.* Nat Rev Cancer, 2004. **4**(2): p. 118-32.

158. Yook, J.I., et al., *Wnt-dependent regulation of the E-cadherin repressor snail.* J Biol Chem, 2005. **280**(12): p. 11740-8.

159. Boutros, M., et al., *Signaling specificity by Frizzled receptors in Drosophila.* Science, 2000. **288**(5472): p. 1825-8.

160. Lee, J.S. and S.S. Thorgeirsson, Functional and genomic implications of global gene expression profiles in cell lines from human hepatocellular cancer. Hepatology, 2002. **35**(5): p. 1134-43.

161. Hsu, H.C., et al., Beta-catenin mutations are associated with a subset of low-stage hepatocellular carcinoma negative for hepatitis B virus and with favorable prognosis. Am J Pathol, 2000. **157**(3): p. 763-70.

162. Dejmek, J., et al., Wnt-5a/Ca2+-induced NFAT activity is counteracted by Wnt-5a/Yes-Cdc42-casein kinase 1alpha signaling in human mammary epithelial cells. Mol Cell Biol, 2006. **26**(16): p. 6024-36.

163. Yamamoto, H., et al., Wnt5a signaling is involved in the aggressiveness of prostate cancer and expression of metalloproteinase. Oncogene, 2010. **29**(14): p. 2036-46.

164. Medrek, C., et al., Wnt-5a-CKIα signaling promotes β-catenin/E-cadherin complex formation and intercellular adhesion in human breast epithelial cells. J Biol Chem, 2009. **284**(16): p. 10968-79.

165. Liu, X., et al., Mutations in the C-terminus of the X protein of hepatitis B virus regulate Wnt-5a expression in hepatoma Huh7 cells: cDNA microarray and proteomic analyses. Carcinogenesis, 2008. **29**(6): p. 1207-14.

8 Supplementary material

8.1 Supplementary material 1: Relative expression levels of β-catenin in HEK293, FOCUS, HepG2 and primary mouse hepatocytes

β-catenin was measured using a suspension bead array on the basis of assays described in 2.7.4. Standard deviations were calculated based on technical triplicates. In Supplementary Figure 1 relative levels of β-catenin measured in human cell lines FOCUS, HepG2 and HEK293 as well as in primary mouse hepatocytes are shown.

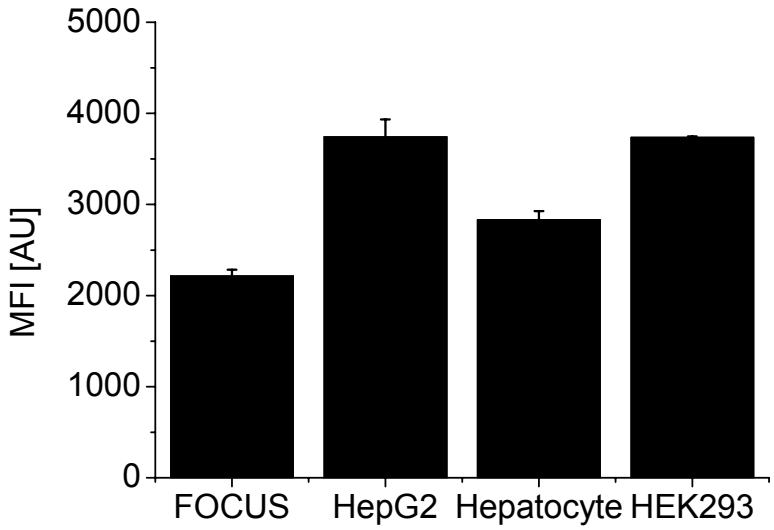

Supplementary Figure 1 Relative levels of β-catenin were measured in FOCUS, HepG2, HEK293 and primary mouse hepatocytes. 10 µg of total protein of untreated cell lysates were analyzed using a bead-based sandwich immunoassay. The result is displayed in median fluorescence intensities. Three technical replicates were performed to calculate the standard deviations. Differences between the overall levels of β-catenin in the investigated cell types were detected.

8.2 Supplementary material 2: Relative levels of the E-cadherin/β-catenin and the N-cadherin/β-catenin complex in HEK293, FOCUS, HepG2 and primary mouse hepatocytes

The E-cadherin/β-catenin complex was detected as described in 2.7.3. For the detection of the N-cadherin/β-catenin complex, an anti human N-cadherin (R&D Systems, Minneapolis, MN, USA) antibody was immobilized on color-coded beads according to the standard protocol (2.7.1). Beads coated with anti N-cadherin antibody were added to the β-catenin bead array panel. All other steps were performed as described in 2.7.3. 3 x 20 µg of non-stimulated cell lysate were used for the analysis. Standard deviations were calculated based on technical triplicates. Due to the lack of a mouse-specific N-cadherin antibody, no results were obtained in primary mouse hepatocytes.

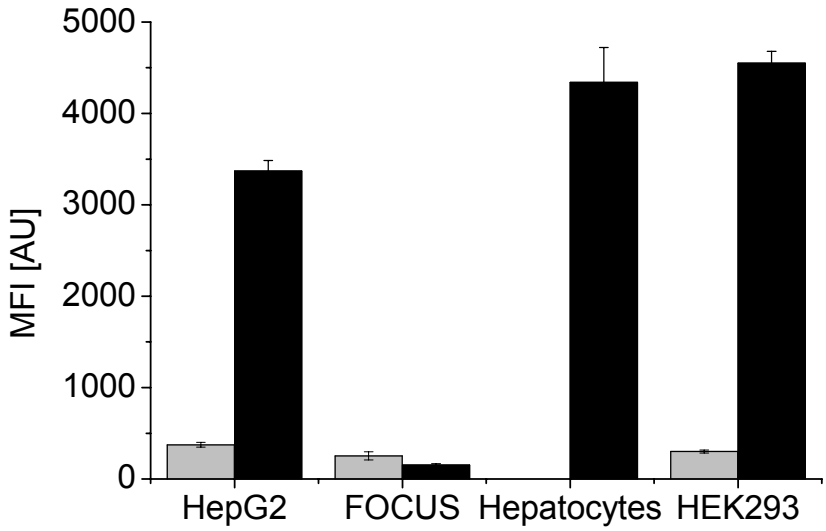

Supplementary Figure 2 Relative levels of the N-cadherin/β-catenin (grey bars) and E-cadherin/β-catenin complex (black bars) were monitored in FOCUS, HepG2, HEK293 and primary mouse hepatocytes. 20 µg of non-stimulated cell lysate were analyzed. Standard deviations were calculated based on technical triplicates. A low amount of N-cadherin-complexed β-catenin was detected in all cell lines. Due to the lack of a mouse-specific N-cadherin capture antibody, no result was gained in primary mouse hepatocytes. The E-cadherin/β-catenin complex was found in HepG2, HEK293 and primary mouse hepatocytes. In FOCUS, the amount of the E-cadherin/β-catenin complex was relatively low.

8.3 Supplementary material 3: Demasking experiment

This experiment aimed to investigate the influence of different lysis conditions on the detection of free β-catenin in primary mouse hepatocytes using the µ-fishing assay. The tested lysis conditions were chosen to demask β-catenin from potential interaction partners which prevent the detection of active β-catenin. Therefore, primary mouse hepatocytes were stimulated with GSK-3 inhibitor SB216763 or DMSO for 3 h. In Supplementary Table 1 the different lysis conditions are listed. Note, condition 1 was routinely used as cell lysis buffer as described in 2.10.1.

Supplementary Table 1 Lysis conditions

	pH	NaCl	Amine Buffer	Triton x-100	Na-Desoxycholate	Urea
1	7.4	150 mM	50 mM Tris	1%		
2	5.8	150 mM	50 mM MES	1%		
3	10.5	150 mM	50 mM Tris	1%		
4	7.4	400 mM	50 mM Tris	1%		
5	7.4	1000 mM	50 mM Tris	1%		
6	7.4	150 mM	50 mM Tris	1%		1M
7	7.4	150 mM	50 mM Tris	1%		2M
8	7.4	150 mM	50 mM Tris	1%		3M
9	7.4	150 mM	50 mM Tris	0.50%	0.50%	

All samples were normalized to 25 µg protein/well with lysis buffer 1 (150 mM NaCl, 50 mM Tris pH 7.4, 1% Triton) and analyzed with the β-catenin bead array panel as described in 2.7.3. The ECT-captured free β-catenin levels of all samples are shown in Supplementary Figure 3.

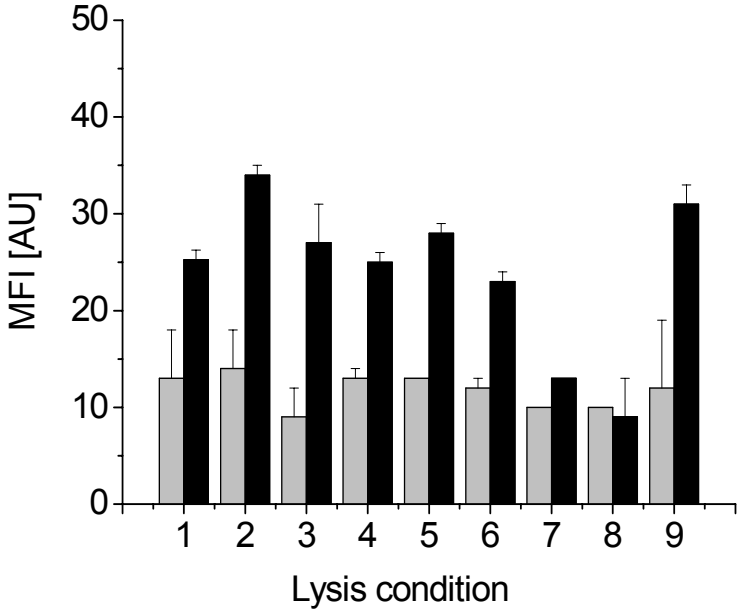

Supplementary Figure 3: The effect of different lysis conditions on the detection of free β-catenin.

Primary mouse hepatocytes were treated with 80 µM SB216763 (or DMSO) for 3 h and lysed with 9 different lysis buffers as listed in Supplementary Table 1. 25 µg of each sample were analyzed in technical replicates with the β-catenin bead array panel. Levels of free β-catenin captured by GST-ECT in stimulated (black) and non-stimulated (grey) samples are displayed in median fluorescence intensities. Strongly denaturating lysis conditions (no 7 and 8) abolished the detection of induced free β-catenin. With respect to the other tested lysis conditions, similar levels of free β-catenin were detected after activation. Thus, none of the tested lysis conditions improved significantly the detection of free β-catenin.

8.4 Supplementary material 4: Expression of Wnt signaling genes in FOCUS and HepG2

Differences between β-catenin signaling in HepG2 and FOCUS were found and described in 3.4 and 3.5. To obtain a more comprehensive comparison of Wnt signaling in these two cell lines, the expression of 84 Wnt signaling genes in serum starved FOCUS and HepG2 cells were analyzed by quantitative PCR. As shown in Supplementary Figure 4A, significant differences in the expression of Wnt receptors, ligands as well as intracellular regulators were detected. Genes and corresponding proteins are listed in Supplementary Table 2. The expression of *FZD2* was found clearly several hundred fold higher in FOCUS compared to HepG2 (Supplementary Figure 4B). The experiments were performed by Taranjit Gujral, Harvard Medical School.

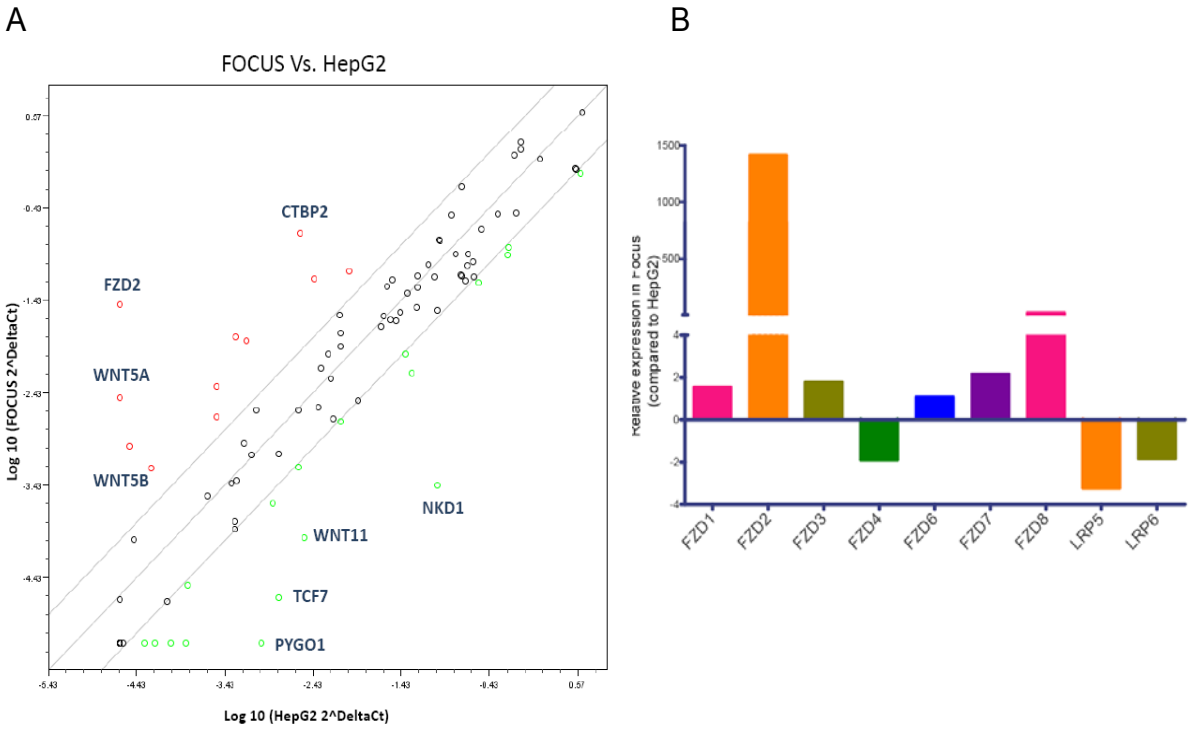

Supplementary Figure 4: Expression of Wnt signaling genes in FOCUS and HepG2.

(A) Significantly altered expression levels of Wnt receptors, ligands as well as intracellular regulators are shown. Genes detected with a higher expression in FOCUS compared to HepG2 are displayed in red circles, while genes measured with a higher expression in HepG2 compared to FOCUS are drawn in green circles. (B) Differently expressed Wnt receptors and co-receptors are displayed separated by color. FZD2 was found to be drastically higher expressed in FOCUS (orange) as in HepG2.

Supplementary Table 2 Wnt signaling genes assessed by quantitative real-time PCR revealing differences between FOCUS and HepG2.

Gene Symbol	Protein
CTBP2	C-terminal binding protein 2
FZD1	Frizzled homolog 1 (Drosophila)
FZD2	Frizzled homolog 2 (Drosophila)
FZD3	Frizzled homolog 3 (Drosophila)
FZD4	Frizzled homolog 4 (Drosophila)
FZD6	Frizzled homolog 6 (Drosophila)
FZD7	Frizzled homolog 7 (Drosophila)
FZD8	Frizzled homolog 8 (Drosophila)
LRP5	Low density lipoprotein receptor-related protein 5
LRP6	Low density lipoprotein receptor-related protein 6
NKD1	Naked cuticle homolog 1 (Drosophila)
PYGO1	Pygopus homolog 1 (Drosophila)
TCF7	Transcription factor 7 (T-cell specific, HMG-box)
WNT11	Wingless-type MMTV integration site family, member 11
WNT5A	Wingless-type MMTV integration site family, member 5A
WNT5B	Wingless-type MMTV integration site family, member 5B

9 List of publications

Poetz, O., Luckert, K., Herget, T., and Joos, T. O., Microsphere-based co immunoprecipitation in multiplex. Anal Biochem (2009).

Luckert, K., Götschel, F., Sorger, P.K. Hecht, A., Joos, T.O., Pötz, O., Snapshots of protein dynamics and posttranslational modifications in one experiment – β-catenin and its functions. Submitted (2010)

Poetz, O., Luckert, K., Hartmann, M., Henzler, T., Kazmaier, C., Herget, T., Joos, T.O., From cells to results: A continuous automated workflow for bead-based sandwich immunoassays. In preparation (2010)

10 Akademische Lehrer

Prof. Bardele

Dr. Bayer

Prof. Bisswanger

Prof. Bohley

Dr. Buchmann

Prof. Dodt

Prof. Duszenko

Prof. Gauglitz

Prof. Hamprecht

Dr. Immanuel Heck

Dr. Iglauer

Prof. Ihringer

Prof. Jäger

PD Dr. Just

Dr. Kalbacher

PD Dr. Klein

Prof. Kohlbacher

Prof. Laufer

Prof. Maier

Dr. Josef Maier

PD Dr. Münzel

PD Dr. Neymeyr

Prof. Nürnberger

Prof. Oberhammer

Prof. Probst

Dr. Sarrazin

Prof. Schott

Prof. Schultz

Prof. Schwarz

Dr. Steinbrück

Prof. Stehle

Prof. Stevanović

PD Dr. Stoeva

PD Dr. Verleysdonk

Prof. Weitz

Prof. Werz

Prof. Weser

PD Dr. Wieder

Prof. Wohlleben

11 Lebenslauf

Persönliche Daten

Katrin Luckert

Geboren am 21.Juli 1982 in Waiblingen

Verheiratet mit Philipp Blaskowitz

Ausbildung

10/2007 - 10/2010	Doktorarbeit
	Titel: “Multiplexe Analyse des dynamischen β-Catenin/Wnt Signalweges”
	„Snapshots of protein dynamics and posttranslational modifications in one experiment – β-catenin and its functions“
	Betreuer: Prof. Dr. Stefan Stevanović, Abteilung Immunologie, Interfakultäres Institut für Zellbiologie der Eberhard-Karls-Universität Tübingen, in Kooperation
	mit Dr. Thomas Joos und Dr. Oliver Pötz, Abteilung Biochemie, Naturwissenschaftliches und medizinisches Institut an der Universität Tübingen (NMI), Reutlingen und
	Prof. Dr. Thilo Stehle, Interfakultäres Institut für Biochemie der Eberhard-Karls-Universität Tübingen
12/2006 – 07/2007	Diplomarbeit
	Titel: „ Multiplexe Interaktionsanalyse von β-Catenin“
	Betreuer: Prof. Dr. Michael Schwarz, Institut für Pharmakologie und Toxikologie an der Eberhard-Karls Universität Tübingen
10/2002 – 11/2006	Studium
	Biochemie, Eberhard-Karls-Universität Tübingen
1993 – 2002	Gymnasium